National Library
of Canada

Bibliothèque nationale
du Canada

Canadian Theses Service

Service des thèses canadiennes

Ottawa, Canada
K1A 0N4

NOTICE

The quality of this microform is heavily dependent upon the quality of the original thesis submitted for microfilming. Every effort has been made to ensure the highest quality of reproduction possible.

If pages are missing, contact the university which granted the degree.

Some pages may have indistinct print especially if the original pages were typed with a poor typewriter ribbon or if the university sent us an inferior photocopy.

Reproduction in full or in part of this microform is governed by the Canadian Copyright Act, R.S.C. 1970, c. C-30, and subsequent amendments.

AVIS

La qualité de cette microforme dépend grandement de la qualité de la thèse soumise au microfilmage. Nous avons tout fait pour assurer une qualité supérieure de reproduction.

S'il manque des pages, veuillez communiquer avec l'université qui a conféré le grade.

La qualité d'impression de certaines pages peut laisser à désirer, surtout si les pages originales ont été dactylographiées à l'aide d'un ruban usé ou si l'université nous a fait parvenir une photocopie de qualité inférieure.

La reproduction, même partielle, de cette microforme est soumise à la Loi canadienne sur le droit d'auteur, SRC 1970, c. C-30, et ses amendements subséquents.

NL 339 (r. 88/04) c

Canada

UNIVERSITY OF ALBERTA

COLLAPSE STRENGTH OF CYLINDERS SUBJECT TO AXIAL TENSION AND EXTERNAL PRESSURE

BY

DUANE D. DEGEER

A THESIS

SUBMITTED TO THE FACULTY OF GRADUATE STUDIES AND RESEARCH
IN PARTIAL FULFILLMENT OF THE REQUIREMENTS FOR THE DEGREE
OF

MASTER OF SCIENCE

DEPARTMENT OF CIVIL ENGINEERING

EDMONTON, ALBERTA
SPRING, 1991

National Library
of Canada

Canadian Theses Service

Ottawa, Canada
K1A 0N4

Bibliothèque nationale
du Canada

Service des thèses canadiennes

The author has granted an irrevocable non-exclusive licence allowing the National Library of Canada to reproduce, loan, distribute or sell copies of his/her thesis by any means and in any form or format, making this thesis available to interested persons.

The author retains ownership of the copyright in his/her thesis. Neither the thesis nor substantial extracts from it may be printed or otherwise reproduced without his/her permission.

L'auteur a accordé une licence irrévocable et non exclusive permettant à la Bibliothèque nationale du Canada de reproduire, prêter, distribuer ou vendre des copies de sa thèse de quelque manière et sous quelque forme que ce soit pour mettre des exemplaires de cette thèse à la disposition des personnes intéressées.

L'auteur conserve la propriété du droit d'auteur qui protège sa thèse. Ni la thèse ni des extraits substantiels de celle-ci ne doivent être imprimés ou autrement reproduits sans son autorisation.

ISBN 0-315-66625-0

Canada

GULF CANADA RESOURCES LIMITED
P.O. BOX 130, CALGARY, ALBERTA T2P 2H7 · TELEPHONE (403) 233-4000

RECEIVED
MAR 19 1991
CENTRE FOR FRONTIER
ENGINEERING RESEARCH

March 14, 1991

Centre for Frontier Engineering Research
200 Karl Clark Road
Edmonton, Alberta
T6N 1E2

ATTENTION: Duane DeGeer

Dear Mr. DeGeer:

RE: AUTHORIZATION FOR RELEASE OF FIGURE 2-1 IN DUANE DEGEER'S MASTER OF SCIENCE THESIS

This letter hereby provides authorization for use of Figure 2-1 with the proviso the title is changed as suggested in the attached letter from Chris Graham. The reference should be modified to reflect work completed by EBA Engineering Consultants Ltd. for Gulf under the appropriate title and text modified on page 10 to reflect "predicted strain profile". Additionally, the reference to Gulf Canada Corporation in the acknowledgement section should be changed to Gulf Canada Resources Limited.

It looks like an excellent report. Good luck!

Yours truly,

Brian Varcoe

Brian Varcoe
Supervisor,
Drilling Operations Projects

BV/lb

C-102(6-87)

INTER-OFFICE MEMO

TO: Brian E. Varcoe
17th floor

Major Projects Department
Frontier Development Division
Technical Services

12 March 1991

RE: RELEASE OF FIGURE FOR PUBLICATION IN DUANE DEGEER'S MASTER OF SCIENCE THESIS

Figure 2.1 of the draft thesis has been taken from a 1987 C-FER report to Gulf, which was in turn taken from a 1985 EBA Engineering Consultants Ltd. report titled "Thaw Subsidence Analysis for East Amauligak". Both studies were funded by Gulf and the Amauligak partners.

The figure is such an isolated and small piece of information from an old, now dated, report that I believe Gulf can release this information without formally informing the Amauligak partners.

Please ask Duane to change the works "Expected Strains" to "Computed Strains" in the figure title. As discussed, the text on page 10 should state that Figure 2.1 is a predicted strain profile based on assumed stratigraphic and permafrost conditions. As you are aware, the Amauligak 3-F24 corehole found permafrost with higher ice contents at depth than had been assumed for the 1985 study.

In summary this memo provides permission for you to release the figure in question subject to the changes noted above. Those changes are required to prevent the figure from being misleading to future readers.

Chris A. Graham

CAG\ts

cc: File ______

(WP-L-M-MAR12.CAG\ts)

UNIVERSITY OF ALBERTA

RELEASE FORM

NAME OF AUTHOR: DUANE DONALD DEGEER

TITLE OF THESIS: COLLAPSE STRENGTH OF CYLINDERS SUBJECT TO AXIAL TENSION AND EXTERNAL PRESSURE

DEGREE: MASTER OF SCIENCE

YEAR THIS DEGREE GRANTED: SPRING, 1991

PERMISSION IS HEREBY GRANTED TO THE UNIVERSITY OF ALBERTA LIBRARY TO REPRODUCE SINGLE COPIES OF THIS THESIS AND TO LEND OR SELL SUCH COPIES FOR PRIVATE, SCHOLARLY OR SCIENTIFIC RESEARCH PURPOSES ONLY.

THE AUTHOR RESERVES OTHER PUBLICATION RIGHTS, AND NEITHER THE THESIS NOR EXTENSIVE EXTRACTS FROM IT MAY BE PRINTED OR OTHERWISE REPRODUCED WITHOUT THE AUTHOR'S WRITTEN PERMISSION.

SIGNED: D. DeGeer

PERMANENT ADDRESS: 104, 1415 LAKEWOOD RD. W.
EDMONTON, AB
T6K 3L2

DATED: APRIL 25, 1991

UNIVERSITY OF ALBERTA

FACULTY OF GRADUATE STUDIES AND RESEARCH

THE UNDERSIGNED CERTIFY THEY HAVE READ, AND RECOMMEND TO THE FACULTY OF GRADUATE STUDIES AND RESEARCH FOR ACCEPTANCE, A THESIS ENTITLED COLLAPSE STRENGTH OF CYLINDERS SUBJECT TO AXIAL TENSION AND EXTERNAL PRESSURE, SUBMITTED BY DUANE D. DEGEER IN PARTIAL FULFILLMENT OF THE REQUIREMENTS FOR THE DEGREE OF MASTER OF SCIENCE.

Dr. J.J. Cheng

Dr. A.E. Elwi

JR Colbourne

Dr. J.R. Colbourne

DATE: April 23, 1991

ABSTRACT

This report presents the results of a study involving the inelastic buckling capacity of cylindrical tubes subject to the load combination of axial tension and external pressure.

The problem originates from frequent collapse of casing in downhole oil and gas producing wells drilled in Arctic environments. The environmental loads on a casing string encountered in the Arctic are permafrost thaw subsidence, imposing large axial loads on the casing, coupled with external pressure loads caused by gas hydrate decomposition. This load combination may extend the casing material behaviour into the plastic range and create an unstable casing string, failing at load levels below those anticipated.

Presented is an improved method of determining the collapse strength of cylinders. The load combination considered is external pressure in combination with constant axial load. The accuracy of the improved method was benchmarked against a large data base of test results gathered in a literature review. A good correlation was found between the predicted strengths in comparison to the test results.

ACKNOWLEDGEMENTS

The author would like to express his appreciation for the effort, guidance, and support offered by Dr. J. J. Cheng, supervisor of the project, and the Department of Civil Engineering. Thanks is also extended to Dr. P. F. Adams for his thoughtful insights and initiation of the study.

The interest in the project and information provided by Gulf Canada Resources Limited is also gratefully acknowledged.

Also acknowledged is the interest and financial support provided by the Centre for Frontier Engineering Research.

TABLE OF CONTENTS

Page

Abstract iv
Acknowledgements v
Table of Contents vi
List of Tables viii
List of Figures ix
List of Symbols xiv

1.0 INTRODUCTION 1

1.1 Statement of the Problem 1
1.2 Objective and Scope 3
1.3 Outline 5

2.0 BACKGROUND 7

2.1 Conditions Unique to the Arctic 7
  2.1.1 Permafrost Thaw Subsidence 7
  2.1.2 Natural Gas Hydrate Decomposition 11
  2.1.3 Summary 12
2.2 Instability of Cylindrical Tubes 13
2.3 Factors Affecting Collapse Strength 16
  2.3.1 Material Anisotropy 17
  2.3.2 Residual Stresses 18
  2.3.3 Poisson's Ratio 21
  2.3.4 L/D Effects 23
  2.3.5 Geometric Imperfections 27
    2.3.5.1 Ovality 29
    2.3.5.2 Eccentricity 30

3.0 PAST WORK 37

3.1 Analysis Methods 37
  3.1.1 Elastic Ring Buckling Equation 37
  3.1.2 Tangent Modulus Approach 37
  3.1.3 Reduced Modulus Approach 40
  3.1.4 Pattillo and Huang (1982) 41
  3.1.5 Gerard (1957) 43
3.2 Design Methods 45
  3.2.1 American Petroleum Institute 45
  3.2.2 Other Design Methods 49
3.3 Test Results 53
  3.3.1 Edwards and Miller (1939) 53
  3.3.2 Stuiver and Tomalin (1959) 55
  3.3.3 Tamano et al. (1982) 56
  3.3.4 Gulf Canada (1987) 59
  3.3.5 Madhavan (1988) 61

Page

3.4 Discussion of Test Results 64
  3.4.1 General 64
  3.4.2 Constant Axial Load Tests 65
3.5 Evaluation of Design and Prediction Methods 67
  3.5.1 Design Methods 69
  3.5.2 Prediction Methods 70

4.0 DERIVATION OF PREDICTION METHOD 112

4.1 Prediction Method 112
  4.1.1 Plasticity Reduction Factor.................114
  4.1.2 Capacity Reduction Factor 118
    4.1.2.1 Tokimasa and Tanaka (1986) 119
    4.1.2.2 Nishioka et al. (1976) 120
    4.1.2.3 Proposed Capacity Reduction Factor 121
    4.1.2.4 Comparison to Test Data 121
4.2 Summary 124

5.0 PARAMETER STUDY 143

5.1 Effect of Inelastic Stiffness 143
5.2 Effect of Yield Stress 145
5.3 Effect of OD/t Ratio 146
5.4 Effect of Ovality 147
5.5 Summary 147

6.0 SUMMARY, CONCLUSIONS, AND RECOMMENDATIONS 153

6.1 Summary 153
6.2 Conclusions 153
6.3 Collapse Prediction Recommendation 155
6.4 Future Research Work 156

REFERENCES 158

LIST OF TABLES

Table **Page**

3.1 API Design Methods 74

3.2 API BUL 5C3 (1985) Minimum Collapse Equations (Units are in psi) 74

3.3 Summary of the Ramberg-Osgood Parameters Used to Model the Test Data Material Properties 75

3.4 Averages and Coefficient of Variations (COV), in percent, for the Test/Predicted Ratios 76

4.1 Ovalities Given for Tamano et al. (1982) and Gulf Canada (1987) Test Data 126

4.2 Averages and Coefficient of Variations for the Test/Predicted Ratio's Using Different Capacity Reduction Factors 127

LIST OF FIGURES

Figure **Page**

1.1 Thaw Subsidence Effect on a Casing String 6

2.1 Computed Strains on a Casing String Over a 30 Year Period 32

2.2 Typical Temperature/Pressure Boundary for Decomposition of Methane Hydrates 33

2.3 Buckling Paths for Perfect and Imperfect Systems with Post-Buckling Instability 34

2.4 Variation of Poisson's Ratio with Axial Strain 35

2.5 Collapse Pressure Reduction Factor for Varying Ovality 36

3.1 Basic Assumptions Behind the Reduced Modulus Theory (Timoshenko and Gere, 1961) 77

3.2 Comparison of Different Reduced Modulus Equations 78

3.3 European Recommendations for Steel Construction Relationship Between λ and P_{cr} 79

3.4 Collapse Chamber for Edwards and Miller (1939) 50mm Tubing 80

3.5 Edwards and Miller (1939) Test Group 6 (OD/t = 16.6) 81

3.6 Edwards and Miller (1939) Test Group 7 (OD/t = 21.7) 82

3.7 Edwards and Miller (1939) Test Group 8 (OD/t = 17.3) 83

3.8 Edwards and Miller (1939) Test Group 9 (OD/t = 11.2) 84

3.9 Edwards and Miller (1939) Test Group 10 (OD/t = 21.7) 85

3.10 Edwards and Miller (1939) Test Group 11 (OD/t = 17.3) 86

3.11 Edwards and Miller (1939) Test Group 12 (OD/t = 11.2) 87

3.12 Collapse Chamber for Stuiver and Tomalin (1959) 25mm Tubing 88

Figure **Page**

3.13 Stuiver and Tomalin (1959) Test Group 1 (OD/t = 27.0) 89

3.14 Stuiver and Tomalin (1959) Test Group 2 (OD/t = 23.5) 90

3.15 Collapse Chamber for Tamano et al. (1982) 178mm Casing.................................. 91

3.16 Tamano et al. (1982) Test Group K55-1 (OD/t = 25.3) 92

3.17 Tamano et al. (1982) Test Group K55-2 (OD/t = 21.8) 93

3.18 Tamano et al. (1982) Test Group K55-3 (OD/t = 18.9) 94

3.19 Tamano et al. (1982) Test Group N80-1 (OD/t = 22.0) 95

3.20 Tamano et al. (1982) Test Group N80-2 (OD/t = 19.3) 96

3.21 Tamano et al. (1982) Test Group N80-3 (OD/t = 15.2) 97

3.22 Tamano et al. (1982) Test Group N80-4 (OD/t = 12.6) 98

3.23 Tamano et al. (1982) Test Group P110-1 (OD/t = 19.4) 99

3.24 Tamano et al. (1982) Test Group P110-2 (OD/t = 15.8) 100

3.25 Tamano et al. (1982) Test Group P110-3 (OD/t = 12.8) 101

3.26 Collapse Chamber for Gulf Canada (1987) 169mm Casing.................................. 102

3.27 Gulf Canada (1987) Test Group 1 (OD/t = 23.8) 103

3.28 Gulf Canada (1987) Constant Axial Strain Test Data (OD/t = 23.8 and 30.7).............. 104

3.29 Schematic of Madhavan (1988) Test Apparatus 105

3.30 Madhavan (1988) Test Group 1, Stainless Steel (OD/t = 36.7) 106

3.31 Madhavan (1988) Test Group 2, Stainless Steel (OD/t = 24.5) 107

Figure **Page**

3.32 Madhavan (1988) Test Group 3, Stainless Steel (OD/t = 18.7) 108

3.33 Madhavan (1988) Test Group 4, Stainless Steel (OD/t = 12.1) 109

3.34 Madhavan (1988) Test Group 5, Stainless Steel (OD/t = 27.3) 110

3.35 Madhavan (1988) Test Group 6, Aluminum (OD/t = 12.2) 111

4.1 Exaggerated Deformed Shape of the Cylinders and Distribution of the Inelastic Region 128

4.2 CRF Comparison for Edwards and Miller (1939) Test Group 6 (OD/t = 16.6) 129

4.3 CRF Comparison for Edwards and Miller (1939) Test Group 7 (OD/t = 21.7) 129

4.4 CRF Comparison for Edwards and Miller (1939) Test Group 8 (OD/t = 17.3) 130

4.5 CRF Comparison for Edwards and Miller (1939) Test Group 9 (OD/t = 11.2) 130

4.6 CRF Comparison for Edwards and Miller (1939) Test Group 10 (OD/t = 21.7) 131

4.7 CRF Comparison for Edwards and Miller (1939) Test Group 11 (OD/t = 17.3) 131

4.8 CRF Comparison for Edwards and Miller (1939) Test Group 12 (OD/t = 11.2) 132

4.9 CRF Comparison for Stuiver and Tomalin (1959) Test Group 1 (OD/t = 27.0) 132

4.10 CRF Comparison for Stuiver and Tomalin (1959) Test Group 2 (OD/t = 23.5) 133

4.11 CRF Comparison for Tamano et al. (1982) Test Group K55-1 (OD/t = 25.3) 133

4.12 CRF Comparison for Tamano et al. (1982) Test Group K55-2 (OD/t = 21.8) 134

4.13 CRF Comparison for Tamano et al. (1982) Test Group K55-3 (OD/t = 18.9)................ 134

4.14 CRF Comparison for Tamano et al. (1982) Test Group N80-1 (OD/t = 22.0) 135

4.15 CRF Comparison for Tamano et al. (1982) Test Group N80-2 (OD/t = 19.3) 135

Figure **Page**

4.16 CRF Comparison for Tamano et al. (1982) Test Group N80-3 (OD/t = 15.2) 136

4.17 CRF Comparison for Tamano et al. (1982) Test Group N80-4 (OD/t = 12.6) 136

4.18 CRF Comparison for Tamano et al. (1982) Test Group P110-1 (OD/t = 19.4) 137

4.19 CRF Comparison for Tamano et al. (1982) Test Group P110-2 (OD/t = 15.8) 137

4.20 CRF Comparison for Tamano et al. (1982) Test Group P110-3 (OD/t = 12.8) 138

4.21 CRF Comparison for Gulf Canada (1987) Test Group 1 (OD/t = 23.8) 138

4.22 CRF Comparison for Madhavan (1988) Test Group 1 (OD/t = 36.7) 139

4.23 CRF Comparison for Madhavan (1988) Test Group 2 (OD/t = 24.5) 139

4.24 CRF Comparison for Madhavan (1988) Test Group 3 (OD/t = 18.7) 140

4.25 CRF Comparison for Madhavan (1988) Test Group 4 (OD/t = 12.1) 140

4.26 CRF Comparison for Madhavan (1988) Test Group 5 (OD/t = 27.3) 141

4.27 CRF Comparison for Madhavan (1988) Test Group 6 (OD/t = 12.2) 141

4.28 Test/Predicted Ratios in Relation to the OD/t Ratio 142

4.29 Test/Predicted Ratios in Relation to the σ_z/σ_y Ratio 142

5.1 Stress Strain Curves for the Variation in Inelastic Stiffness 149

5.2 Predicted Collapse Pressures for the Variation in Inelastic Stiffness 149

5.3 Stress Strain Curves for the Variation in Yield Strength 150

5.4 Predicted Collapse Pressures for the Variation in Yield Strength 150

5.5 Stress Strain Curve for the Variation in OD/t Ratio 151

Figure **Page**

5.6 Predicted Collapse Pressures for the Variation in OD/t Ratio 151
5.7 Stress Strain Curve for the Variation in Ovality 152
5.8 Predicted Collapse Pressures for the Variation in Ovality 152

LIST OF SYMBOLS

A = parameter for the reduction factor for ovality

a = API RP 2A (1982) buckling stress coefficient

α = capacity reduction factor (CRF)

α_{11} = Pattillo and Huang (1982) buckling parameter

α_{12} = Pattillo and Huang (1982) buckling parameter

α_{22} = Pattillo and Huang (1982) buckling parameter

α_m = modified capacity reduction factor

API = American Petroleum Institute

B = parameter for the reduction factor for ovality

b = API RP 2A (1982) buckling stress coefficient

COV = Coefficient of Variation, = standard deviation/ mean

CRF = capacity reduction factor

D = average diameter, = (OD-t)

Δ = ovality

δ = elastic volume change

D/t = average diameter/thickness ratio, = (OD/t-1)

Δ_2 = ovality

E = elastic modulus

ε = strain or effective strain

E_r = reduced modulus

E_s = secant modulus, = σ/ε

E_t = tangent modulus, = slope of the stress strain curve

ε_z = strain in the axial direction

η = plasticity reduction factor (PRF)

η_m = plasticity reduction factor (PRF) for a cylinder of moderate length

κ = residual stress parameter, = 1-2/(OD/t)

kN = KiloNewton

L = axial length

Λ = design buckling parameter

λ = buckling parameter from the European Recommendations for Steel Construction (1984)

L/D = axial length/average diameter ratio

L/OD = axial length/average outside diameter ratio

mm = millimetre

MPa = MegaPascal, = one Newton per square millimetre

ν = Poisson's ratio, elastic or plastic

n = Ramberg-Osgood hardening parameter

ν_e = elastic Poisson's ratio

ν_{inel} = Ratzlaff's (1985) inelastic Poisson's ratio

ν_p = plastic Poisson's ratio

OD = average outside diameter

OD/t = average outside diameter/thickness ratio

OD_{max} = maximum value of the outside diameter

OD_{min} = minimum value of the outside diameter

$OD_{nominal}$ = nominal value of the outside diameter

OR = average outside radius

p = applied pressure

P_c = critical collapse pressure used in the proposed collapse prediction method

P_{cr} = critical collapse pressure

P_e = elastic collapse pressure for a cylinder of infinite length

P_y = pressure causing first material yield, $= 2\sigma_y/(D/t)$

P_{el} = elastic collapse pressure for a cylinder influenced by length

PRF = plasticity reduction factor

R = average radius

ρ = DnV buckling imperfection parameter

r_Δ = reduction factor for ovality

$r_{\Delta,\Xi}$ = reduction factor for ovality and eccentricity

r_Ξ = reduction factor for eccentricity

σ = effective stress

$\sigma_{\alpha,\eta}$ = buckling stress, accounting for the effects of the capacity reduction factor and plasticity reduction factor

σ_{cr} = critical buckling stress

$\sigma_{e,\alpha}$ = elastic buckling stress, accounting for the effects of the capacity reduction factor (CRF)

σ_{max} = maximum stress value

σ_p = proportional limit

S_θ = circumferential anisotropic parameter

σ_θ = stress in the circumferential direction

$\sigma_{R\theta,OP}$ = optimum value of the circumferential residual stress

σ_y = yield stress, = stress at 0.5% strain

$\sigma_{y,r}$ = yield stress, reduced by the effects of axial load

$\sigma_{y\theta}$ = yield stress in the circumferential direction

σ_{yz} = yield stress in the axial direction

σ_z = stress in the axial direction

t = average thickness

t_{max} = maximum thickness

t_{min} = minimum thickness

Ξ = eccentricity

$f(\sigma_{ij})$ = yield surface function

1.0 INTRODUCTION

1.1 Statement of the Problem

As the development of petroleum reserves in Arctic regions continues, present engineering technology must be enhanced to overcome unique problems associated with the North. One such problem is the thaw-subsidence of soil, or soil compaction, around a producing well drilled through permafrost. As warm oil is produced, ice in the surrounding soil melts, providing a soil volume decrease, subsequent compaction, and pore pressure reduction, imposing large downdrag forces on the casing. These forces, along with the loss of lateral support of the soil around the casing can produce abnormally high compressive strains through the thawing stratum, while the casing above and below the thaw zone may be subjected to tension. Depending on the relative compressibility of the various soil layers, the strains induced in the casing can be extremely large, deforming segments of the casing well into the inelastic range. Figure 1.1 illustrates the permafrost thaw effect on the casing string for varying soil layers of sand and silt.

In certain zones of the thaw annulus, the decomposition of gas hydrates over time may take place, causing external pressures on the casing. This pressure, coupled with the imposed axial strains which have already yielded portions of the casing, creates a severe loading effect on the casing. Instability and subsequent failure may occur at load levels below those anticipated.

Considerable research has been directed towards understanding the behaviour of cylindrical shells subject to external pressure, and solutions do exist that predict the external pressure causing collapse. The major problem, however, occurs with the addition of axial strains. These strains, acting along the length of the cylindrical shell, reduce its ability to resist the applied external pressures. A local buckling motion in a direction perpendicular to the casing length may result due to the reduced effective strength of the casing. Unfortunately, little information exists on the effect these axial loads have on the collapse resistance of cylindrical shells, particularly under loads that deform the shell well past its yield value.

This study was initiated by a need for a better understanding of the collapse strength of cylindrical tubes subject to axial tension and external pressure in order to accurately predict casing collapse. Identifying and understanding the casing behaviour under these unique conditions is essential for the determination of its collapse strength. A prediction method is proposed that determines the collapse strength of cylindrical shells, and its accuracy is benchmarked to test results for all types of cylindrical shells, including casing.

The problem of cylinder collapse under combinations of load is a general one, and the work performed in this study, along with the solutions presented, can be used to address problems which undergo similar loading situations. Examples include high pressure containers, deep submersibles, pipelines (both onshore and offshore), and underground protective conduits.

1.2 Objective and Scope

Previous prediction and design methods have been centred towards empirically based procedures to assess casing strength. As well, some experimental programs have been accompanied by analytical solutions to predict their test results, but they do not necessarily consider all the factors which affect casing collapse strength, nor do they accurately predict the test results obtained from other work. Several factors contribute to these inconsistencies, including experimental variations and interpretation of the results obtained.

The objective of this study is to assess past work in this area, investigate the experimental differences and results obtained from the previous tests, evaluate the prediction and design methods currently available, and derive an accurate analytical procedure for determining the collapse strength of cylindrical tubes subject to axial tension and external pressure.

A large data base of previous test results has been developed in order to assess the predictive reliability of the analytical procedure presented in this study. The test results in this data base were performed under various loading and environmental conditions, and include many of the parameters which have a significant effect on the collapse strength of cylindrical tubes. These parameters include diameter-to-thickness (D/t) ratio, material yield strengths, material stiffness (both elastic and inelastic), initial geometric imperfections, and axial tension (both constant load and constant deformation).

The D/t ratio ranges from 10 to 36 in the test results obtained, representing a realistic range of values that might be expected in a casing string. Complete effective stress strain curves characterizing the material behaviour are utilized, ranging from an elastic-perfectly plastic material to those with significant post yield stiffness. The axial tension ranges from zero to values in excess of yield, for both the constant axial load and constant axial deformation conditions.

1.3 Outline

Background information is provided in Chapter 2 to give the reader a general knowledge of the permafrost thaw subsidence and gas hydrate decomposition phenomena, and of the type of loads they might realistically place on a casing string drilled in the Arctic. Chapter 2 also provides background information on the buckling of cylindrical tubes, and the factors that affect collapse resistance. Chapter 3 describes in detail the previous test procedures and results used in this study, along with several design methods currently in use, and methods for predicting the collapse strength of cylindrical tubes under the loading conditions specific to this study. The information in Chapter 3 is used in Chapter 4 to derive an appropriate analytical procedure for estimating the casing collapse strength, comparing this procedure with the past test results. Chapter 5 includes a parametric study, evaluating the effects of the different variables on collapse resistance. Chapter 6 summarizes the findings of this study and outlines the important conclusions drawn from the work performed.

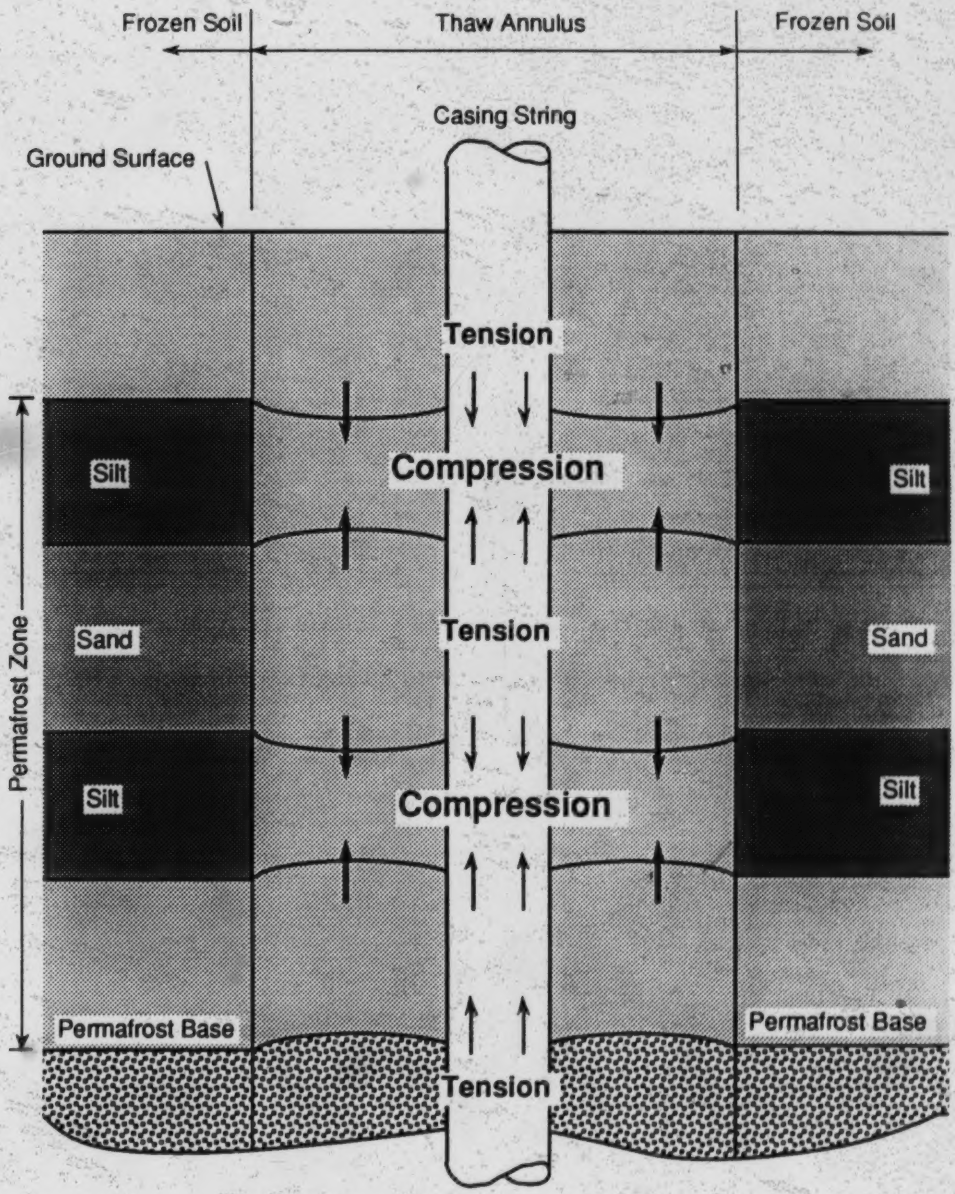
Frozen Soil
Thaw Annulus
Frozen Soil
Casing String
Ground Surface
Tension
Compression
Tension
Compression
Tension
Silt
Sand
Silt
Silt
Sand
Silt
Permafrost Zone
Permafrost Base
Permafrost Base

Figure 1.1 - Thaw Subsidence Effect on a Casing String

2.0 BACKGROUND

2.1 Conditions Unique to the Arctic

2.1.1 Permafrost Thaw Subsidence

Simply stated, permafrost is permanently frozen soil with ice occupying the pore spaces. Permafrost can be continuous from the surface, or discontinuous with intermittent unfrozen soil layers in between. In Canada, approximately 50% of the land surface is underlain by permafrost (Hnatiuk and Randall, 1977), with depths ranging from a few metres (discontinuous zone) to several hundred metres (continuous zone). In the Mackenzie Delta area, where oil and gas reserves are known to exist, the permafrost layer begins at approximately 150 metres below ground level and continues down to about 600 metres.

Permafrost thaw subsidence is the soil compaction due to the thawing of the ice in the soil pores resulting from a temperature increase, such as that provided by a producing well. It is possible that a frozen soil which is fully consolidated will not compact, nor produce strain in a casing string. However, most in situ soils, frozen or unfrozen, are not fully consolidated and deformations in the soil can result from thaw subsidence.

The type of permafrost can be described by its lithology and mechanical properties, both of which are parameters influencing thaw subsidence that cannot be controlled. The lithology is the layer arrangement, thickness and layer position of the soil types relative to one another. Mitchell and Goodman (1976) indicate that a lithology with layers will produce larger strains during permafrost thaw subsidence than a uniform lithology without layers. This means that a lithology consisting of alternating layers of compressible and noncompressible materials (such as the silt and sand arrangement shown previously in Figure 1.1) will produce alternating tensile and compressive strains along the length of the casing, with the highest strain magnitudes occurring when the layers are about three metres thick. For thinner layers, the loads producing the strains are low and the casing resistance prohibits thaw subsidence. In larger layers, large strain magnitudes cannot develop due to the increased difficulty for vertical compaction to occur over the large depth, particularly when the thaw radius around a producing well is small (a typical thaw zone is roughly cylindrical and, after about 20 years of production, the radius of the cylinder is less than 2% of the length (Mitchell and Goodman, 1976)). For a larger thaw radius, however, such as that found around multiple wellbores, vertical compaction is not so difficult, and the maximum strains may occur in layer thicknesses greater than 3 metres.

Generally, the compressive strains will occur in the more compressible layers, such as silt, while the tensile strains will occur in the non-compressible layers, such as sand. Mitchell and Goodman (1976) determined that, for alternating sand and silt layer thicknesses of about 3 metres, the strain attained will be about 90% of the soil's maximum possible value. They also indicate that localized compressive strains are highest when an isolated layer of silt is embedded in a thick sand layer, while the highest tensile strains in casing result from a multi-layered sand/silt system.

Parameters influencing thaw subsidence that can be controlled in the drilling and completion operations include production time, amount of insulation used to surround the wellbore, and the proximity of nearby wellbores that contribute to the overall thaw area (Hirshberg et al., 1988). When a thaw zone from a single wellbore is overlapped with other zones, a large overall thaw area is produced. Hirshberg et al. (1988) mentions that currently proposed wellhead spacings as close as 4.6 metres for offshore islands are expected to produce higher soil strains than those predicted for original Prudhoe Bay wells spaced about 37 metres apart.

From a casing design standpoint, the axial load in a casing string resulting from the thawing of permafrost around a production well drilled in the arctic is perhaps the single most important factor influencing well design. Information on the soil and permafrost thaw conditions at specific drilling locations in the Arctic region is generally regarded as proprietary, and in most cases one can only generalize about certain conditions. However, Mitchell and Goodman (1976) indicate that the permafrost thaw mechanism may impose on the casing assembly axial strains as high as 1%, placing the casing material well into its inelastic range of material behaviour. Also, Figure 2.1 shows a predicted strain profile obtained from Gulf Canada (1987) for a well in the Beaufort Sea area, based on assumed stratigraphic and permafrost conditions. This Figure indicates that vertical strains as high as 1.1% in tension and 0.7% in compression might be developed over a thirty year period. A close examination of Figure 2.1 also tells us that the permafrost lithology is generally layered, with alternating zones of compression and tension.

2.1.2 Natural Gas Hydrate Decomposition

Gas hydrates are solid, ice-like mixtures of natural gas and water that can occupy the pore spaces of soil and rocks in regions where natural gas and water coexist in cool, high pressure environments. The hydrate structure consists of gas molecules surrounded by a latticework of water molecules held together by hydrogen bands.

Bily and Dick (1974) have identified gases in the hydrate form under the permafrost in the Mackenzie Delta at least 600 metres below the surface. The cap of the hydrate zone is generally at the base of the permafrost and, in the Prudhoe Bay area, may extend tens of kilometres vertically and laterally.

While these natural gas hydrates are looked upon by some as a source of recoverable gas (Makogon, 1981), they are generally thought of as a hinderance to oil drilling and production operations at greater depths. Figure 2.2 shows the boundary for which hydrates begin to decompose, varying with pressure and temperature. The hydrate in its in situ state does not present a problem, but, as production proceeds and warm oil passes up through the wellbore in the hydrate zone, pressure and temperature changes may decompose the hydrate, increasing its volume many times. This change results in a zone around the wellbore that is under extreme pressure. This produces an external pressure on the casing assembly that can be as high as 25 MPa depending on the specific pressure and temperature conditions (Bily and Dick, 1974; Goodman, 1977). In some instances, however, this pressure is allowed to release. Some release mechanisms to consider are fracturing of the overlying formation, pressure release along the cement-soil interface of the producing well, general elastic expansion of the soil, or pressure flow through the soil acting as a porous membrane.

Given the soil type and conditions in the Beaufort Sea area, it is felt that a pressure release mechanism formation is entirely possible, and that the 25 MPa pressure value suggested by Bily and Dick (1974) represents an absolute maximum. A more realistic value for the external pressure applied to a casing assembly would be in the 10-15 MPa range. A pressure of 14 MPa is suggested by Goodman (1977) if there is no permeable path for fluid or pressure relief.

2.1.3 Summary

Gas hydrates exist in the Beaufort Sea-Mackenzie Delta area, and can be found just below the permafrost base. In view of Figure 2.1, the base of the permafrost is a location of high axial tensile strains as a result of the permafrost thaw subsidence. This tension, coupled with the external pressure generated from gas hydrate decomposition, creates a severe loading condition which may result in an unstable casing string. Buckling and subsequent failure may occur.

This unique loading condition and the resulting field problems with casing failure have provided the motivation for this study.

2.2 Instability of Cylindrical Tubes

An oil well casing string can undergo two basic types of failure modes: that of an ultimate strength failure, or failure modes related to structural instability. An ultimate strength failure implies that the material strength of the structural member has been attained and can no longer resist any increases in load. Instability of a structural member is a condition where that member loses its ability to resist increasing compressive loads and a decrease in load carrying capacity results (Galambos, 1988). Instability occurs at the maximum point on the load deflection curve, and may not necessarily correspond to the point of maximum material strength.

Instability can further be subdivided into two categories: bifurcation of equilibrium and limit load instability. A limit load instability will exhibit a single mode of deformation up to its maximum load without any bifurcation. Examples of this category of instability include the buckling of shallow arches and spherical caps, where a symmetric mode of deformation is present until the limit load point is attained, and collapse occurs. A member which buckles as a result of bifurcation will initially deform in one mode and, at the bifurcation point, suddenly change to another deformation mode. When subjected to circumferential compression, geometrically perfect cylindrical shells will experience bifurcation buckling, where the initial axisymmetric mode of deformation changes to a non-axisymmetric mode at the bifurcation point.

Madhavan (1988) and Thompson and Hunt (1983) indicate that the presence of initial geometric imperfections (in the form of eccentricities and ovalities) and subsequent material yielding changes the response of the tube, and collapse occurs when a limit point is reached along the elastic-plastic equilibrium path. If the tube is imperfection sensitive (that is, sensitive to initial geometric imperfections such as ovality), these imperfections lower the limit load to below the bifurcation load.

Figure 2.3 illustrates the different buckling paths for perfect and imperfect systems which exhibit imperfection sensitivity. A perfect member (no imperfections) will trace the path of the dashed line in Figure 2.3 and bifurcate at the buckling load. An imperfect member will exhibit a limit load instability which is lower than the bifurcation point, and trace the path of the solid line in Figure 2.3. A limit load buckling response is followed by unstable postbuckling behaviour. Under a load controlled situation, this limit load corresponds to the collapse load.

The other factors which affect the value of the collapse load of a cylinder with initial imperfections are the material properties and D/t ratio. The imperfections have less influence on cylinders with low D/t ratios that buckle inelastically than on those that buckle elastically (Galambos (1988)). The material properties of the tube affect the ultimate capacity by way of its stiffness and yield strength.

Geometry differences and boundary conditions will also affect the buckling strength of cylindrical tubes. They may change the number of circumferential waves that develop at buckling by preventing the lower energy buckling modes from occurring. An example of this is how the length-to-diameter (L/D) ratio affects a tube's buckling strength when the ends are prevented from deflecting radially. If the L/D ratio is large, the end effects are insignificant in the middle of the tube and buckling under external pressure will exhibit two circumferential waves, or an ovalized shape. This is the minimum energy buckling mode. If, however, the L/D ratio is small, buckling in two circumferential waves is prevented and a higher buckling mode will develop as the external pressure is increased. Radial and longitudinal stiffeners on a cylindrical tube also increase the buckling strength in the same manner.

2.3 Factors Affecting Collapse Strength

Examples of factors affecting collapse strength are the loading condition, material behaviour (yield strength, elastic and inelastic stiffness), and geometric parameters like D/t (ratio of the outside tube diameter to its mean thickness). These factors are taken into account in most analyses, and their effect on collapse will be discussed later in the parameter study.

The effects of other factors, though, like material anisotropy, residual stresses, Poisson's ratio, L/D and initial geometric imperfections are not always considered in theoretical derivations. These factors may significantly affect cylinder collapse resistances, and are worthy of some discussion.

2.3.1 Material Anisotropy

Tube material anisotropies, mostly in the form of yield strength differences in the axial and circumferential directions, are due primarily to the manufacturing process. Cold drawing of small stainless steel tubes often creates an axial/circumferential yield strength ratio of up to 1.29 (Madhavan, 1988), while normalizing a material tends to create a near isotropic tube. The coupon testing of tubes for material properties is usually performed in the longitudinal direction. If the yield strength in the circumferential direction is less, lower collapse strengths than predicted may result.

Yeh and Kyriakides (1986a) discuss anisotropy and, along with Madhavan (1988), outline a method to account for material yield strength differences, adopted from an anisotropic plasticity model first developed by Hill (1950). The method assumes an isotropic elastic deformation, but that the yield stress is different in the three principal directions (this assumes that material properties are known in the axial, radial, and circumferential directions). Basically, the yield function developed for a biaxial loading condition takes the form:

$$f(\sigma_{ij}) = \sqrt{\sigma_z^2 - \left(\frac{1}{S_\theta^2}\right)\sigma_z\sigma_\theta + \frac{1}{S_\theta^2}\sigma_\theta^2} = \sigma_{max} \qquad [2.1]$$

where σ_{max} is the maximum value of stress along the uniaxial stress strain curve, σ_z and σ_θ are the axial and circumferential stresses, and S_θ is the circumferential anisotropic parameter, given by:

$$S_\theta = \frac{\sigma_{y\theta}}{\sigma_{yz}} \qquad [2.2]$$

where $\sigma_{y\theta}$ and σ_{yz} are the yield strengths in the circumferential and axial directions.

An incremental method is used to solve the equilibrium equations for the cylinder collapse problem. By assigning a value of one to S_θ, the equations reduce to the von Mises effective stress formulation for an element that is biaxially stressed in two principal directions.

2.3.2 Residual Stresses

The effect of residual stresses on tube collapse strength is discussed by numerous authors, most notably Yeh and Kyriakides (1986a, 1986b), Simonen and Shippell (1982), Tokimasa and Tanaka (1986), Mimura et al. (1987), and Mehdizadeh (1975). Generally, the presence of residual stresses tends to reduce the collapse pressure. There are, however, some instances where residual circumferential stresses may increase collapse resistance.

Two manufacturing operations are mainly responsible for introducing residual stresses in the material of a cylinder: nonuniform rates of cooling as a result of quenching, and the cylinder straightening process. Quenching depends to a large extent on the chemical composition of the cylinder, the wall thickness, and the manufacturers' particular method of quenching. Straightening, however, is the main cause of residual stress formation. Mehdizadeh (1975) indicates that the main type of straightening used by manufacturers is of a rotary type. This type of straightening introduces residual stresses of up to 40% of the yield strength in the casing (Mehdizadeh, 1975). This magnitude of residual stress may reduce the collapse pressure by as much as 40%.

The effect of residual stresses increasing or decreasing the collapse resistance can be explained as follows: through the wall thickness of a casing, the circumferential stress distribution resulting from the application of an external pressure is not uniformly distributed. The magnitude of the circumferential stress at the inner surface of a casing under external pressure is considerably higher than that at the outer surface. Therefore, a casing with no residual stresses and under external pressure will yield at the inner surface before the outer surface. If residual stresses are present, and are compressive at the inner surface, the collapse resistance decreases since the inner surface reaches its yield stress at a lower external pressure value than if no residual stresses were present. The opposite is true for tensile residual stresses at the inner surface; the collapse resistance will be increased because the tensile stresses at the inner surface must be reduced to zero before compressive stresses can build up.

Mimura et al. (1987) and Tokimasa and Tanaka (1986) have also looked at the effect of residual stresses on casing collapse performance and have come up with an "optimum" residual stress, or the residual stress distribution through the casing wall thickness that produces the greatest collapse resistance. This theoretically occurs when all portions of the casing wall yield at the same external pressure load. The optimum circumferential residual stress of a perfectly round pipe is given by:

$$\sigma_{R\theta,OP} = \frac{1 - \kappa^4}{7/3 + 2\kappa^2 + \kappa^4}\,\sigma_P \qquad [2.3]$$

where:

$$\kappa = \frac{\text{inside diameter}}{\text{outside diameter}} = 1 - \frac{2}{OD/t} \qquad [2.4]$$

and σ_P is the proportional limit.

Using realistic casing values of OD/t and a linearly varying residual stress distribution through the casing wall thickness, Mimura et al. (1987) indicate that the optimum residual stress should be a tensile stress on the inner surface between 5 and 15% of the material proportional limit, and a compressive stress of the same value on the outer face of the casing.

Residual stresses appear to have the greatest effect on medium walled pipe, in which collapse occurs at a mean effective stress level just past the material proportional limit, assuming a uniform circumferential stress distribution. For thick walled pipes, the effect on collapse resistance is small because collapse occurs when the material has plastified considerably, and manufacturing attempts at optimizing the residual stresses in thick walled pipes may be ineffective. There is no effect of residual stresses on the elastic collapse of thin walled pipes when the critical collapse stress is below the proportional limit.

2.3.3 Poisson's Ratio

Generally, Poisson's ratio is assumed to be 0.3 for steel materials in the elastic range, and 0.5 (no volume change) past the elastic limit, assuming fully plastic behaviour. Ratzlaff (1985) refers to an equation developed by Stang et al. (1946) who derives the following expression for Poisson's Ratio in the inelastic range:

$$\nu_{inel} = \frac{1 - \sqrt{\frac{1 + \delta}{1 + \varepsilon}}}{\varepsilon} \qquad [2.5]$$

where ν_{inel} is the inelastic Poisson's ratio and δ is the volume change occurring prior to yielding.

For an isotropic material, MacKenzie et al. (1986) refers to Gerard's (1962) derivation and gives the relation for Poisson's ratio as:

$$\nu = \nu_p - \frac{E_s}{E}(\nu_p - \nu_e) \qquad [2.6]$$

where ν_p is the fully plastic Poisson's ratio, equal to 0.5, ν_e is the elastic Poisson's ratio (=0.3), and E_s is the secant modulus (= σ/ε). Figure 2.4 illustrates the variation in Poisson's ratio with strain using Equations 2.5 and 2.6, and the normally assumed values of 0.3 (elastic) and 0.5 (inelastic). Also shown is the stress strain curve assumed in the calculations.

The Ratzlaff (1985) curve in Figure 2.4 was based on a specific type of steel, and the volume changes were measured on an experimentally tested tension coupon. The reason for the downward trend of the curve is not known, but one might speculate that the steel began to fracture as it was nearing failure, changing the overall specimen volume. If this is the case, then different steels will perhaps exhibit different curves.

The difference between Gerard's (1962) curve and that of Ratzlaff's (1985) at the high strain levels is of little concern, however, because the effective strains at collapse in cylinders with OD/t ranging from 10 to 30 are typically less than about 4%.

The difference between these two curves and the theoretical 0.3 to 0.5 transition may relate to the differences in section yielding. A transition of Poisson's ratio may seem appropriate when analysing the cylinder section properties because portions of the tube are yielding while others are not, but the local buckling behaviour of cylinders subject to axial tension and external pressure may be influenced by local behaviour only. A comparison of the prediction methods in Chapter 3 to the test data using different Poisson's ratio models resulted in a better data fit when using the 0.3 to 0.5 transition method, and is the method that will be used in this study.

2.3.4 L/D Effects

A long circular cylinder subjected to external pressure will buckle in two circumferential waves, forming an oval shape. As the cylinder length decreases, the number of circumferential waves increases, and so does the collapse resistance of the cylinder. For very short cylinders approaching zero length, the behaviour corresponds to that of a long flat plate under longitudinal compression, with edge boundary conditions corresponding to those along the cylinder edges (Gerard, 1957). When a cylinder is considered "infinitely long", one can neglect the boundary conditions at the end of the cylinder, but when the cylinder is short, end effects must be taken into account.

The test results reported in Chapter 3 have been assumed to be unaffected by the end effects of the testing apparatus, and corresponding to the behaviour of an infinitely long cylinder. In other words, the cylinders were assumed long enough such that the radial restraint provided by the test apparatus end caps did not affect collapse results. Yeh and Kyriakides (1986a) concluded that a cylinder with a L/OD ≥ 12 was sufficient to assume negligible end effects. The critical length as given by Stuiver and Tomalin (1959), in reference to Southwell (1915), is:

$$\frac{L}{D} \geq 1.73 \sqrt{\frac{D}{t}} \qquad [2.7]$$

where L/D is the Length-to-Diameter ratio.

Using Equation 2.7 for D/t ranging from 10 to 25, the corresponding minimum L/D ranges from 5.47 to 8.65. Fowler et al. (1983) provides a theoretical solution for the effect of L/D on the elastic collapse pressure of a tube simply supported at the ends (free to rotate, but fixed radially) as:

$$p_{el} = p_e \left[1 + \frac{7 - \nu_e}{3\left(1 + \left\{ 4L/\pi D \right\}^2\right)^2} + \left(\frac{D}{t}\right)^2 \frac{1 - \nu_e^2}{3\left(1 + \left\{ 4L/\pi D \right\}^2\right)^2} \right] \qquad [2.8]$$

where p_{el} is the elastic collapse pressure for a cylinder of finite length buckling in two circumferential waves, and p_e is the elastic collapse pressure of a tube of infinite length. Using Equation 2.8, length effects are virtually negligible for $L/D \geq 8$. Tokimasa and Tanaka (1986) provide a similar equation to that of Equation 2.8, but indicate that the plastic collapse strength of casing is unaffected by L/D. The test results of Tamano et al. (1982) follow this pattern. Their test specimens had L/D values ranging from 6.4 to 6.8 (L/OD = 6.7), below the limits set above. Their collapse results, however, have been predicted reasonably well (as will be illustrated in Chapter 3), with no artificially high collapse strengths. This does not necessarily indicate that cylinders collapsing in the plastic range are unaffected by L/D, but it does indicate that the results reported by Tamano et al. (1982) were not influenced by end effects.

Theoretically, the assumptions employed by Gerard (1957) in his derivations for cylinder collapse strengths differ between those of a long cylinder ($L/D > 0.79\sqrt{D/t}$) free to rotate and translate at the cylinder ends, and those of a moderate length cylinder ($7.07\sqrt{t/D} < L/D < 0.79\sqrt{D/t}$), also free at the ends. For most materials in the inelastic range, the difference in the inelastic collapse strengths for a moderate length cylinder and a long cylinder is generally quite small (Gerard, 1962).

Huang and Pattillo (1984) discuss L/D effects in relation to the cylinder ends being "fixed" and "free" from rotation at the ends (both cases are fixed from radial translation). They conclude that, for fixed ends and $L/D = 8$, collapse resistance calculation errors amount to less than 4% in comparison to those for an infinitely long tube. Also concluded was the fact that the presence of axial loads had little effect on the value of L/D for which the cylinder may be considered infinite in length.

Tschoepe and Maison (1983) indicate that an $L/OD \geq 10$ models an infinitely long tube quite well, and that significant increases in collapse pressures occurred for an L/OD = 5, when the cylinder is fixed from radial translation and rotation.

Hirakawa et al. (1982) say that the critical L/OD value (that is, the minimum value of L/OD for which one can assume an infinitely long tube) strongly depends on whether the collapse is elastic or plastic. In their study, they used two OD/t values: 15 (plastic collapse) and 25 (elastic collapse). For OD/t=15, an L/OD=2 was found to give < 5% error, and for OD/t=25, the same error was found at L/OD=10. Hirakawa et al. (1982) also indicate the dependence of the critical L/OD on out-of-roundness. The effect of out-of-roundness is significant for low L/OD and high OD/t values.

It seems reasonable to conclude that, while the critical L/OD depends on many factors, if L/OD ≥ 12, end effects of any kind can be ignored and the resulting errors will be small.

2.3.5 Geometric Imperfections

For the purposes of this study, geometric imperfections can be categorized into ovality and eccentricity. Ovality accounts for the out-of-roundness of the cylinder, and eccentricity is a function of cylinder wall thickness variations. Depending on the magnitude of imperfections present in a cylinder, its collapse strength may be reduced to 30% of that of a perfect cylinder (Arbocz and Babcock, 1969). Madhavan (1988) and Heise and Esztergar (1970) indicate that ovality is the most significant geometric imperfection parameter, and that generally, eccentricity will have a relatively small effect.

The effect of geometric imperfections on collapse strength is also a function of the magnitude of axial stresses present in the cylinder. Mimura et al. (1987) point out that the effect of ovality is greatest on medium-walled pipe (OD/t=19.34) when axial tensile stresses are less than about 50% of the yield stress. For thick-walled pipe (OD/t=12.96), the effect is less, and for thin-walled pipe (OD/t=30.30), ovality has its largest influence when axial tensile stresses range from 40-75% of the yield stress. In all cases, the effect of ovality is negligible at axial tensile stress levels above 75% of the yield stress. Also, for thick- and medium-walled pipe, the effect of ovality decreases with increasing axial tension.

These trends have been noted by others, including Pattillo and Huang (1985), API BUL 2U (1987), and Madhavan (1988). The effect of ovality on collapse strength seems to be most significant when collapse occurs and the material is near or below the elastic-plastic transition. Its effect becomes insignificant when the cylinder material has undergone substantial material deformations and has yielded considerably.

2.3.5.1 Ovality

All methods of defining ovality appear to assume that the initial out-of-roundness is similar in form to the assumed buckling mode shape. That is, for long cylinders which buckle in two circumferential waves, the ovality is also assumed to initially form two circumferential waves. API BUL 2U (1987) and Mimura et al. (1987) define ovality as:

$$\Delta = \frac{OD_{max} - OD_{min}}{OD_{nominal}} \qquad [2.9]$$

Yeh and Kyriakides (1986a,1986b), Nishioka et al. (1976), and Tokimasa and Tanaka (1986) define ovality as:

$$\Delta_2 = \frac{OD_{max} - OD_{min}}{OD_{max} + OD_{min}} \qquad [2.10]$$

Tokimasa and Tanaka (1986) include the effects of ovality on collapse strength by using a reduction factor given by:

$$r_\Delta = 1 - [0.0856(OD/t) - 1.14]\left(1 - \frac{2}{A + \sqrt{A^2 - 4B}}\right) \qquad [2.11]$$

where

$$A = 1 + 3\Delta_2(D/t) + B \qquad [2.12]$$

and

$$B = \frac{\text{calculated collapse pressure}}{\text{elastic collapse pressure}} \qquad [2.13]$$

For collapse pressures where the material behaves inelastically, the calculated collapse pressure will be different than that of the elastic collapse pressure, and B in Equation 2.13 will deviate from unity.

2.3.5.2 Eccentricity

The equations that define eccentricity are identical to Equations 2.9 and 2.10 with the substitution of thickness values instead of diameter values. The basic equation for eccentricity is of the form:

$$\Xi = \frac{t_{max} - t_{min}}{t_{max} + t_{min}} \qquad [2.14]$$

The reduction factor for the effect of eccentricity on plastic collapse is given by Tokimasa and Tanaka (1986) as:

$$r_{\Xi} = 1 - \Xi \qquad [2.15]$$

To make use of the reduction factors defined by Tokimasa and Tanaka (1986), one simply multiplies the calculated collapse pressure for a geometrically perfect tube by both r_Δ and r_Ξ.

Nishioka et al. (1976) provide the following reduction factor for collapse pressures, which includes both the effects of ovality and eccentricity:

$$r_{\Delta,\Xi} = \frac{1 - \Xi}{1 + 3\Delta_2 (OD/t)_{max}} \qquad [2.16]$$

where Δ_2 and Ξ are defined by Equations 2.10 and 2.14, respectfully. With $\Delta_2 = 0$, $r_{\Delta,\Xi}$ reduces to r_Ξ defined by Tokimasa and Tanaka (1986) in Equation 2.15.

Figure 2.5 illustrates the comparison of the reduction factors defined by Nishioka et al. (1976) and Tokimasa and Tanaka (1986) for ovalized casing. The reduction factor for Tokimasa and Tanaka (1986) is much more sensitive to OD/t, indicating a relatively small reduction for low OD/t casing. A closer examination of the test data used by the two methods reveals an OD/t range of 16 to 25 for Tokimasa and Tanaka's (1986) data, while that of Nishioka et al. (1976) ranged from 18.9 to 21.2, a substantially smaller range.

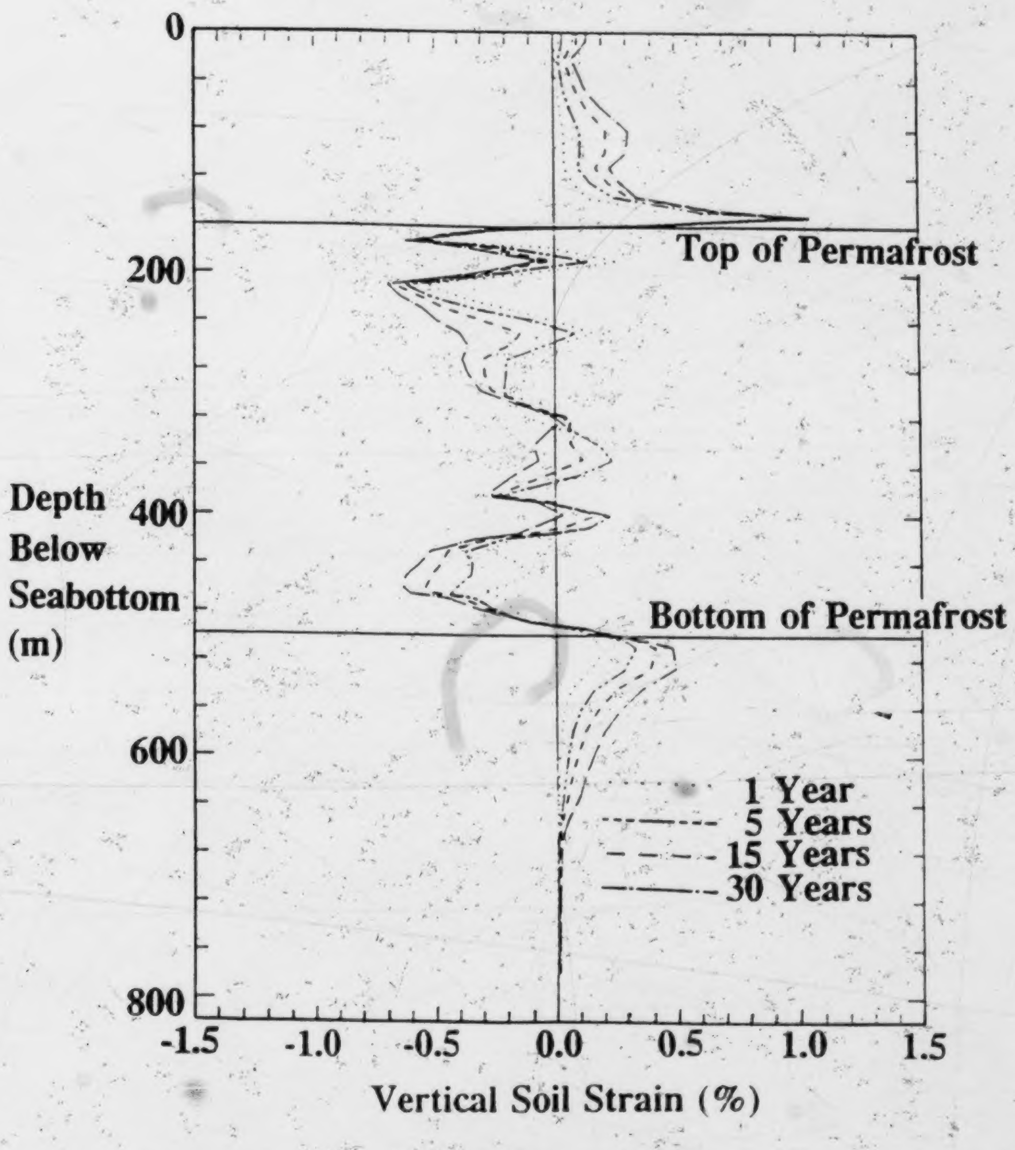

Figure 2.1 - Computed Strains on a Casing String Over a 30 Year Period (from Gulf Canada (1987) and EBA (1985))

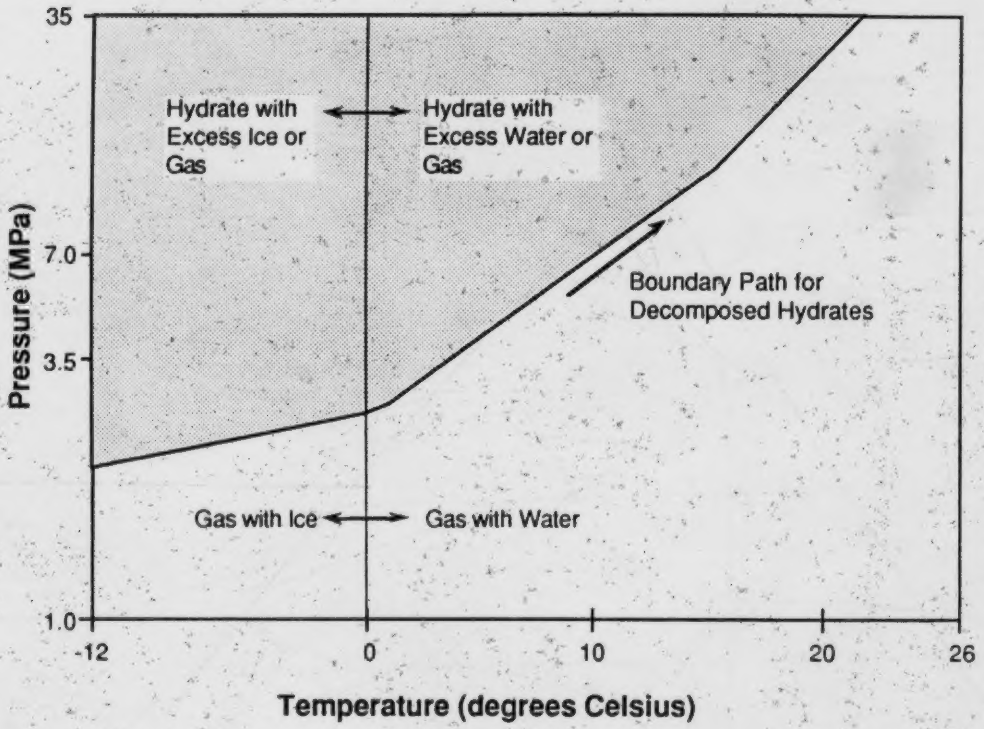

Figure 2.2 - Typical Pressure/Temperature Boundary for Decomposition of Methane Hydrates

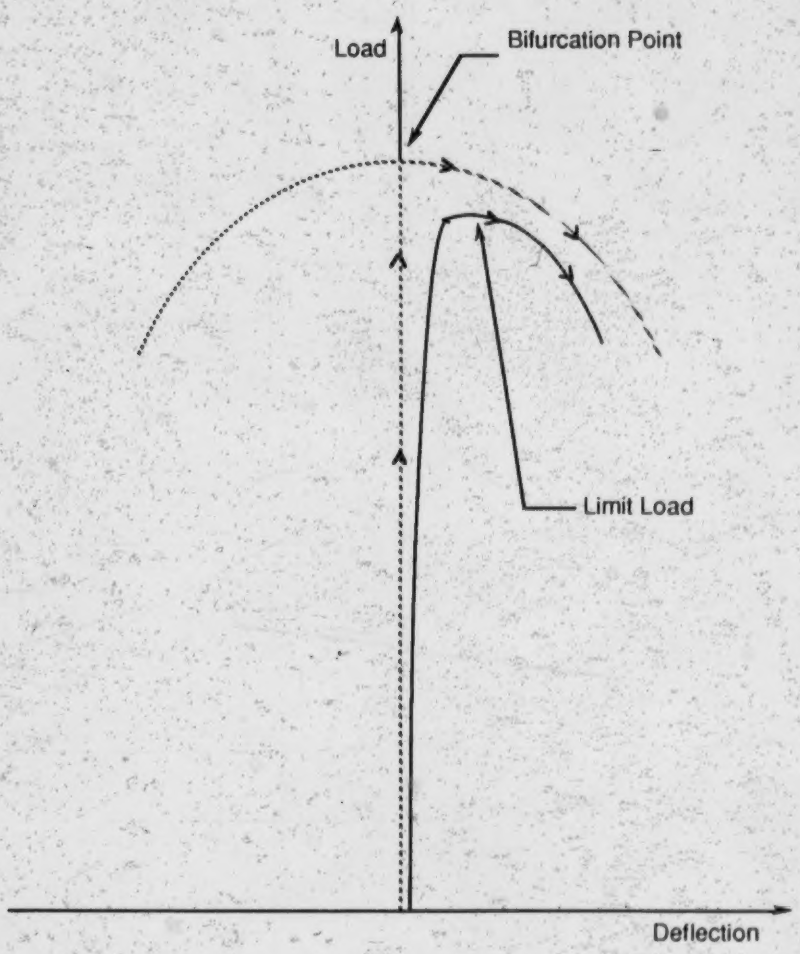

Figure 2.3 - Buckling Paths for Perfect and Imperfect Systems with Post-Buckling Instability

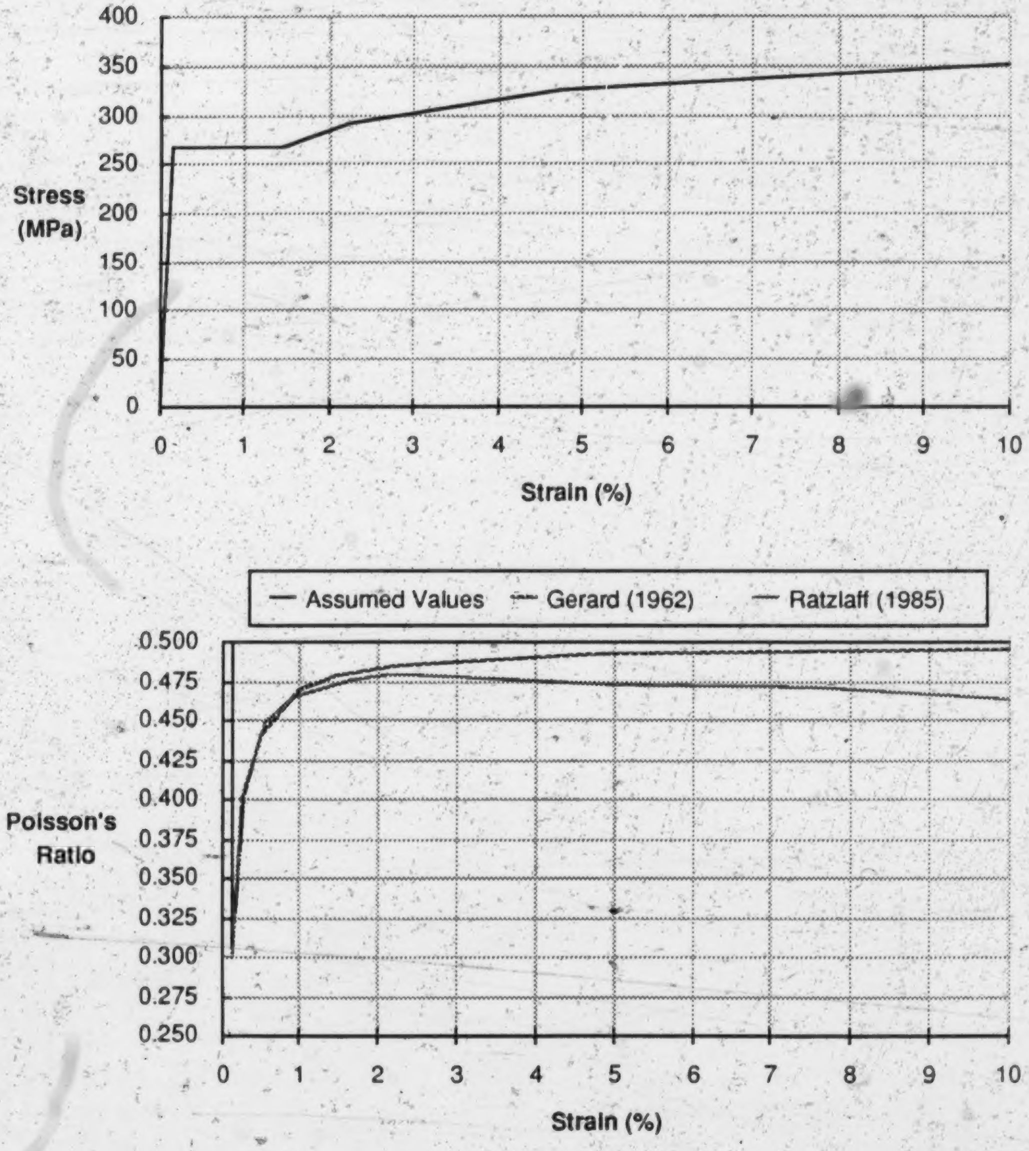

Figure 2.4 - Variation of Poisson's Ratio with Axial Strain

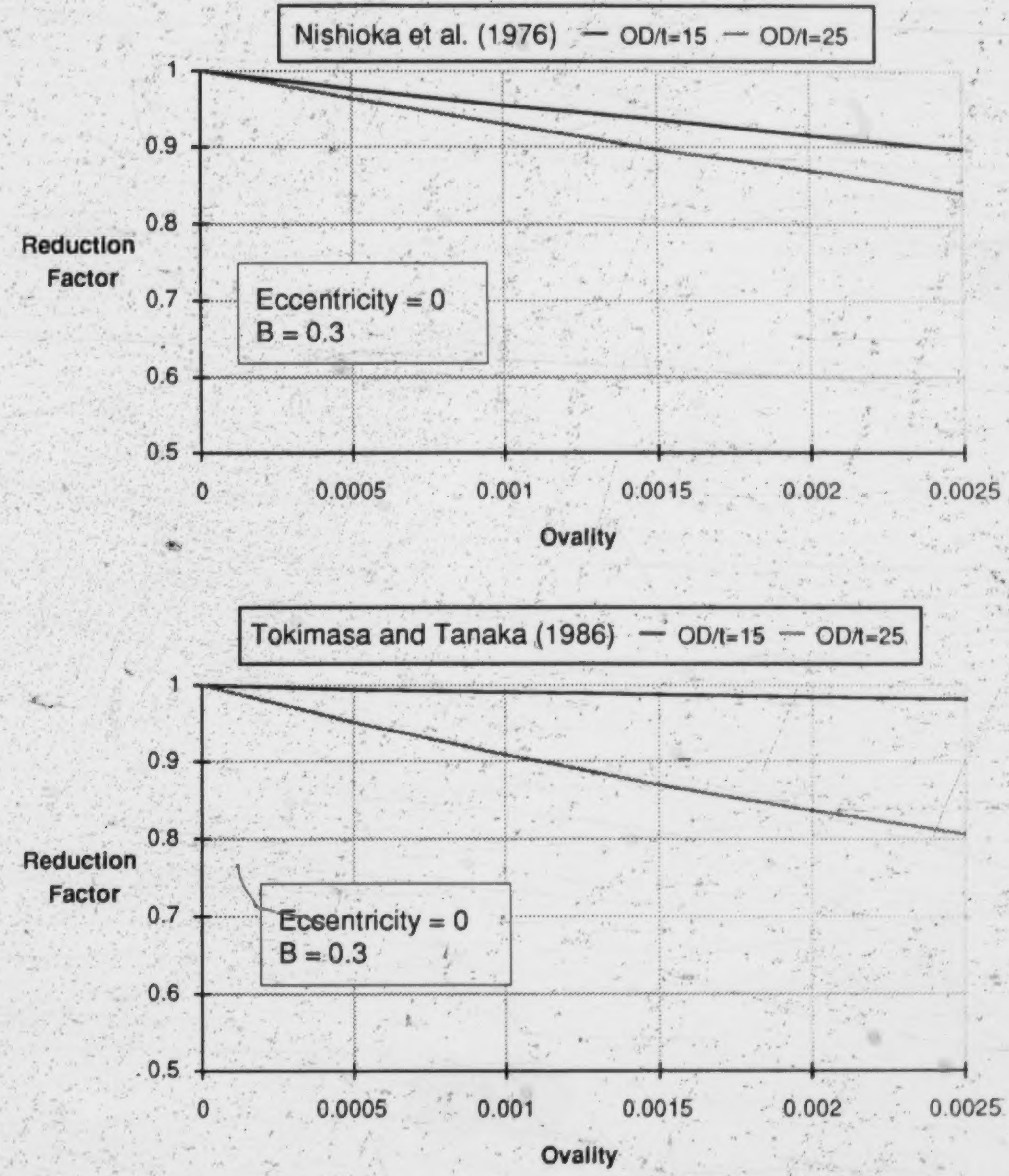

Figure 2.5 - Collapse Pressure Reduction Factor for Varying Ovality

3.0 PAST WORK

3.1 Analysis Methods

3.1.1 Elastic Ring Buckling Equation

The classical elastic ring buckling equation given by, among others, Timoshenko and Gere (1961), is as follows:

$$p_e = \frac{2E}{\left(1 - \nu_e^2\right)} \left(\frac{t}{D}\right)^3 \qquad [3.1]$$

where p_e is the critical external pressure causing elastic collapse, and E is the Elastic Modulus. This equation assumes a long, geometrically and materially perfect circular cylinder buckling in a mode involving two circumferential waves. The first portion of Equation 3.1 is the material parameter, while the second term can be thought of as the geometric parameter. Equation 3.1 predicts the collapse of tubes when the material behaviour is elastic only, but it does form a solid foundation from which the elastic-plastic analysis methods below have been derived.

3.1.2 Tangent Modulus Approach

The tangent modulus approach extends the usefulness of Equation 3.1 into the inelastic range of material behaviour. The tangent modulus theory is based on the assumption that, at a certain critical stress, a deflected equilibrium state is possible. This state is controlled by the tangent modulus, E_t, and it is assumed that, as a result of the buckling deflections, there is no strain reversal at the critical stress. The tangent modulus equation for the collapse strength of cylindrical tubes is (Timoshenko and Gere, 1961):

$$P_{cr} = \frac{2E_t}{\left(1 - \nu^2\right)} \left(\frac{t}{D}\right)^3 \qquad [3.2]$$

where ν is Poisson's Ratio (elastic or plastic) and E_t is the tangent modulus, or the slope of the stress strain curve at a given stress level.

Stress strain curves can be modelled using a variation of the Ramberg-Osgood (1943) curve fit used by Workman (1982), in which:

$$\varepsilon = \frac{\sigma}{E} + \left(0.005 - \frac{\sigma_y}{E}\right)\left(\frac{\sigma}{\sigma_y}\right)^n \qquad [3.3]$$

where σ is the effective stress given below in Equation 3.4, ε is the corresponding effective strain, σ_y is the yield stress of the material (equal to the stress at 0.5% strain), and n is a hardening parameter which determines the inelastic slope of the stress strain curve.

The effective stress, σ, is determined from the Hencky-von Mises distortion energy criterion for a biaxially stressed field with the shear stress taken as zero (Galambos, 1988):

$$\sigma = \sqrt{\sigma_\theta^2 + \sigma_z^2 - \sigma_\theta\sigma_z} \qquad [3.4]$$

where σ_z is the axial stress of the ring or cylinder, and σ_θ is the circumferential stress , given by:

$$\sigma_\theta = \frac{pD}{2t} \qquad [3.5]$$

with p corresponding to the externally applied pressure (σ_θ is negative for compression).

By differentiating Equation 3.3 with respect to σ and rearranging, E_t may be expressed as:

$$E_t = \frac{1}{\left[\frac{1}{E} + \frac{n\left(0.005 - \frac{\sigma_y}{E}\right)}{\sigma_y}\left(\frac{\sigma}{\sigma_y}\right)^{n-1}\right]} \qquad [3.6]$$

The procedure for calculating the critical pressure is iterative: for a given axial stress, one assumes a critical pressure to cause buckling and calculates the corresponding material stress state using Equations 3.4 and 3.5. One then computes E_t using Equation 3.6, followed by the critical pressure from Equation 3.2. This critical pressure should match the assumed pressure. If it doesn't, one repeats the procedure until a match is made, within a given tolerance.

3.1.3 Reduced Modulus Approach

The basic assumption of the tangent modulus theory is that, at the critical stress there is no strain reversal. This leads to lower predicted values of the critical external buckling pressures because strain reversal, or unloading, does take place. The reduced modulus theory takes this into account. The action of unloading can be seen in Figure 3.1. As the concave portion of the tube section increases in deflection past the yield stress (corresponding to a stiffness of E_t), the convex side of the tube section decreases in stress and unloads (corresponding to the unloading curve stiffness, E). Therefore, the section stiffness of the tube lies somewhere between the elastic stiffness and the inelastic stiffness defined by the tangent modulus. The reduced modulus buckling equation assumes the form:

$$p_{cr} = \frac{2E_r}{\left(1 - \nu^2\right)} \left(\frac{t}{D}\right)^3 \qquad [3.7]$$

where E_r is the reduced modulus, whose value depends on the shape of the cross section and the material properties. For a circular cylinder under external pressure, Galambos (1988) gives the reduced modulus as:

$$E_r = \sqrt{E_s\, E_t} \qquad [3.8]$$

where E_s is the secant modulus, equal to σ/ε.

Equation 3.8 is also given by Stephens et al. (1982), who refer to NASA (1968). Holmquist and Nadai (1939), Clinedinst (1939), and Timoshenko and Gere (1961) define the reduced modulus as:

$$E_r = \frac{4EE_t}{\left[\sqrt{E} + \sqrt{E_t}\,\right]^2} \qquad [3.9]$$

For practical values of E, E_t, and E_S, Equations 3.8 and 3.9 yield virtually the same values for E_r. This is illustrated in Figure 3.2 for a material consisting of a rounded stress strain curve and that of an elastic-perfectly plastic steel.

The iterative procedure discussed for the tangent modulus approach is also used for determining the collapse pressure using the reduced modulus approach.

3.1.4 Pattillo and Huang (1982)

Pattillo and Huang (1982) have derived an analytical procedure for determining the collapse pressure of casing of infinite length in the presence of an imposed axial tensile load (the mathematical details of their method are described in Huang and Pattillo, 1982). Two possible sources of plastic collapse are discussed: collapse that occurs as a result of exceeding the ultimate strength of the material, and collapse associated with plastic buckling. For the latter case (the case of interest), the authors have provided a derivation using thin shell theory, and regard the casing as an orthotropic elastic shell subject to a uniform axial load and external pressure. The elastic bending stiffness of the shell, EI, is replaced by factors which depend on the inelastic material properties and the loading condition. The required terms are obtained by using the deformation theory of plasticity and assuming an effective stress state for the material based on the biaxial stress condition in the axial and circumferential directions. Two basic assumptions are used in the derivation: radial stresses are ignored and the average circumferential stress is used rather than a stress distribution through the wall thickness of the casing. The errors associated with these approximations are minimized as the OD/t ratio of the casing increases and approaches a thin shell.

The collapse pressure equation is given as:

$$p_{cr} = 2\left(\frac{\alpha_{22}}{\alpha_{11}\alpha_{22} - \alpha_{12}^{2}}\right)\left(\frac{t}{D}\right)^{3} \qquad [3.10]$$

This equation is similar to Equation 3.1, but the $E/(1-\nu_e^2)$ material term is replaced with the "α" terms, defined as follows:

$$\alpha_{11} = \frac{1}{E_s} + \frac{1}{4\sigma^2}\left(\frac{1}{E_t} - \frac{1}{E_s}\right)(2\sigma_\theta - \sigma_z)^2 \qquad [3.11]$$

$$\alpha_{22} = \frac{1}{E_s} + \frac{1}{4\sigma^2}\left(\frac{1}{E_t} - \frac{1}{E_s}\right)(2\sigma_z - \sigma_\theta)^2 \qquad [3.12]$$

$$\alpha_{12} = -\frac{\nu}{E} - \frac{1}{2}\left(\frac{1}{E_s} - \frac{1}{E}\right) + \frac{1}{4\sigma^2}\left(\frac{1}{E_t} - \frac{1}{E_s}\right)(2\sigma_\theta - \sigma_z)(2\sigma_z - \sigma_\theta) \qquad [3.13]$$

The solution for Equation 3.10 is determined by successive iterations until assumed values of p_{cr} agree within a specific tolerance to the calculated values.

Pattillo and Huang (1982) have presented a comparison of their prediction method to the test data of Edwards and Miller (1939) and Tamano et al. (1982). The correlation presented by the authors is reasonably good.

3.1.5 Gerard (1957)

Gerard (1957, 1962) has derived a set of equilibrium differential equations for the plastic buckling of thin shells of constant unequal radii. With a set of assumptions for a particular buckling problem, these equilibrium equations can be reduced to solvable equations for the problem at hand. The equations have been formulated on the basis that, at the buckling load, an exchange of stable equilibrium configuration occurs between the straight form and the slightly bent form of a cylinder. Because the load remains constant during the exchange, a strain reversal must occur on the convex side, concurring with the concepts of the reduced modulus approach discussed earlier.

For a long cylinder ($L/D > 0.79\sqrt{D/t}$) subject to external lateral pressure, the buckling occurs with two circumferential waves and the solution obtained by Gerard (1957) can be suitably reduced to provide the following collapse equation:

$$p_{cr} = \eta \frac{2E}{\left(1 - \nu^2\right)} \left(\frac{t}{D}\right)^3 \qquad [3.14]$$

where η is termed the plasticity reduction factor, given by:

$$\eta = \left[\frac{1 - \nu_e^2}{1 - \nu^2}\right] \left(\frac{E_s + 3E_t}{4E}\right) \qquad [3.15]$$

Gerard (1957) also provides a plasticity reduction factor for moderate length cylinders subject to external pressure ($7.07\sqrt{t/D} < L/D < 0.79\sqrt{D/t}$):

$$\eta_m = \left[\frac{1 - \nu_e^2}{1 - \nu^2}\right] \left(\frac{E_s}{E}\right) \sqrt[4]{\frac{E_t}{E_s}} \sqrt{\frac{1}{4} + \frac{3}{4}\frac{E_t}{E_s}} \qquad [3.16]$$

3.2 Design Methods

3.2.1 American Petroleum Institute

The American Petroleum Institute (API) has developed several guides and bulletins regarding the design of long cylinders or casing subject to external pressure and axial load. The Recommended Practice for Planning, Designing, and Constructing Fixed Offshore Platforms (API RP 2A, 1982), Bulletin on Formulas and Calculations for Casing, Tubing, Drill Pipe, and Line Pipe Properties (API BUL 5C3, 1985), Recommended Practice for Planning, Designing, and Constructing Tension Leg Platforms (API RP 2T, 1987), and the Bulletin on Stability Design of Cylindrical Shells (API BUL 2U, 1987) all contain provisions for the design of cylinders (API RP 2T, however, refers the designer to API BUL 2U, 1987). All the API procedures contain semi-empirical formulations for evaluating the buckling strength of stiffened and unstiffened cylindrical shells. The basic methodology for determining the buckling strength is to reduce the elastic ring buckling equation (Equation 3.1) by capacity reduction factors and plasticity reduction factors which have been determined from approximate lower-bound values of test data on shells with initial imperfections. The recommendations of API, therefore, are intended to predict a statistically acceptable minimum collapse, not an average collapse. Safety factors are also given by API, but will not be used in this study.

Table 3.1 summarizes the purpose of each guide and the imposed considerations and limitations.

API BUL 2U (1987) and API RP 2A (1982) follow the same procedure to determine the collapse strength due to external pressure only, but they differ when the reduction in strength due to axial tension is considered. The critical elastic ring buckling pressure is given by:

$$p_e = 0.275\,E\left(\frac{t}{R}\right)^3 \qquad [3.17]$$

where R is the mean cylinder radius. Equation 3.17 assumes Poisson's ratio to be 0.3. The API RP 2A (1982) equation is slightly different in that it uses the outside radius in lieu of the mean radius in Equation 3.17.

The elastic buckling stress is then given by:

$$\sigma_{e,\alpha} = \alpha\, p_e\left(\frac{OR}{t}\right) \qquad [3.18]$$

where OR is the outside radius and α is the capacity reduction factor, which depends on the maximum differences in residual stresses, material anisotropies, the cross section diameter, and the local deviation of the cylinder from a true circle. API BUL 2U (1987) recommends that a constant value of $\alpha = 0.8$ be used for cylinders which meet its imperfection tolerances, but has provisions for determining other values of α when those provisions are not met. API RP 2A (1982) will only allow the use of $\alpha = 0.8$, and not allow the use of cylinders that do not meet the tolerance requirements.

If $\sigma_{e,\alpha} > 0.55\sigma_y$, $\sigma_{e,\alpha}$ must be reduced by a plasticity reduction factor, η, whose value can range anywhere from zero to one. η basically depends on the magnitude of $\sigma_{e,\alpha}$ in relation to σ_y, and is calculated by the following:

$$\text{for} \quad \begin{array}{ll} \Lambda \le 0.55, & \eta = 1 \\ 0.55 < \Lambda \le 1.6, & \eta = \dfrac{0.45}{\Lambda} + 0.18 \\ 1.6 < \Lambda \le 6.25, & \eta = \dfrac{1.31}{1 + 1.15\Lambda} \\ 6.25 < \Lambda, & \eta = \dfrac{1}{\Lambda} \end{array} \qquad [3.19]$$

where $\Lambda = \sigma_{e,\alpha}/\sigma_y$, and $\sigma_{\alpha,\eta}$ is now equal to $\eta\sigma_{e,\alpha}$, the plastic buckling stress.

The final step in determining the collapse strength is to apply a reduction to $\sigma_{\alpha,\eta}$ to account for the axial load. The reduced critical buckling stress, σ_{cr}, as determined by API BUL 2U (1987), is solved for in the following interaction equation:

$$\sigma_{cr} = \sigma_{\alpha,\eta}\left[1 - 0.25\left(\frac{\sigma_z}{\sigma_y}\right)\right] \qquad [3.20]$$

but not greater than the value of σ_y minus σ_z. The API RP 2A (1982) reduced buckling stress is given by the following interaction equation:

$$a^2 + b^2 + 2v_e ab \leq 1.0 \qquad [3.21]$$

where:

$$a = \frac{\sigma_z}{\sigma_y} \qquad [3.22]$$

$$b = \left|\frac{\sigma_{cr}}{\sigma_{\alpha,\eta}}\right| \qquad [3.23]$$

The critical pressure for both procedures is then calculated from:

$$p_{cr} = \sigma_{cr}\left(\frac{t}{OR}\right) \qquad [3.24]$$

Based on casing collapse test data, API BUL 5C3 (1985) has adopted four modes of collapse, namely elastic collapse, transition collapse, plastic collapse, and yield collapse. Each mode has an applicable OD/t range which is dependent on the yield stress. The procedure used in API BUL 5C3 (1985) is to reduce the yield stress of the casing based on the magnitude of axial tension, then determine the collapse resistance assuming no axial load using the reduced yield strength.

The reduced yield strength is calculated by:

$$\sigma_{y,r} = \sigma_y \left[\sqrt{1 - \frac{3}{4}\left(\frac{\sigma_z}{\sigma_y}\right)^2} - \frac{1}{2}\left(\frac{\sigma_z}{\sigma_y}\right) \right] \qquad [3.25]$$

Table 3.2 summarizes the API BUL 5C3 (1985) minimum collapse equations. The value determined from Equation 3.25 is used in place of σ_y in the equations in Table 3.2 to determine the collapse pressure. Pattillo (1985a, 1985b) provides a more in-depth look at how the axial load adjustment is made, and the formulations of the minimum collapse equations.

3.2.2 Other Design Methods

Other design rules for the determination of the collapse strength of cylinders are the ASME Boiler and Pressure Vessel Code Case N-284 (1986), the European Recommendations for Steel Construction, Section 4.6: Buckling of Shells (1984), and the DnV Rules for the Design, Construction, and Inspection of Offshore Structures, Appendix C (1977). Miller (1981) also provides an adaptation to the rules described by the ASME Code.

Code Case N-284 has been approved by ASME as an alternate method for determining allowable compressive stresses for metal containment shells. The purpose of the Case is to provide stability criteria for shells with more loading conditions and complex geometries than that of the ASME Boiler and Pressure Vessel Code. The criteria provided in the Case were primarily developed by Miller (1979, 1981).

For long cylindrical shells subject to external pressure and axial tension, the method used in Code Case N-284 is similar to that described for API BUL 2U (1987) and API RP 2A (1982). However, Case N-284 does not appear to include provisions for the addition of axial tension. The plasticity reduction factors given are also somewhat different that of the API design guidelines.

Miller (1981) provides adaptations to Code Case N-284 to account for axial tensile loads. For the combination of external pressure and axial tension, Equation 3.20 must be satisfied for elastic buckling, and both Equation 3.20 and the following form of the von Mises equation must be satisfied for inelastic buckling:

$$\left(\frac{\sigma_z}{\sigma_y}\right)^2 - 1.5\frac{\sigma_z}{\sigma_y}\frac{\sigma_\theta}{\sigma_y} + \left(\frac{\sigma_\theta}{\sigma_y}\right)^2 = 1 \qquad [3.26]$$

Miller (1981) provides the same $\sigma_{\alpha,\eta}$ as that calculated in API BUL 2U (1987) and API RP 2A (1982), using the same plasticity factor, but the capacity reduction factor is given by:

$$\alpha = 1-0.2\sqrt{\frac{OD_{max}-OD_{min}}{0.01(OD_{nominal})}} \qquad [3.27]$$

but α cannot be greater than 0.8.

The European Recommendations for Steel Construction, Section 4.6: Buckling of Shells (1984) has been written by the European Convention for Constructional Steelwork (ECCS). Its method for determining the critical collapse pressure is somewhat different than the methods described so far. The pressure causing material yield, p_y, is first calculated and compared to the elastic ring buckling formula (Equation 3.1) by way of the following formula:

$$\lambda = \sqrt{\frac{p_y}{p_e}} \qquad [3.28]$$

For λ greater than one, elastic buckling occurs, and the critical pressure causing collapse, p_{cr}, is equal to $0.5p_y$. For λ between zero and one, the collapse pressure will vary from p_y to $0.5p_y$. Figure 3.3 illustrates the relationship between p_{cr} and λ for $0 \leq \lambda \leq 1$.

The combination of axial load and external pressure is taken care of by using the following interaction equation:

$$\frac{\sigma_z}{\sigma_{cr}} + \frac{p}{p_{cr}} \leq 1 \qquad [3.29]$$

where σ_{cr} is the critical buckling stress in the axial direction for axial loading only, calculated in another section of the ECCS Recommendations.

The ECCS method above applies only to cylinders which are circular to within 0.5% of the radius measured from the true centre. Measurements for this should be made at a minimum of 24 equally spaced positions around the circumference. These measurements are not necessary if tests are performed to show that the cylinder can attain an external pressure equal to the design load.

The Det norske Veritas (DnV) Rules for the Design, Construction, and Inspection of Offshore Structures, Appendix C (1977) provide criteria for determining the elastic buckling resistance of cylindrical shells using the following equation:

$$\sigma_e = \rho \, p_e \left(\frac{R}{t}\right) \qquad [3.30]$$

where ρ is the factor due to imperfections. For long cylinders, $\rho = 0.87$. An interaction equation is provided for several combinations of load, but does not include axial tension. No mention is made of inelastic buckling, but the Rules do indicate that a more refined analysis or results of model tests may be used as alternate methods for the determination of buckling resistance.

The DnV Rules also have strict tolerance requirements for cylindrical shells, and includes taking measurements of the local deviation from the true circle, as well as out-of-roundness.

3.3 Test Results

3.3.1 Edwards and Miller (1939)

Perhaps the earliest experimental investigation into the problem of casing collapse under combinations of axial tension and external pressure was that of Edwards and Miller (1939). Over two hundred tests were performed on 50mm OD (outside diameter) seamless steel tubes with varying material properties, OD/t ratios, and combined load magnitudes. The following test parameters were used:

OD/t: 11-22
L/OD: 18
σ_y: 207-552 MPa
σ_z: 0-σ_y

Edwards and Miller (1939) have chosen 50mm OD tubes on the basis that previous work by Stewart (1906) and Carman (1917) has shown that small scale collapse tests can give results comparable to full size tests provided that the OD/t ratios are the same. This can be assumed to be true if the material property and geometric imperfection differences are accurately established and accounted for in the analysis.

The test apparatus used by Edwards and Miller (1939) is illustrated schematically in Figure 3.4. The packing around the seals was maintained throughout the tests to obtain uniformly leakproof joints and to minimize the frictional force of the packing, which interferes with the free longitudinal movement of the tube in the chamber.

As end fittings were threaded to the specimen, it was important for the specimens to have a sufficient L/OD ratio in order to eliminate any end effects. Using the criteria outlined in Section 2.3.4, L/OD for the test specimens exceeds the minimum and the effect of end cap radial restraint on specimen collapse performance is negligible.

The test procedure involved a loading sequence of first applying a predetermined fixed tension load, then increasing the external pressure until collapse occurred. Collapse was detected by a sudden decrease in pressure. In a few of the tests, significant elongation of the specimen occurred in the axial direction. In these tests, the force of the packing friction (as a result of repacking), which imposed an axial tension restraint on the specimen, was found to be about 4.5 kN for each joint. This value was applied as a correction to the tension load in all cases when significant stretching of the specimen necessitated repacking of the seals.

The results of the tests performed by Edwards and Miller (1939) are illustrated in Figures 3.5 to 3.11, along with predicted results of Sections 3.1 and 3.2, and the corresponding stress strain curves for each test group cited. In total, Edwards and Miller (1939) provided the results for twelve test groups. The stress strain curves for test groups one to five, however, were not provided, and were therefore not included in this study.

3.3.2 Stuiver and Tomalin (1959)

Stuiver and Tomalin (1959) performed two series of tests on small diameter tubing to determine the loading combinations of axial tension and external pressure which produce collapse. Twenty tests were performed on 25mm OD seamless steel tubing with wall thicknesses machined to 1.08 and 0.94mm. Because of the machining, the out of roundness of the tube specimens was found to be negligible. Wall thickness variations were measured, but did not appear to affect the test results or the position of the failure. The following test parameters were used:

OD/t: 23.5 and 27.0

L/OD: $>1.73\sqrt{OD/t}$

σ_y: 543 MPa

σ_z: $0-\sigma_y$

The test apparatus is illustrated in Figure 3.12. In view of the potential longitudinal restraint of the specimen by the O-ring seals, Stuiver and Tomalin (1959) felt that the seal flexibility was such that movement of the specimen was not restricted as the test progressed. Axial tension was provided independently by the use of a universal testing machine.

The stress strain curve for the material used was obtained by axially loading a tube in tension in which strain gages had been mounted. The test procedure for the remaining tube specimens involved applying an initial axial tension followed by an increase in external pressure until collapse occurred. Collapse pressures and loads were taken as the maximum values reached during the tests. The results of these tests are illustrated in Figures 3.13 and 3.14, comparing them to the prediction methods.

3.3.3 Tamano et al. (1982)

Over fifty tests were performed by Tamano et al. (1982) on API grade casing material under various conditions of axial tension and external pressure. The nominal diameter of the test specimens was 178mm OD for all grades of casing tested. Test results for specimens of grades K55, N80, and P110 seamless pipe are reported. Material properties of the casing varied considerably, and a wide range of OD/t ratios was investigated in order to envelop the range of values expected in a commercial casing string. The test parameters are as follows:

OD/t: 15.2 - 25.3
L/OD: 6.7
σ_y: 439-906 MPa
σ_z: 0-σ_y

The low L/OD ratio casts some doubt as to the validity of the test results. It is below the "8" limit set by Fowler et al. (1983), and at the low end of the $1.73\sqrt{OD/t}$ limit imposed by Stuiver and Tomalin (1959). Simonen and Shippell (1982) were faced with the same problem of having a seemingly low L/OD, creating a potential error in the accuracy of the test results. Finite element calculations were performed by Simonen and Shippell (1982) to estimate the extent of end effects, and their results indicated that the centre portion of the specimens were unaffected by the end restraint. The L/OD they used was about 5.7. Using this value as a minimum is a considerable deviation from the previous criteria, and indicates the wide range of end effects that could exist as different end capping techniques are used.

The apparatus used for the Tamano et al. (1982) tests is illustrated in Figure 3.15. There is no mention of any longitudinal restraint at the specimen/frame interface, but with the larger specimen sizes and larger axial loads, any O-ring restraint is probably ineffective.

Both proportional loading (tension and pressure applied simultaneously) and constant loading (tension held constant while pressure is increased) conditions were used in these tests. Tamano et al. (1982) indicate a slight but definite difference in the collapse pressure was found between the two loading conditions, but there was no discussion on why, nor which tests were subject to which loading sequence. In all tests, the collapse pressure was defined as the maximum applied pressure.

Stress strain curves for the pipe materials were obtained from longitudinal tension test coupons cut from the pipe. The results of the casing collapse tests are illustrated in Figures 3.16 to 3.25, along with the corresponding representative stress strain curves for each grade of pipe, and the various prediction methods.

3.3.4 Gulf Canada (1987)

The experimental program performed by Gulf Canada (1987) was to determine the collapse strength of model segments of downhole casing subject to constant axial tension and external pressure. The test program is described in a separate report to Gulf Canada Corporation from Southwest Research Institute (1987), and consisted of thirteen API grade X-56 casing specimens tested under the following conditions:

- external pressure and constant axial load
- external pressure and constant axial strain
- external pressure only.

Test parameters were as follows:

OD/t: 23.6-31.0
L/OD: 8-11
σ_y: 475 MPa
σ_z: 0-σ_y
ε_z: 0-4%

The initial loads for the constant axial load tests varied from 0 to the yield load, while the initial strains for the constant axial strain tests ranged from 0 to 4% strain.

The test apparatus is illustrated in Figure 3.26. Specially machined end plugs were welded to the ends of the specimen, and O-rings provided the seal for external pressure. No mention is made of the O-ring axial restraint, but, because the specimens tested were full scale, the magnitude of potential end restraint load is negligible in comparison to the axial load magnitude.

The test procedure was one of applying an initial axial load, followed by an increase in external pressure to the collapse level. For the constant axial strain tests, the specimen was initially axially loaded in increments to the target strain. Pressure was then increased while maintaining the original axial strain.

Stress strain curves for the material used in all tests were obtained from longitudinal tension test coupons cut from the pipe. The results of the collapse tests are illustrated in Figures 3.27 and 3.28, along with the representative stress strain curve for the material. Figure 3.27 also shows the predicted results for the constant axial load case, using the prediction and design methods outlined in Sections 3.1 and 3.2. The constant axial strain tests in Figure 3.28 have not been predicted, and will be discussed further in Section 3.4.

3.3.5 Madhavan (1988)

Over fifty tests on 30mm OD seamless tubing were performed by Madhavan (1988) under conditions of axial tension and external pressure. The following test parameters were used:

OD/t: 12-37
L/OD: 20
σ_y: 66-383 MPa
σ_z: 0-1.2σ_y
E: 71,700 MPa (aluminum)
207,000 MPa (steel)

The two material types used were annealed stainless steel and aluminum. Stainless steel was chosen because of its availability and its similarity to the material behaviour of typical pipeline grade steel. Aluminum was chosen for its good isotropic characteristics with respect to yielding. Using both materials in this test program provided a large range of material yield stress and elastic moduli, as noted above.

The testing apparatus used by Madhavan (1988) is illustrated in Figure 3.29. End plugs were bonded to the ends of the tube specimen, designed to give proper gripping in applying axial tension to the tubes. O-rings with teflon backup rings were used for sealing purposes.

Testing consisted of both paths of loading: constant axial load followed by increasing external pressure, and constant external pressure followed by increasing axial tension. Madhavan (1988) indicates that the experimental results for the two loading paths show that the effect of load sequence on collapse is not significant.

Material property testing was performed on tensile specimens that were machined from both ends of each tube in the lot from the supplier. Actual stress strain data was not provided, but rather a Ramberg-Osgood (1943) curve fit to the data was given, in which

$$\varepsilon = \frac{\sigma}{E}\left[1 + \frac{3}{7}\left(\frac{\sigma}{\sigma_y}\right)^{n-1} \right] \qquad [3.31]$$

The parameters E, n, and σ_y were obtained from a least squares fit. Proper modelling of the material behaviour (by way of a stress strain curve) is of prime concern when attempting to predict collapse pressures. Because no actual stress strain data was provided, it is uncertain how accurately this modelling was done. This potential inaccuracy is transferred directly to the prediction methods, placing a degree of uncertainty on their validity.

Another set of tests were performed to assess the frictional resistance of the seals in the testing apparatus. Varying pressures were applied while measuring the force required to slide the tube specimens. It was found that the force fluctuated within a 10% variation for the range of pressures tested. This correction was applied to the collapse test results accordingly.

The results of the collapse tests are illustrated in Figures 3.30 to 3.35, along with the predicted results and associated stress strain curves. One of the suspicions of Madhavan (1988) in discussing his test results is that, with the lower OD/t ratio specimens, large axial elongations created an interference between the seals and the tube specimen. The end plugs were made to provide minimum friction at the seals. However, the elongation of the tubes may have exceeded the length of the end plug, causing the tube specimen itself to come in contact with the seal. The increase in frictional resistance caused a slight axial unloading of the tubes, increasing their resistance to external pressure. Collapse results for these tube specimens are therefore artificially high. This can be seen in all of the reported test results at the higher axial stress/yield stress ratios, where the trend towards lower collapse pressures stops. This is especially noticeable for the test specimens with low OD/t ratios, as shown in Figures 3.33 and 3.35.

3.4 Discussion of Test Results

3.4.1 General

Two data sets of test results have been collected: constant axial load tests and constant axial strain tests. A constant axial load test is one in which the axial load is maintained as the external pressure is increased. A constant axial strain test is one in which the cylinder is initially loaded to a desired strain level. The external pressure is then applied and the axial load is allowed to decrease to ensure there is no change in the axial deformation. Both conditions can exist in casing strings of wells drilled in northern regions.

The constant axial strain case involves loading in the circumferential direction and, because of the Poisson strain effect, unloading in the axial direction takes place when the circumferential compressive stress is increased. The test results involving constant axial strain (Figure 3.28) illustrate no decrease in the critical pressure causing collapse for increases in initial axial strain. This interesting trend is worthy of further study, but the solution to this problem involves plasticity formulations and is beyond the scope of this study. Suffice it to say at this point that the critical pressure causing collapse does not appear to depend on the magnitude of initial axial strain, and will not be discussed any further in this study. Collapse strengths, however, for the constant axial load tests do depend on the magnitude of initial axial load. Axial tensile loads decrease collapse strengths and, because of this, the constant axial load case will be considered a lower bound to the problem of collapse of casing in northern regions.

3.4.2 Constant Axial Load Tests

A couple of points are worthy of note regarding the constant axial load test data. Most of the experimental procedures seemed to have a problem with potential longitudinal end restraint as a result of friction generated at the seal of the cylinder specimens tested. For the small diameter specimens tested, this problem may lead to artificially high collapse pressures for two reasons. First, because the seal takes some of the axial load, the actual load on the specimen is lower than expected. This seems to have been taken care of in the test results, with the authors applying a correction to the axial load. Errors may still be present, however, due to the uncertainty of seal load. Secondly, as external pressure is applied to the tube specimen, Poisson strains are transmitted as tensile strains in the axial direction.

If the seal restraining load increases as deformations increase in the axial direction, an axial unloading on the specimen takes place. The problem then becomes similar to the constant axial strain case discussed in Section 3.4.1. This axial unloading will affect the tube a great deal, altering the true collapse test results. Both of these potential problems will likely occur at the higher axial load levels of lower OD/t specimens, where large axial deformations exist. The results reported by Madhavan (1988) are clearly affected by seal load, but the results reported by the other references do not seem to be nearly as affected, if at all.

Variations in test results may occur if the material properties of the test specimens were averaged or rounded off. Tamano et al. (1982) provided only representative stress strain curves for the materials and the 2% offset yield stresses. For this study, though, specific stress strain curves were developed assuming the same shape of curve for each set of data, differing only in yield strength. The Ramberg-Osgood curve for the Edwards and Miller (1939) Test Groups 7, 8, and 9 stress strain data (Figures 3.6, 3.7, and 3.8) has a considerably high slope at the extrapolated end of the curve. The stress strain data provided by the authors only goes to 0.65% strain, and it is quite likely that the real curve has a lower slope. Because of the sensitivity of inelastic buckling strengths to the slope of the stress strain curve, this may be why the results have been over predicted for those tests where significant inelastic material properties have developed.

Table 3.3 summarizes the Ramberg-Osgood material parameters for the curve fitting to all the stress strain curves provided in the test data references. For Madhavan's (1988) data, the Ramberg-Osgood parameters were used up to a strain level of 1.5%. After this level, a constant tangent modulus was used, equal to the slope of the stress strain curve at 1.5% strain.

3.5 Evaluation of Design and Prediction Methods

The following are items of importance for the evaluation of the prediction methods:

- the value of OD/t influences the amount of plastic straining that has occurred prior to buckling. A lower OD/t value implies more plastic straining;
- the effect of geometric imperfections. This effect appears to be greatest for elastic collapse, but is not a factor when collapse occurs as the material progresses well into the plastic range;
- the conservatism of the design approaches;

- the design methods include a capacity reduction factor, but the prediction methods do not;
- the ease with which each of the prediction and design methods can be used.

To further evaluate the accuracy of the prediction methods, the mean and coefficient of variation (COV), in percent, have been calculated for the test/predicted ratios, and are shown in Table 3.4 (the COV is equal to the standard deviation divided by the mean). The calculations in Table 3.4 included all the constant axial load data reported in Section 3.3, except for the results that had initial axial loads above yield. These results, which amount only to about 5% of the total number of test results, have been excluded to make use of the design equations in the comparison. The design methods are only useful when the initial axial load is below the yield value.

In Table 3.4, the E_t, E_r, Pattillo, and Gerard Test/Predicted columns represent the results obtained using the analysis methods described in Sections 3.1.2, 3.1.3, 3.1.4, and 3.1.5, respectively. It is important to note that these methods include a reduction in collapse strength due to plasticity, but do not include the effects of geometric imperfections, residual stresses, or material anisotropy.

Also in Table 3.4 are the Test/Design ratios for two design methods: that described by Miller (1981) in Section 3.2.2, and the API BUL 5C3 (1985) design method, summarized in Section 3.2.1. These design methods include the effects of geometric imperfections, residual stresses and material anisotropy by using a capacity reduction factor.

3.5.1 Design Methods

Both of the design methods used in this evaluation utilize the empirical results of previous tests and provide "knockdown" factors which include the effects of imperfections and plasticity to obtain a lower bound to the test data. Their predictions are therefore conservative. The mean test/design ratios in Table 3.4 also show this conservatism.

Observing Figures 3.5 to 3.35, Miller's (1981) design method appears to be more conservative than the API BUL 5C3 (1985) method when σ_z/σ_y approaches unity, but the opposite is true for lower values of σ_z/σ_y. The API predictions reported herein are based on actual yield stress values. Technically, the method requires the designer to use the minimum specified yield strength, introducing even more conservatism. In the calculations using Miller's (1981) method, the capacity reduction factor was assumed to be the maximum value, α=0.8. Miller (1981) indicated that this factor will be less than 0.8 for cylinders whose ovality is high. Using a value of less than 0.8 will add a margin of safety to the design.

The use of the design methods in this study are intended to provide a good comparison to the other predictions and to the test data, as well as demonstrate the conservatism used in present design. The method described by Miller (1981), however, is a good approach to use in a design situation, incorporating all the parameters that affect collapse strength of cylindrical shells. It is well structured, easy to use and, even though the use of the API BUL 5C3 (1985) method results in less variation, Miller's (1981) method is the recommended method for use in a design situation.

3.5.2 Prediction Methods

The tangent modulus, reduced modulus, Pattillo and Huang (1982), and Gerard (1957) methods of prediction do not make use of a capacity reduction factor to account for geometric imperfections, residual stresses, or material anisotropies. Because of this, these methods over-predict the collapse strength when a reduced buckling strength results from the imperfections. This occurs at the lower σ_z/σ_y values. When collapse occurs plastically, the effect of the imperfections reduces or vanishes.

When the stress strain curve of a cylinder has a well defined yield plateau, the results of the prediction method reported by Pattillo and Huang (1982) are generally lower than the test results and the other prediction methods. When the stress strain curve is of the rounded type, the results are lower when σ_z/σ_y is small, but higher and unconservative when σ_z/σ_y becomes large and approaches unity. The mean and coefficient of variation values in Table 3.4 for Pattillo and Huang's (1982) method are good in comparison to the other prediction methods, but if capacity reduction factors are applied to the other methods, it is anticipated that they will exhibit better statistical predictions. The method reported by Pattillo and Huang (1982) is also a difficult method to use, with excessive calculations (Equations 3.10-3.13).

The tangent modulus approach is a conservative approach for the reasons discussed in Section 3.1. It predicts the collapse of cylinders as well as the other methods when the stress strain curve has a definite yield plateau, but under-predicts collapse when the curve is of the round house type. The buckling of perfect tubes with definite yield plateaus, however, are not difficult to predict. When the buckling is not elastic, the critical stress is the yield value. This is because the material loses all its stiffness when the yield plateau is reached. Under conditions of constant loading, cylinders exhibit no increase in load carrying capacity after buckling, and the critical pressure causing collapse is p_y for a geometrically perfect tube.

The predictions of the reduced modulus approach and that of Gerard (1957) perhaps predict the buckling loads the best. An examination of Figures 3.5 to 3.35 indicates that both of these methods will likely improve their mean and coefficient of variation values for the test/predicted ratios once their predictions include a capacity reduction factor. Predictions of the two methods are virtually identical for the test results of Edwards and Miller (1939), Stuiver and Tomalin (1959), and Tamano et al. (1982), but differ for the data of Gulf (1987) and Madhavan (1988). The test/predicted ratios for Madhavan's (1988) data are quite high due to the end seal problems encountered in the testing program, and are not considered representative of the true collapse values. The reduced modulus approach appears to predict lower values of collapse pressure than that of Gerard (1957) when the OD/t ratio is small, but when OD/t is large, the reduced modulus method predicts higher values when σ_z/σ_y is small.

The plasticity reduction factors used in the reduced modulus, tangent modulus, and Gerard (1957) prediction methods will be discussed further in Chapter 4 in the derivation of the proposed prediction method.

Design Guide	Generally Used for:	Limits of Applicability
API RP 2A	General design of fixed offshore structure cylinder members with medium D/t	- Limitations on materials and geometric imperfections - $D/t \leq 300$
API BUL 2U	Stability design of cylinders fabricated from steel plates with high D/t	- $D/t \leq 2000$, $t \geq 4.76$mm - some reduction factors apply only to materials with a well defined yield point
API BUL 5C3	Design of downhole casing, tubing, drillpipe and line pipe, all with relatively low D/t	- empirical equations based on casing only limits use to downhole tubulars

Table 3.1 - API Design Methods

Applicable D/t Range	Formula	Mode of Failure
$OD/t \geq \frac{2+B/A}{3B/A}$	$P_E = \frac{46.95\times10^6}{(OD/t)(OD/t-1)^2}$	Elastic
$\frac{2+B/A}{3B/A} \geq OD/t \geq \frac{\sigma_y(A-F)}{C+\sigma_y(B-G)}$	$P_T = \sigma_y\left(\frac{F}{OD/t}-G\right)$	Transition
$\frac{\sigma_y(A-F)}{C+\sigma_y(B-G)} \geq OD/t \geq \frac{\sqrt{(A-2)^2+8(B+C/\sigma_y)}+(A-2)}{2(B+C/\sigma_y)}$	$P_P = \sigma_y\left(\frac{A}{OD/t}-B\right)-C$	Plastic
$OD/t \leq \frac{\sqrt{(A-2)^2+8(B+C/\sigma_y)}+(A-2)}{2(B+C/\sigma_y)}$	$P_P = 2\sigma_y\left(\frac{OD/t-1}{(OD/t)^2}\right)$	Yield

$A = 2.8762+1.0679\times10^{-6}\sigma_y+2.1301\times10^{-11}\sigma_y^2-5.3132\times10^{-17}\sigma_y^3$ $B = 0.026233+5.0609\times10^{-7}\sigma_y$ $C = -465.93+0.030867\sigma_y-1.0483\times10^{-8}\sigma_y^2+3.6989\times10^{-14}\sigma_y^3$	$F = \frac{46.95\times10^6 H^3}{\sigma_y(H-B/A)(1-H)^2}$ $G = FB/A$ $H = \frac{3B/A}{2+B/A}$

Table 3.2 - API BUL 5C3 (1985) Minimum Collapse Equations (Units are in psi)

Test Data Source	Test Group	Nominal OD/t	Ramberg - Osgood Parameters		
			E	σy	n
Edwards & Miller (1939)	6	16.6	207348	281.2	120.0
	7	21.7	207348	560.0	11.0
	8	17.3	207348	560.0	11.0
	9	11.2	207348	560.0	11.0
	10	21.7	207348	360.0	55.0
	11	17.3	207348	360.0	55.0
	12	11.2	207348	375.0	110.0
Stuiver & Tomalin (1959)	1	27.0	180000	537.8	150.0
	2	23.5	180000	537.8	150.0
Tamano et al (1982)	K55-1	25.3	189700	509.0	1000
	K55-2	21.8	189700	439.0	1000
	K55-3	18.9	189700	439.0	1000
	N80-1	22.0	189700	702.0	1000
	N80-2	19.3	189700	678.0	1000
	N80-3	15.2	189700	661.0	1000
	N80-4	12.6	189700	733.0	1000
	P110-1	19.4	189700	904.0	1000
	P110-2	15.8	189700	875.0	1000
	P110-3	12.8	189700	906.0	1000
Gulf (1987)	1	23.8	178000	475.0	31.0
	2	23.8	178000	475.0	31.0
		30.7	178000	475.0	31.0
Madhavan (1988)	1	36.7	202696	280.0	11.0
	2	24.5	199249	352.0	11.7
	3	18.7	189596	338.0	10.3
	4	12.1	191665	357.0	9.6
	5	27.3	193044	382.0	12.7
	6	12.2	71702	66.6	5.0

Table 3.3 - Summary of the Ramberg-Osgood Parameters Used to Model the Test Data Material Properties

Test Data Source	Test Group	Et Test/Pred Mean	Et Test/Pred COV %	Er Test/Pred Mean	Er Test/Pred COV %	Gerard Test/Pred Mean	Gerard Test/Pred COV %	Pattillo Test/Pred Mean	Pattillo Test/Pred COV %	Miller Test/Design Mean	Miller Test/Design COV %	API 5C3 Test/Design Mean	API 5C3 Test/Design COV %
Edwards & Miller (1939)	6	1.04	7.61	1.00	6.17	0.98	6.42	1.03	7.10	1.12	9.99	1.10	6.46
	7	1.19	28.92	0.94	19.64	0.91	19.14	0.83	14.86	1.15	21.80	1.15	12.07
	8	1.26	21.69	1.04	16.45	1.00	15.42	0.95	15.01	1.40	33.49	1.26	15.92
	9	1.08	8.25	0.98	10.98	0.96	12.51	0.99	15.00	1.19	3.23	1.24	4.98
	10	0.93	18.38	0.86	12.38	0.84	10.81	0.84	8.43	1.05	6.15	1.03	4.83
	11	0.97	15.26	0.91	6.79	0.88	5.88	0.90	6.83	1.03	12.41	0.99	6.10
	12	0.94	8.51	0.91	8.89	0.89	9.62	0.97	10.90	1.00	8.89	1.09	8.91
Stuiver & Tomalin (1959)	1	0.90	16.70	0.89	18.15	0.89	18.93	0.89	20.95	1.12	19.68	1.25	26.30
	2	0.94	11.59	0.92	11.78	0.92	12.92	0.92	12.34	1.15	10.04	1.30	18.28
Tamano et al (1982)	K55	1.04	17.80	1.03	17.69	1.03	17.67	1.08	17.71	1.36	13.92	1.47	8.23
	N80	1.07	31.92	1.07	30.60	1.06	29.07	1.13	28.88	1.40	34.06	1.43	25.10
	P110	0.99	15.37	0.98	14.82	0.98	13.61	1.04	12.78	1.31	17.12	1.32	11.85
Gulf (1987)*	1	0.76	0.80	0.75	0.75	0.75	0.77	0.79	0.79	1.05	1.49	1.19	1.09
Madhavan (1988)**	1	1.94	70.99	1.26	43.56	1.22	37.42	0.91	20.93	1.01	40.61	0.90	11.30
	2	1.26	33.64	1.00	20.39	0.98	17.66	0.88	10.29	1.04	23.50	1.04	9.54
	3	1.30	36.82	0.97	19.16	0.93	16.45	0.84	3.82	1.26	47.52	1.13	37.58
	4	1.30	24.04	1.07	18.56	1.04	17.75	1.03	11.59	1.39	32.43	1.41	26.76
	5	0.97	18.83	0.79	8.64	0.80	8.65	0.68	6.25	0.73	6.67	0.85	9.64
	6	0.98	14.33	0.82	10.45	0.81	10.18	0.86	1.99	0.92	24.61	1.03	17.04
All Data *, **		1.09	34.74	0.97	20.76	0.95	19.58	0.95	18.59	1.18	27.60	1.18	21.13

* - Gulf's (1987) data does not include those tests where $\sigma_z \ge \sigma_y$.

* - Gulf (1987) Test Group 2 (constant axial strain) results were not used

** - Madhavan's (1988) data does not include those tests where $\sigma_z \ge \sigma_y$

Table 3.4 - Averages and Coefficient of Variations (COV), in percent, for the Test/Predicted Ratios

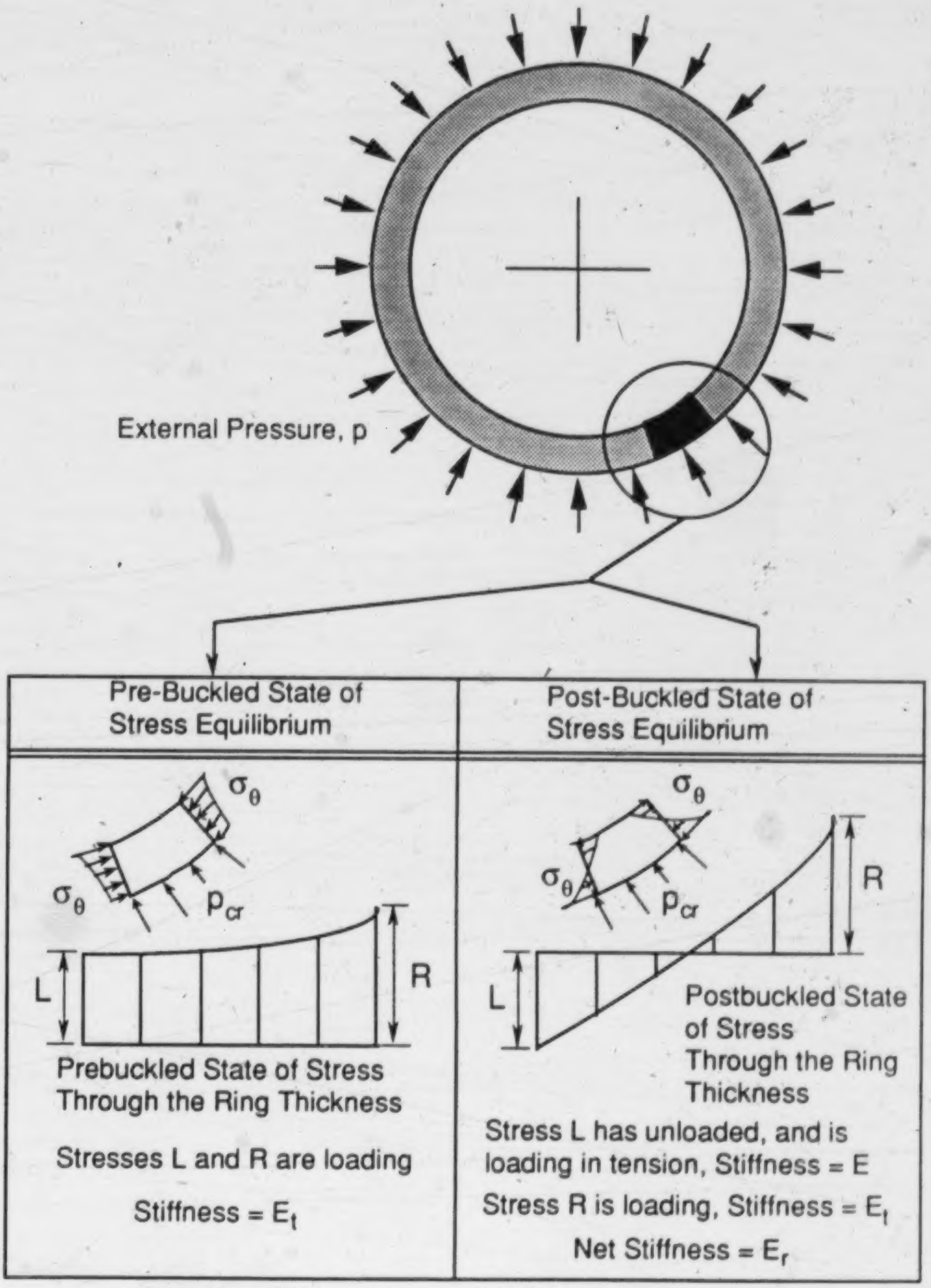
External Pressure, p
Pre-Buckled State of Stress Equilibrium
Post-Buckled State of Stress Equilibrium
σθ
σθ
pcr
L
R
Prebuckled State of Stress Through the Ring Thickness
Stresses L and R are loading
Stiffness = Et
σθ
σθ
pcr
R
L
Postbuckled State of Stress Through the Ring Thickness
Stress L has unloaded, and is loading in tension, Stiffness = E
Stress R is loading, Stiffness = Et
Net Stiffness = Er

Figure 3.1 - Basic Assumptions Behind the Reduced Modulus Theory (Timoshenko and Gere, 1961)

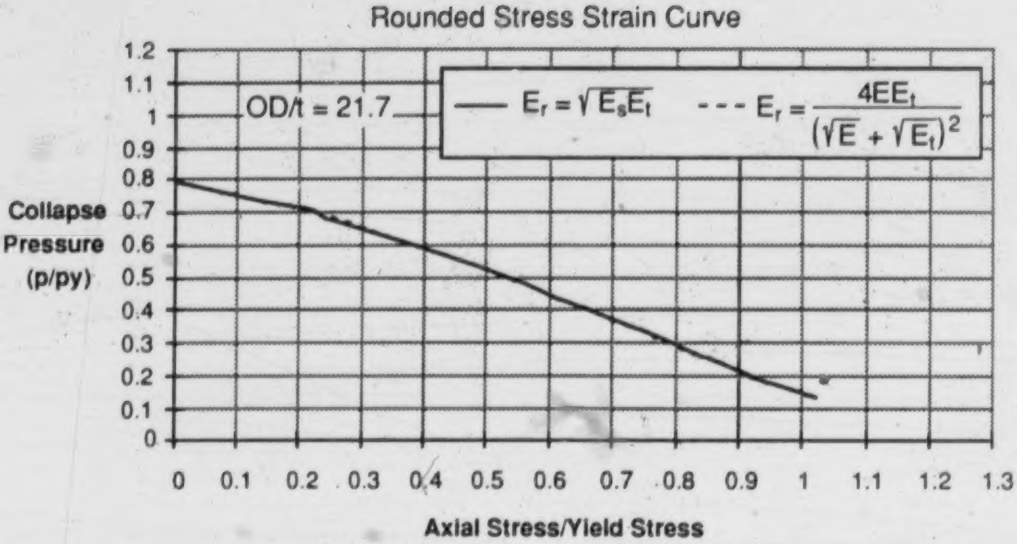

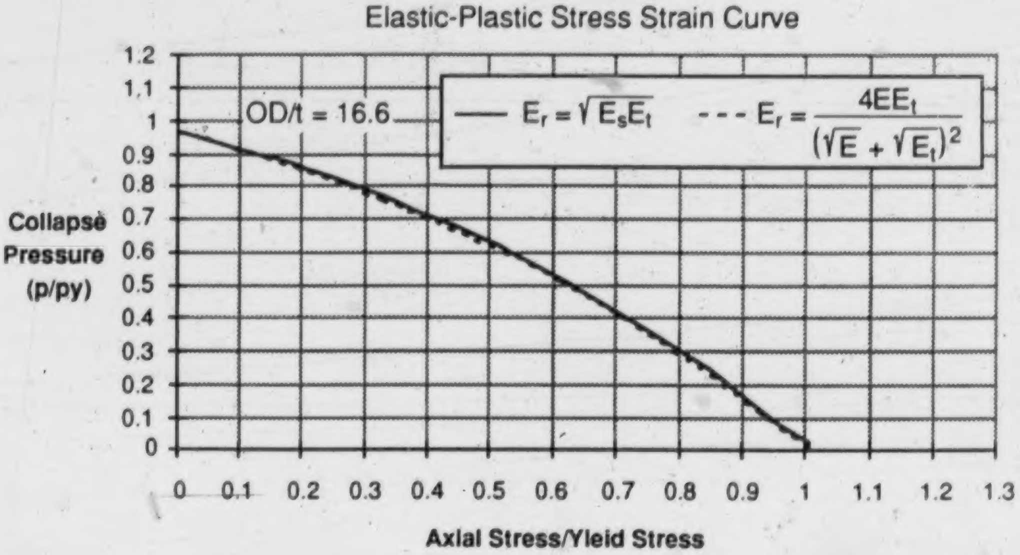

Figure 3.2 - Comparison of Different Reduced Modulus Equations

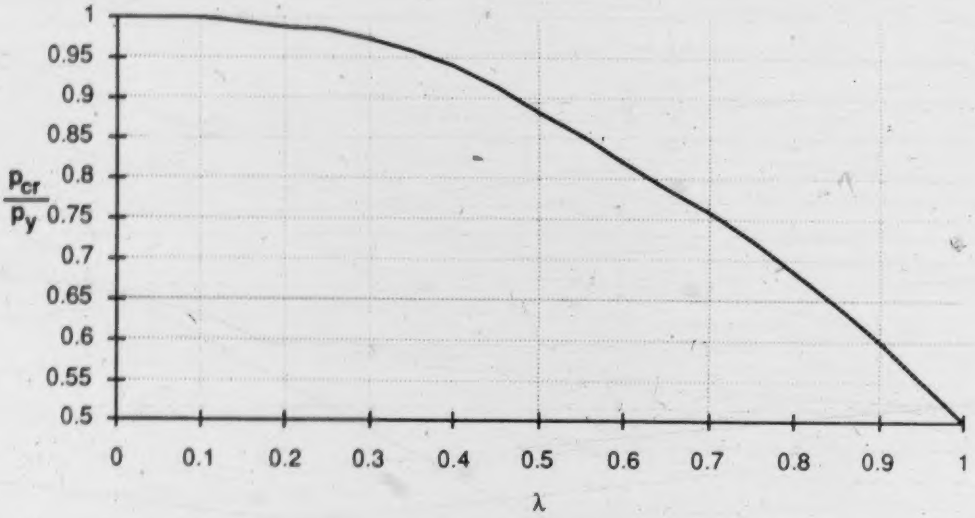

Figure 3.3 - European Recommendations for Steel Construction Relationship Between λ and P_{cr}.

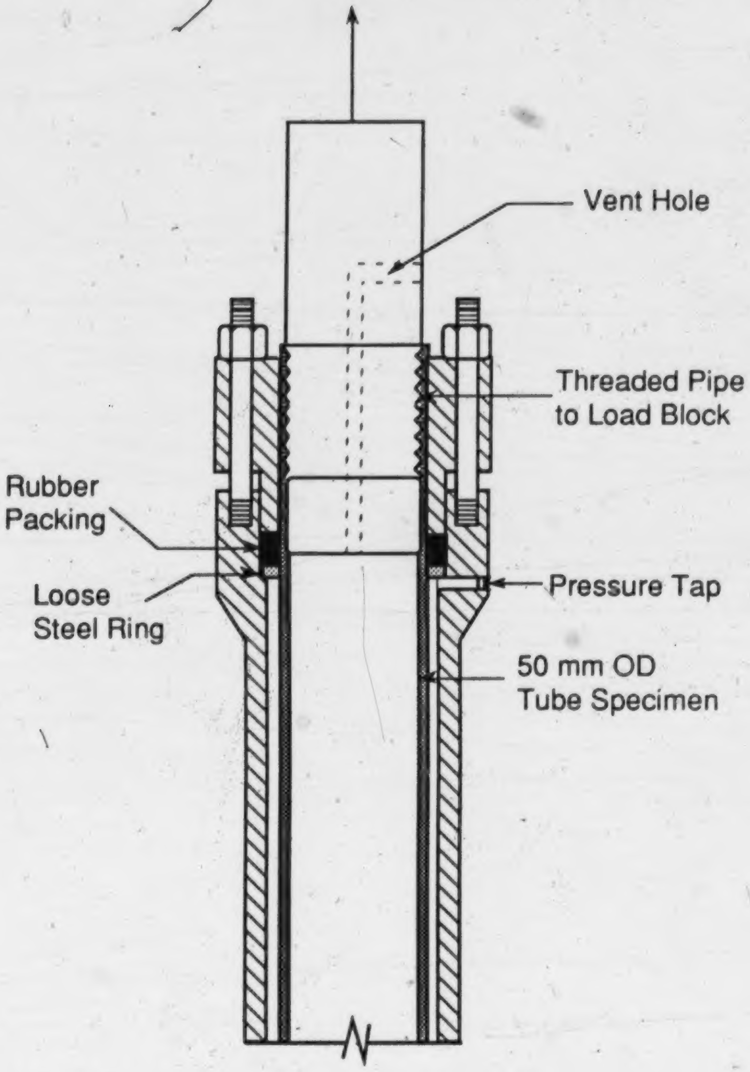
Vent Hole
Threaded Pipe to Load Block
Rubber Packing
Pressure Tap
Loose Steel Ring
50 mm OD Tube Specimen

Figure 3.4 - Collapse Chamber for Edwards and Miller (1939) 50mm Tubing

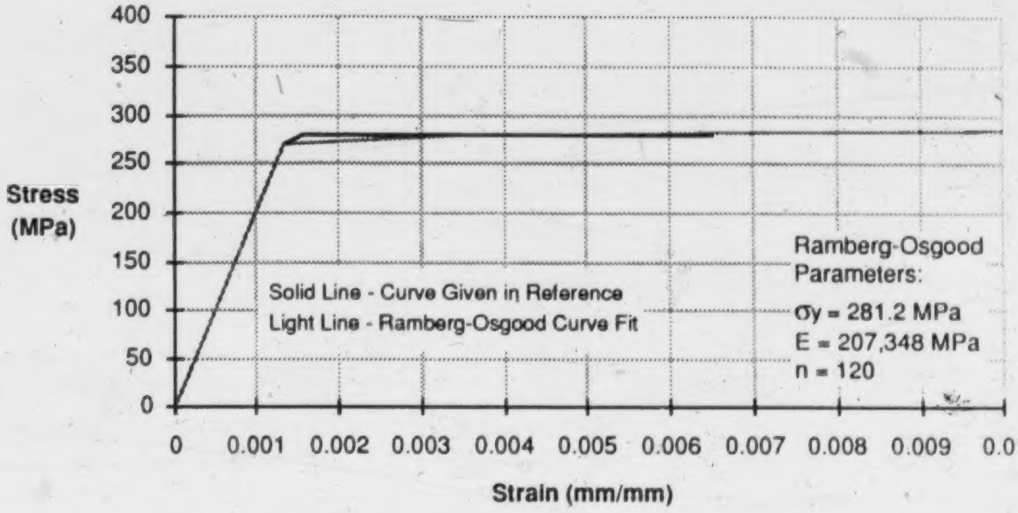

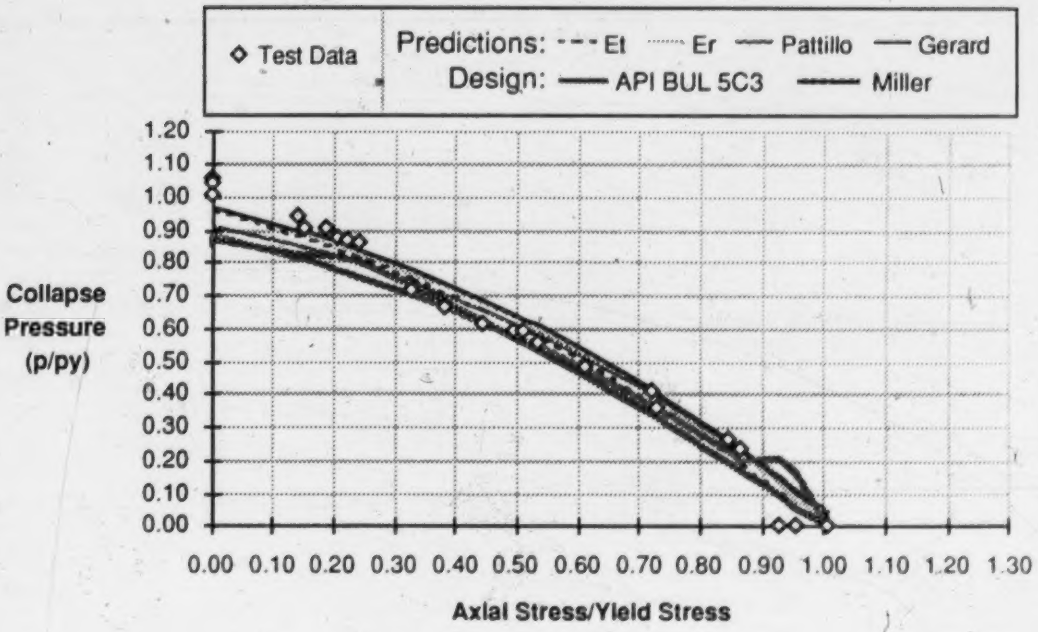

Figure 3.5 - Edwards and Miller (1939) Test Group 6 (OD/t = 16.6)

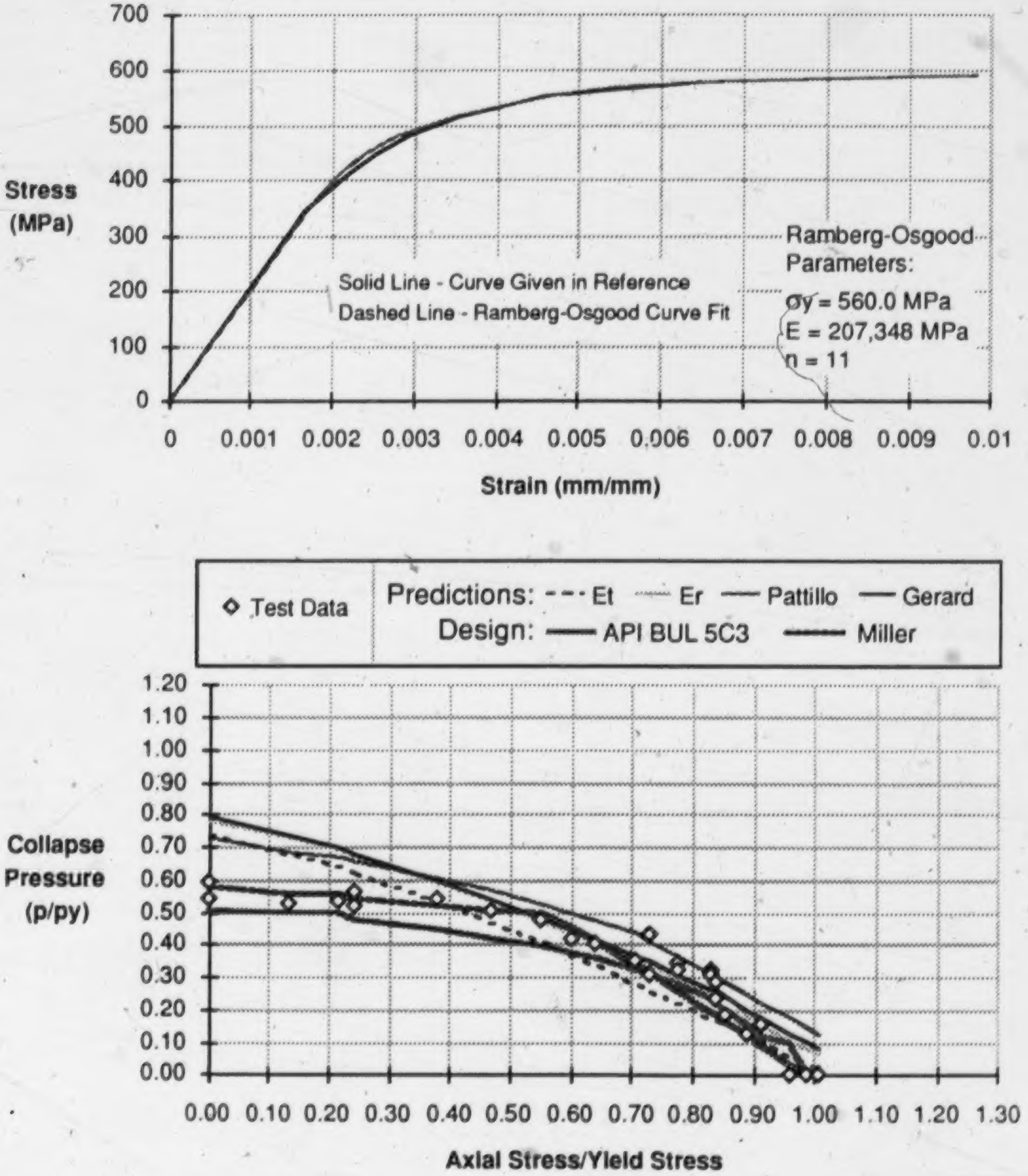

Figure 3.6 - Edwards and Miller (1939) Test Group 7 (OD/t = 21.7)

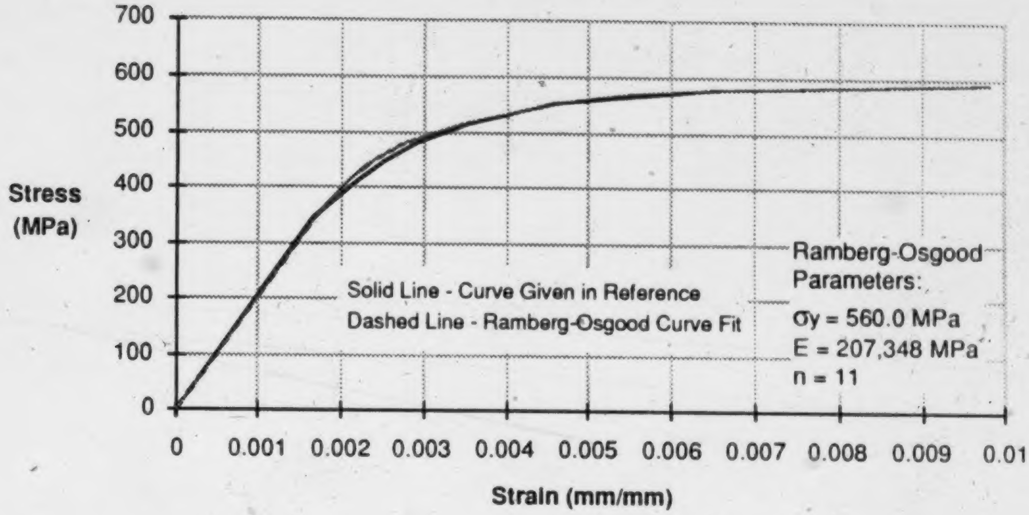

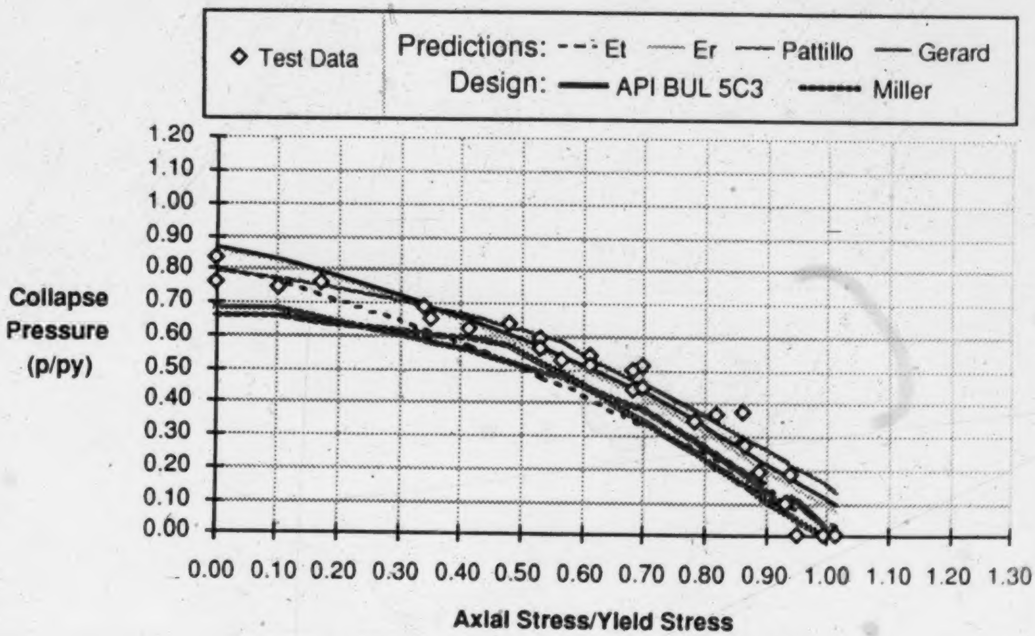

Figure 3.7 - Edwards and Miller (1939) Test Group 8 (OD/t = 17.3)

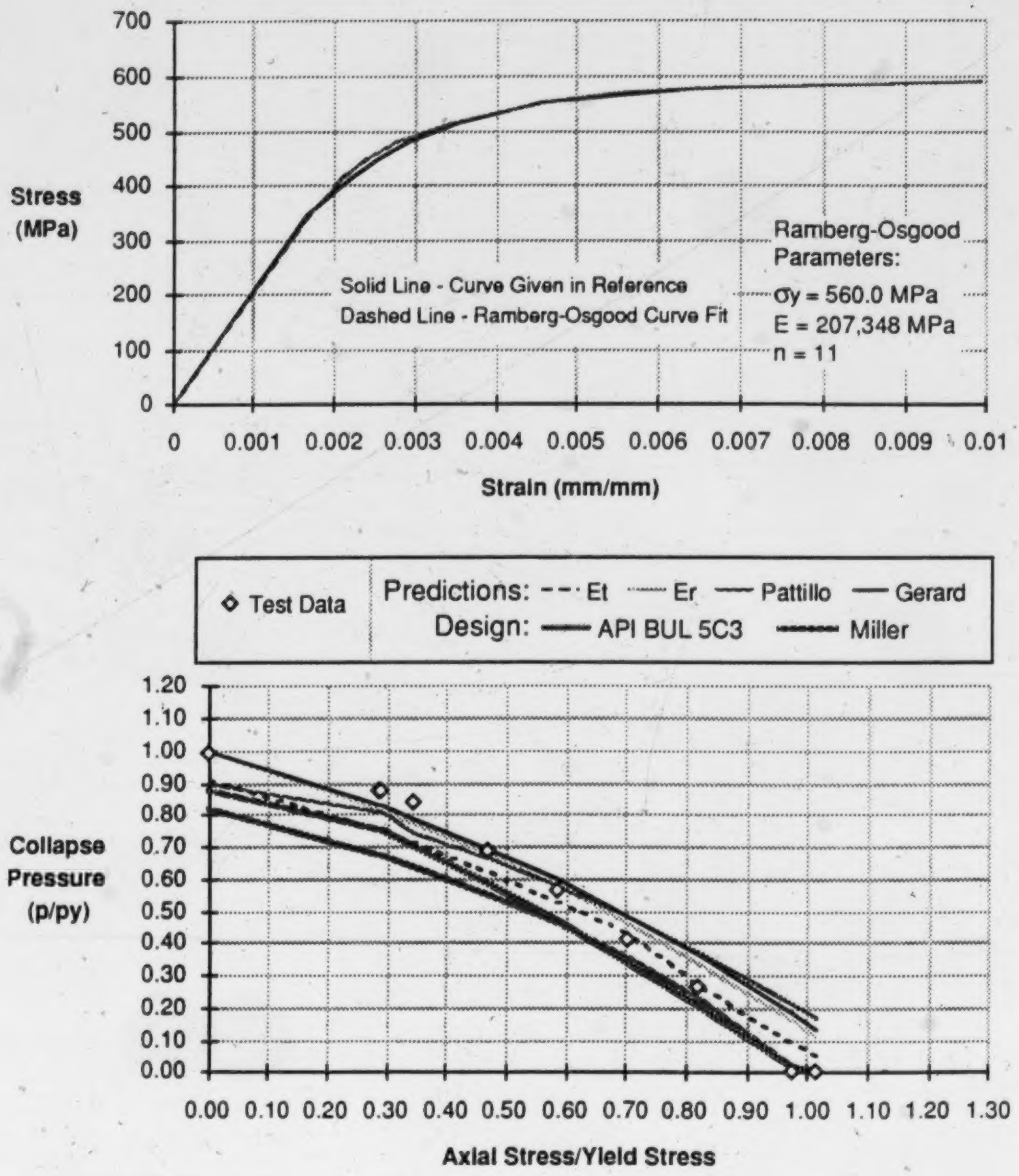

Figure 3.8 - Edwards and Miller (1939) Test Group 9 (OD/t = 11.2)

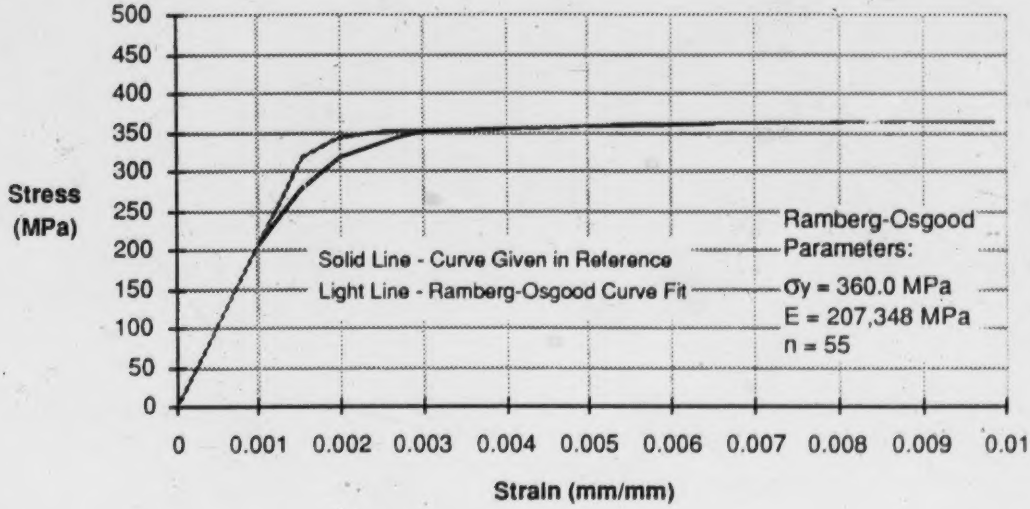

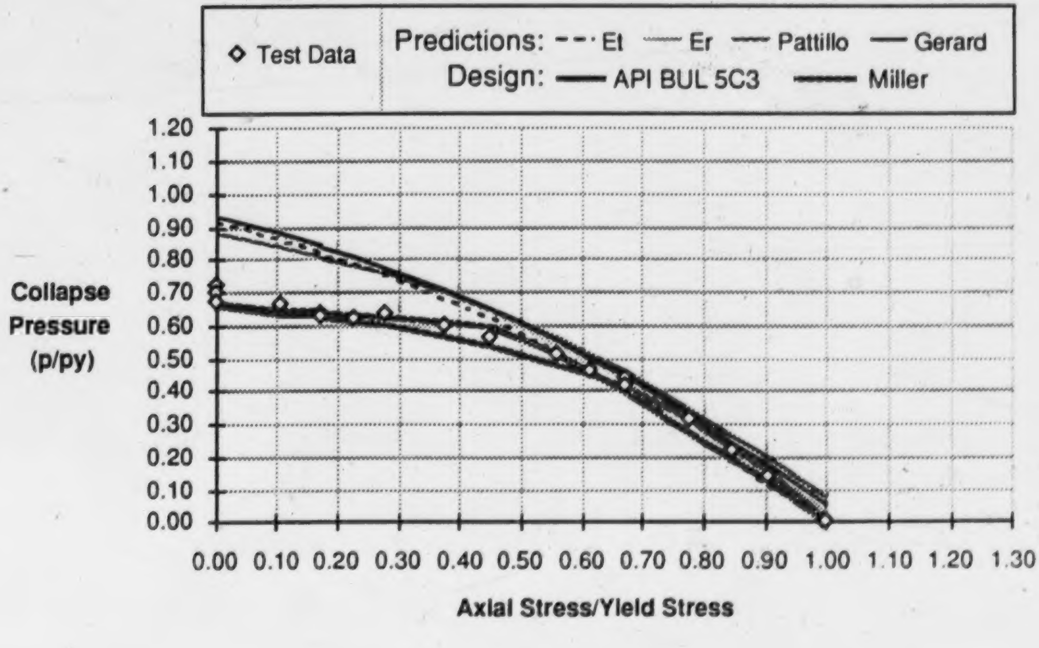

Figure 3.9 - Edwards and Miller (1939) Test Group 10 (OD/t = 21.7)

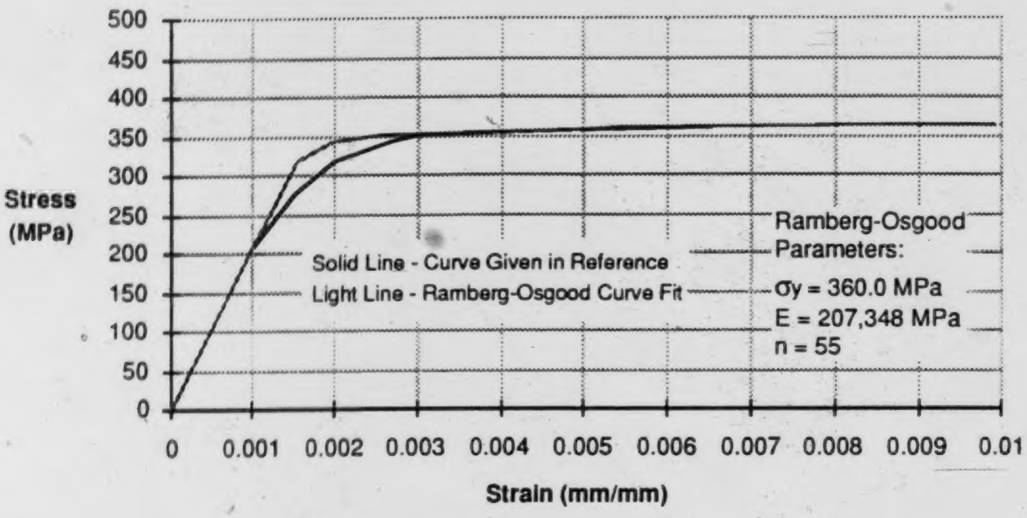

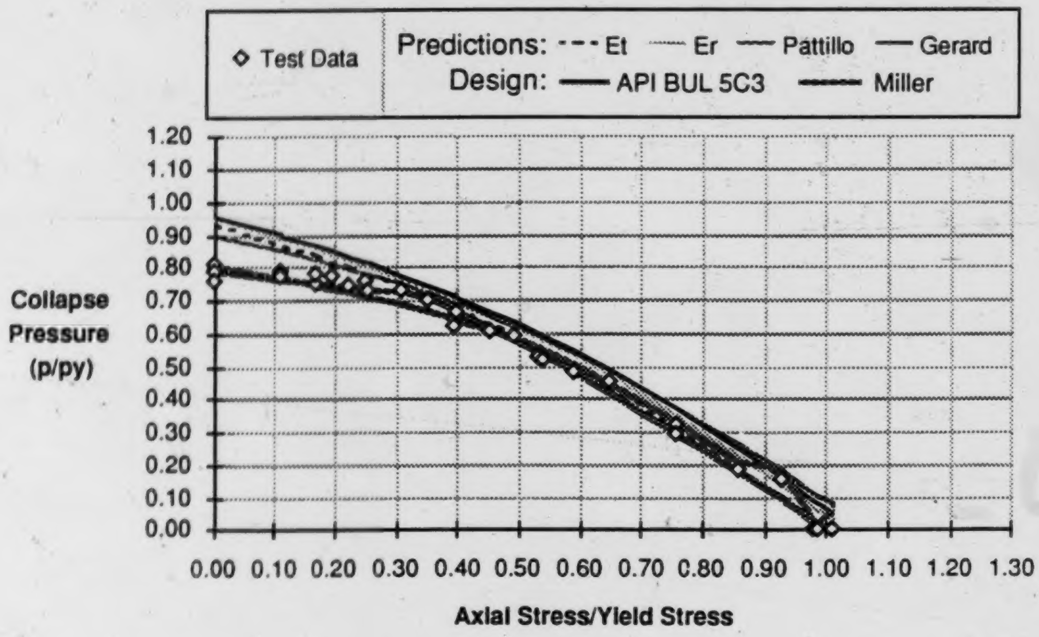

Figure 3.10 - Edwards and Miller (1939) Test Group 11 (OD/t = 17.3)

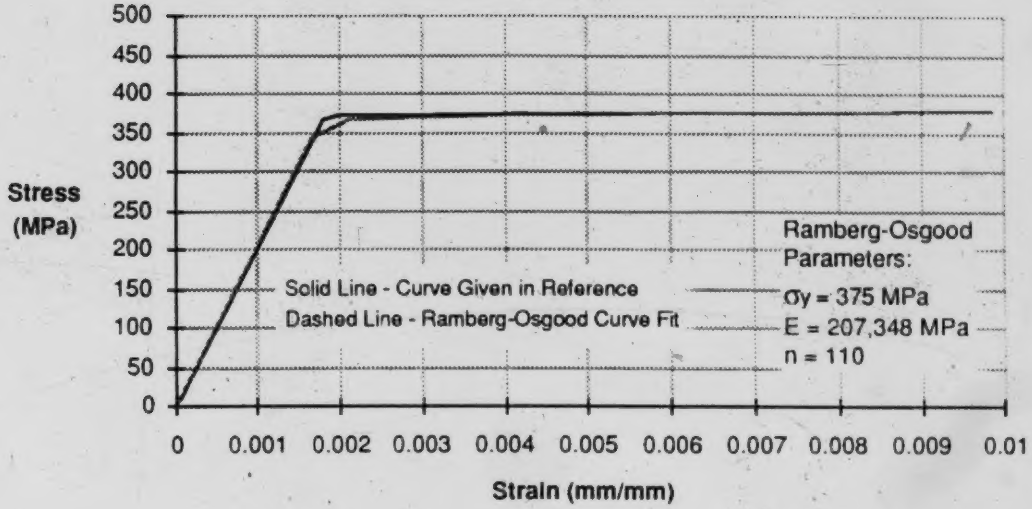

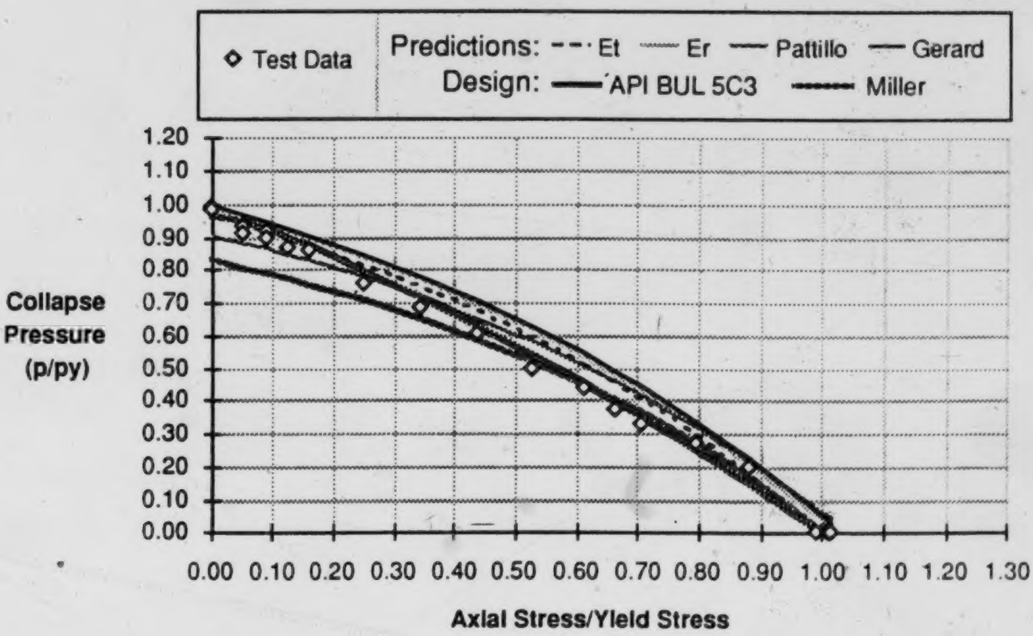

Figure 3.11 - Edwards and Miller (1939) Test Group 12 (OD/t = 11.2)

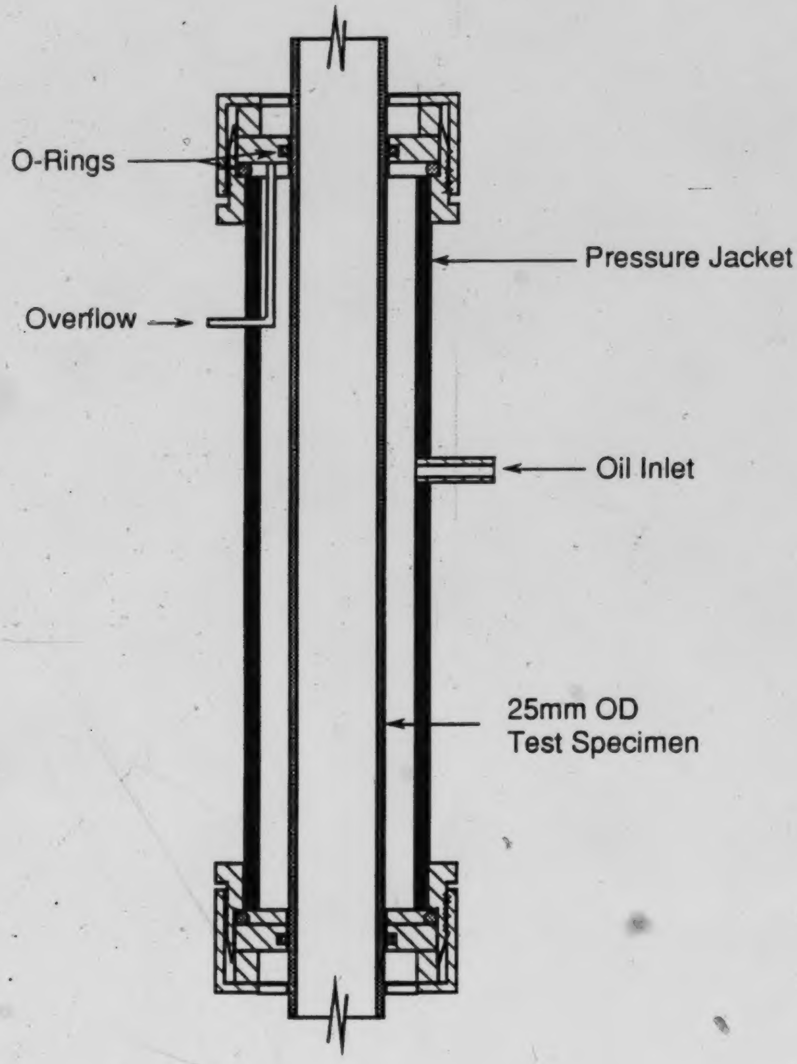
O-Rings
Pressure Jacket
Overflow
Oil Inlet
25mm OD
Test Specimen

Figure 3.12 - Collapse Chamber for Stuiver and Tomalin (1959) 25mm Tubing

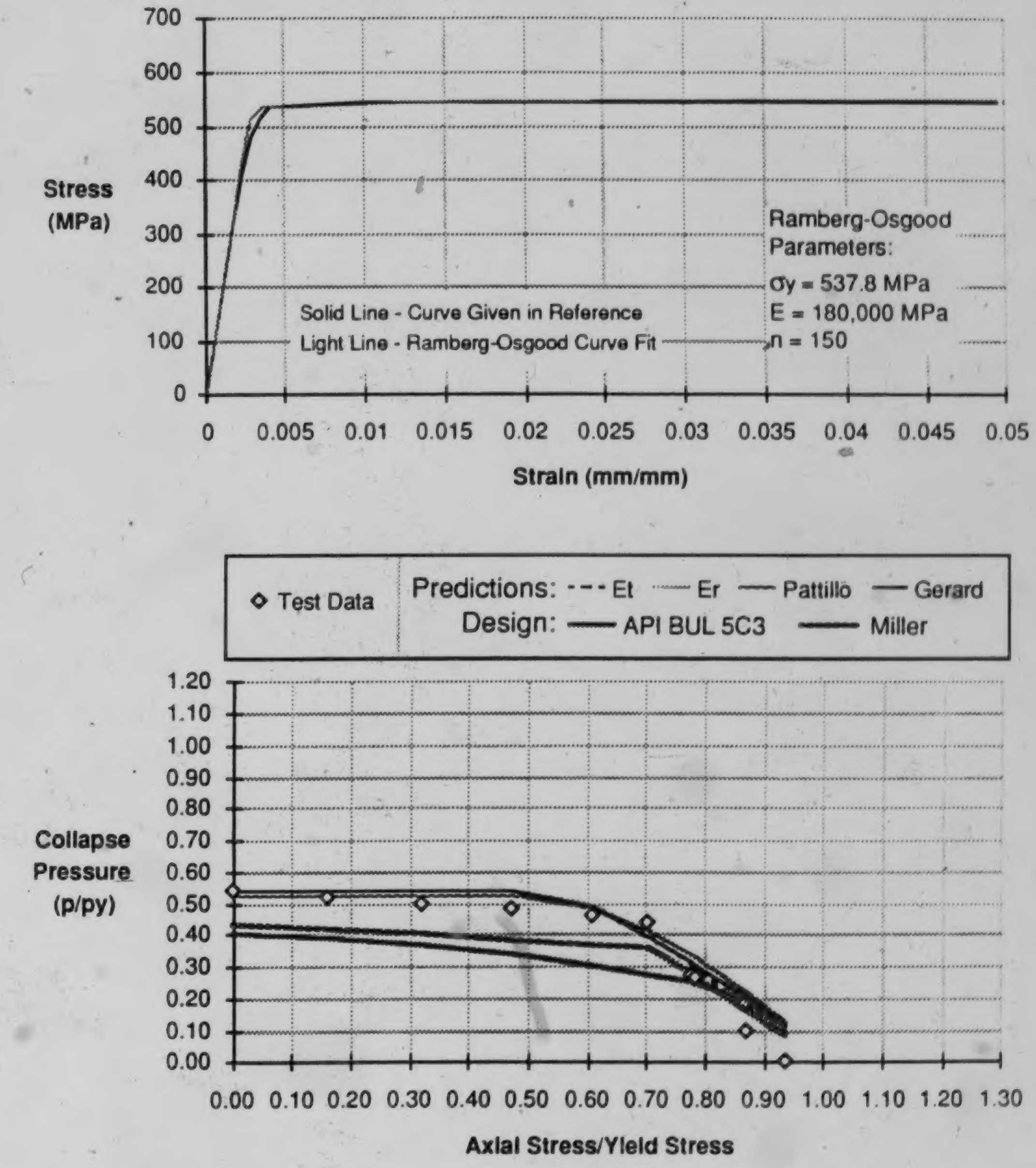

Figure 3.13 - Stuiver and Tomalin (1959) Test Group 1 (OD/t = 27.0)

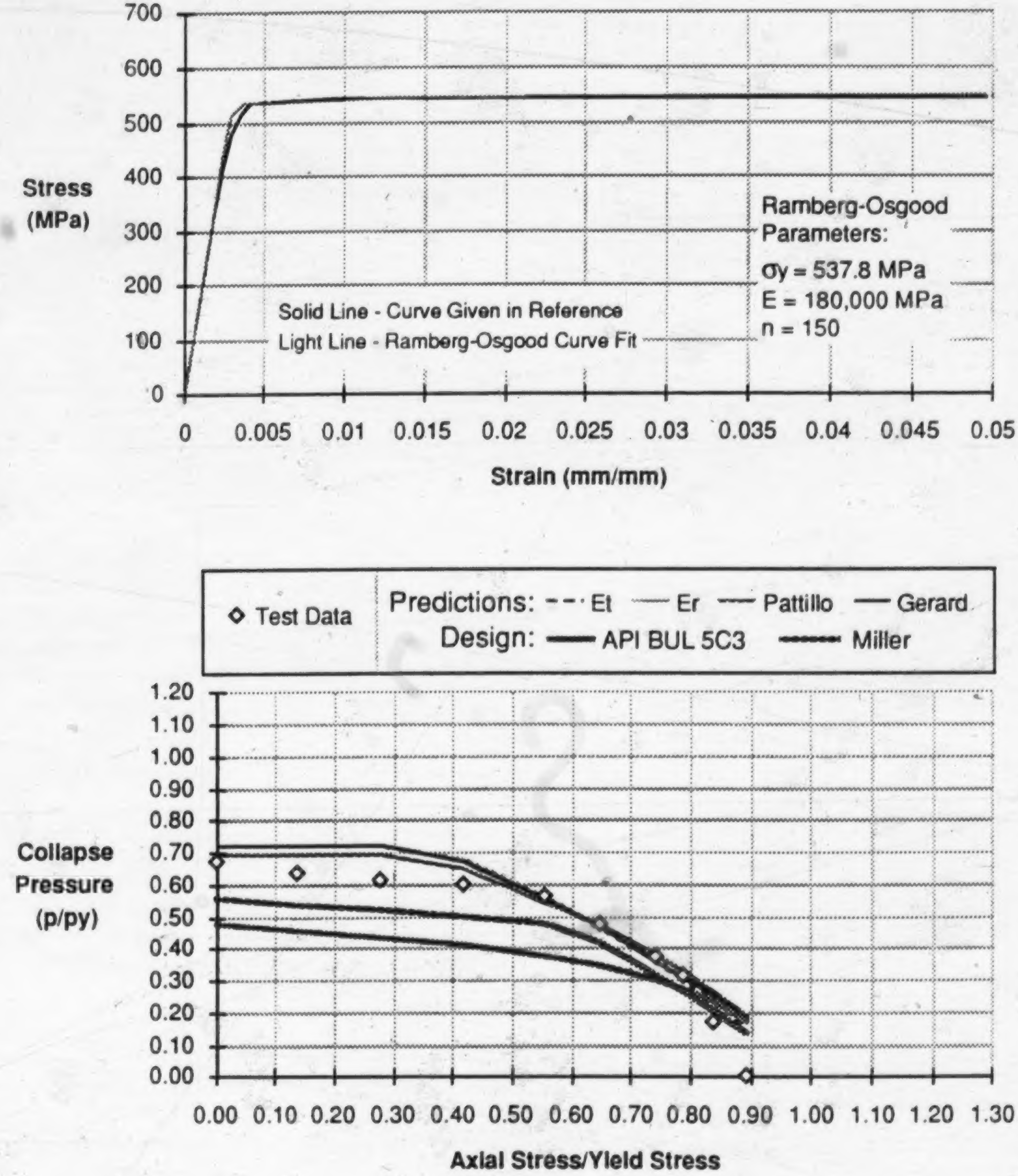

Figure 3.14 - Stuiver and Tomalin (1959) Test Group 2 (OD/t = 23.5)

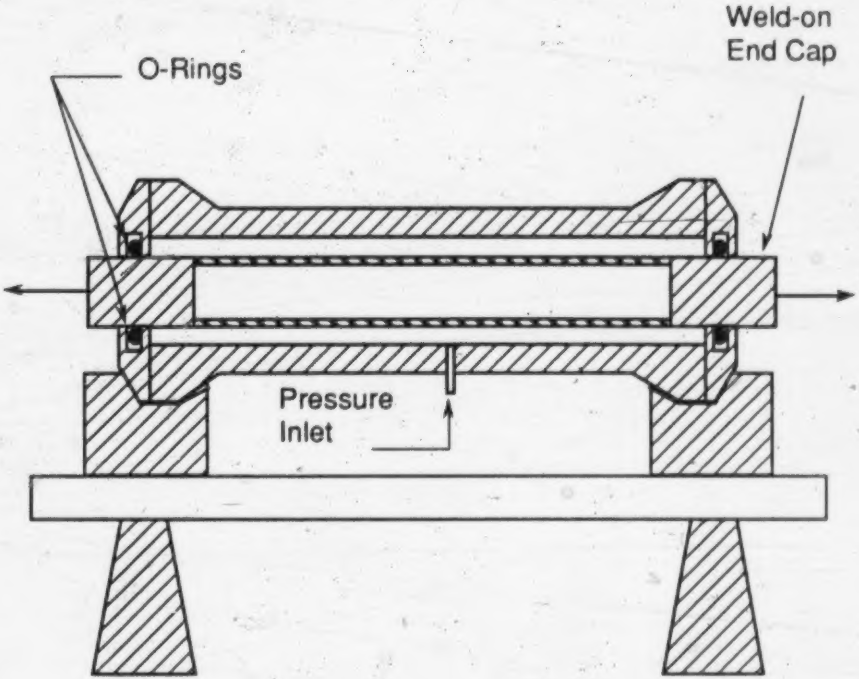
O-Rings
Weld-on
End Cap
Pressure
Inlet

Figure 3.15 - Collapse Chamber for Tamano et al. (1982) 178mm Casing

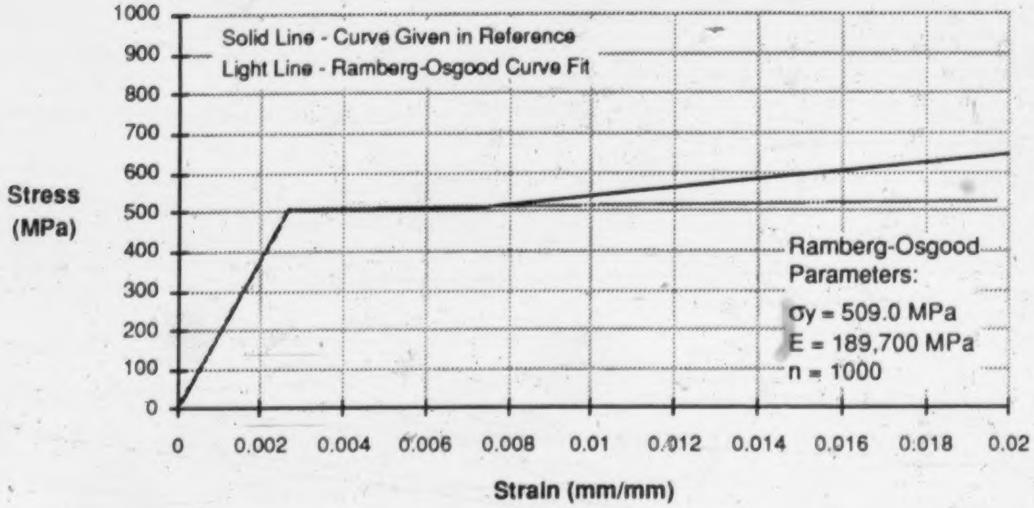

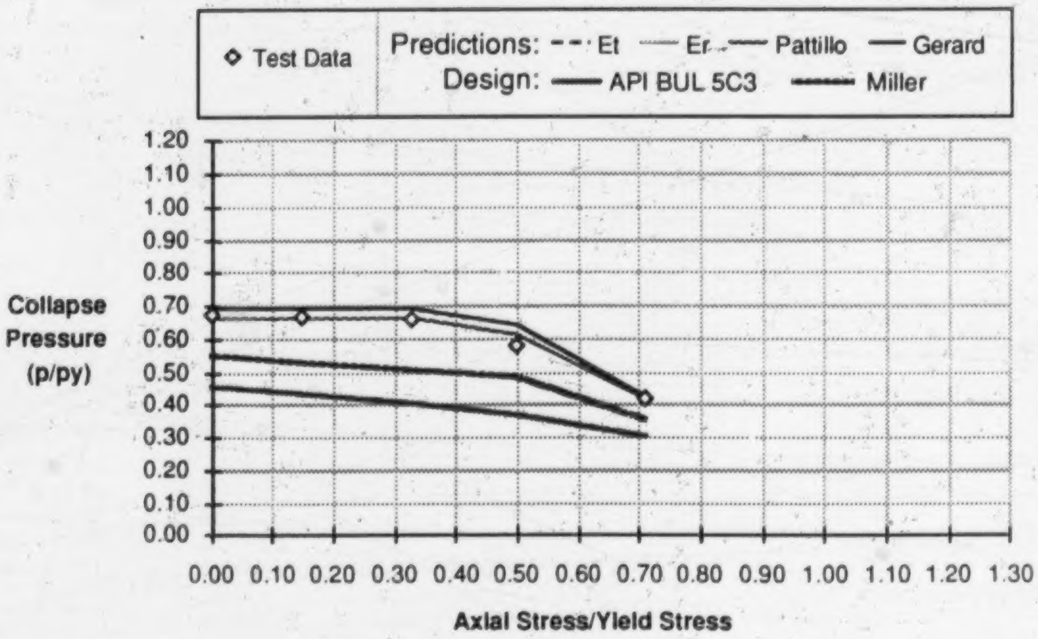

Figure 3.16 - Tamano et al. (1982) Test Group K55-1 (OD/t = 25.3)

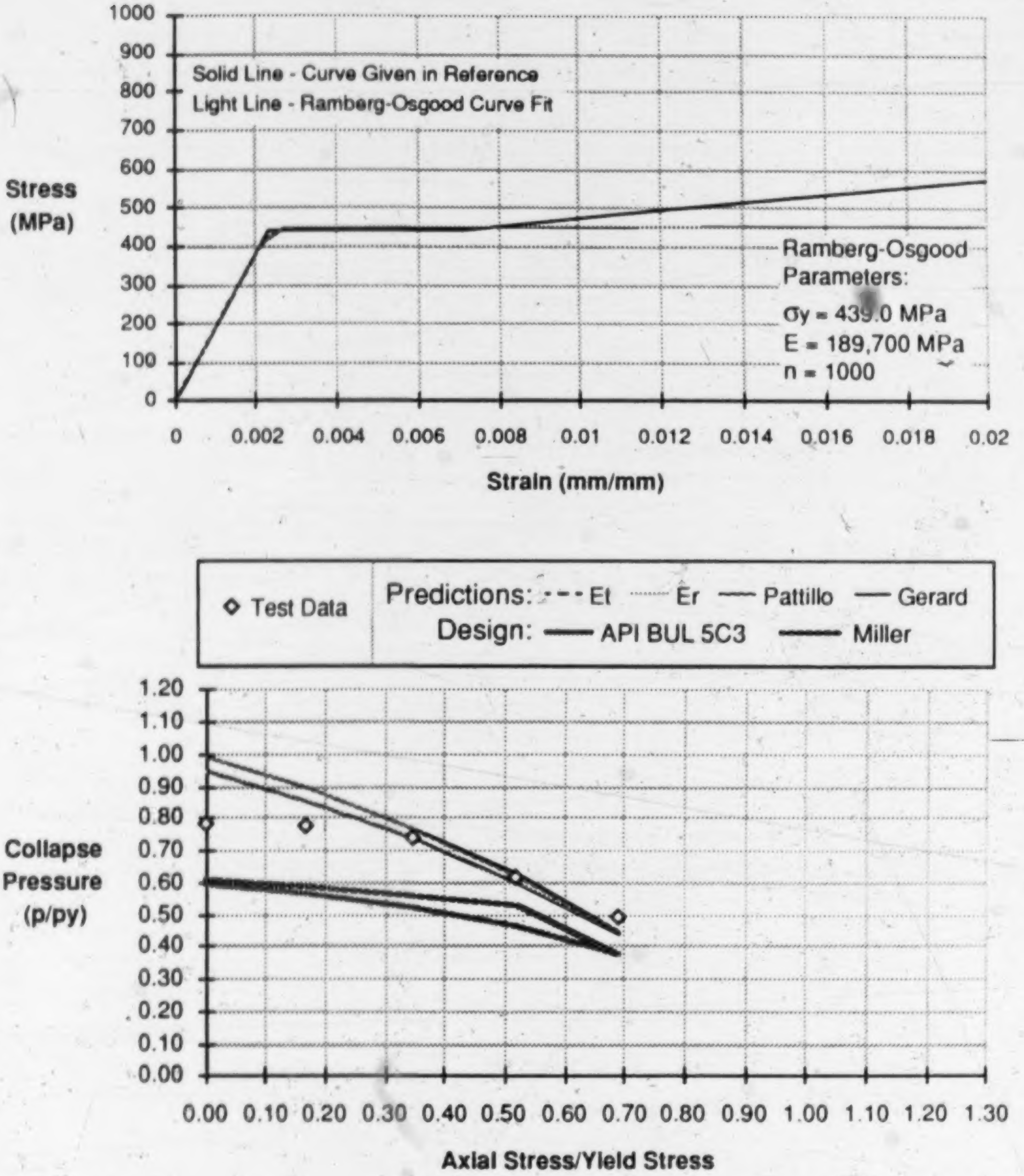

Figure 3.17 - Tamano et al. (1982) Test Group K55-2
(OD/t = 21.8)

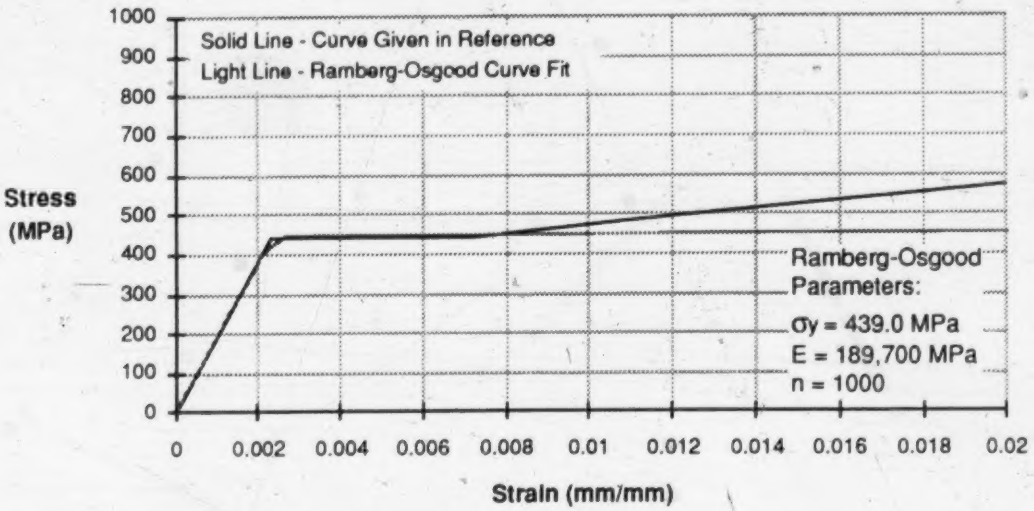

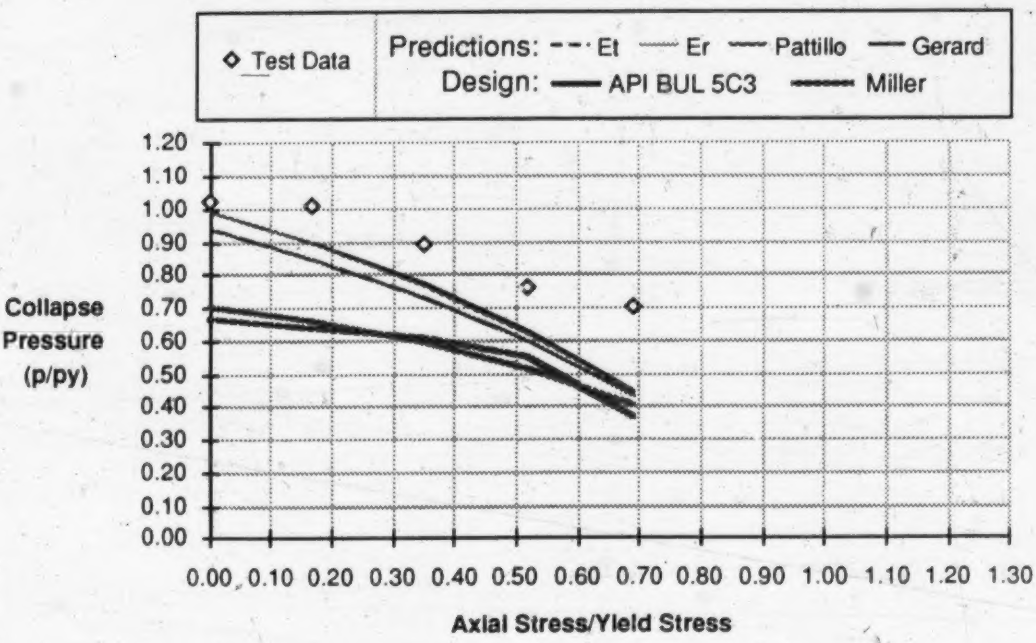

Figure 3.18 - Tamano et al. (1982) Test Group K55-3
(OD/t = 18.9)

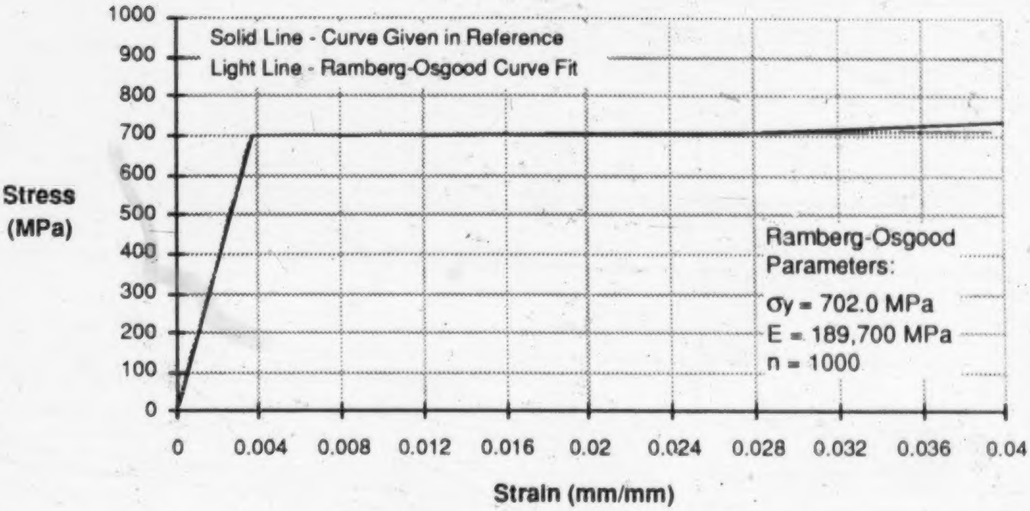

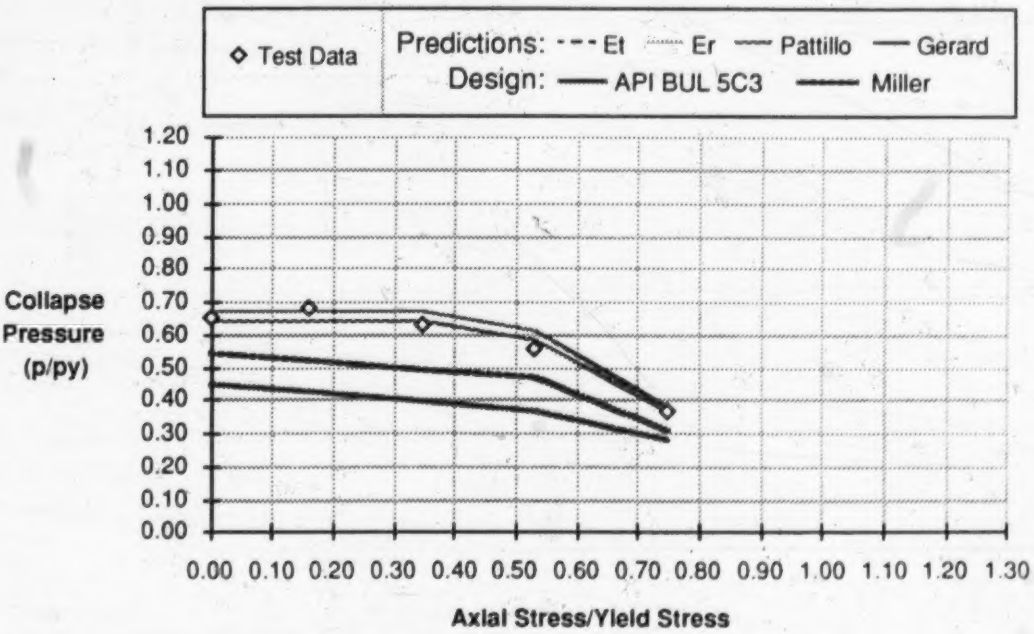

Figure 3.19 - Tamano et al. (1982) Test Group N80-1 (OD/t = 22.0)

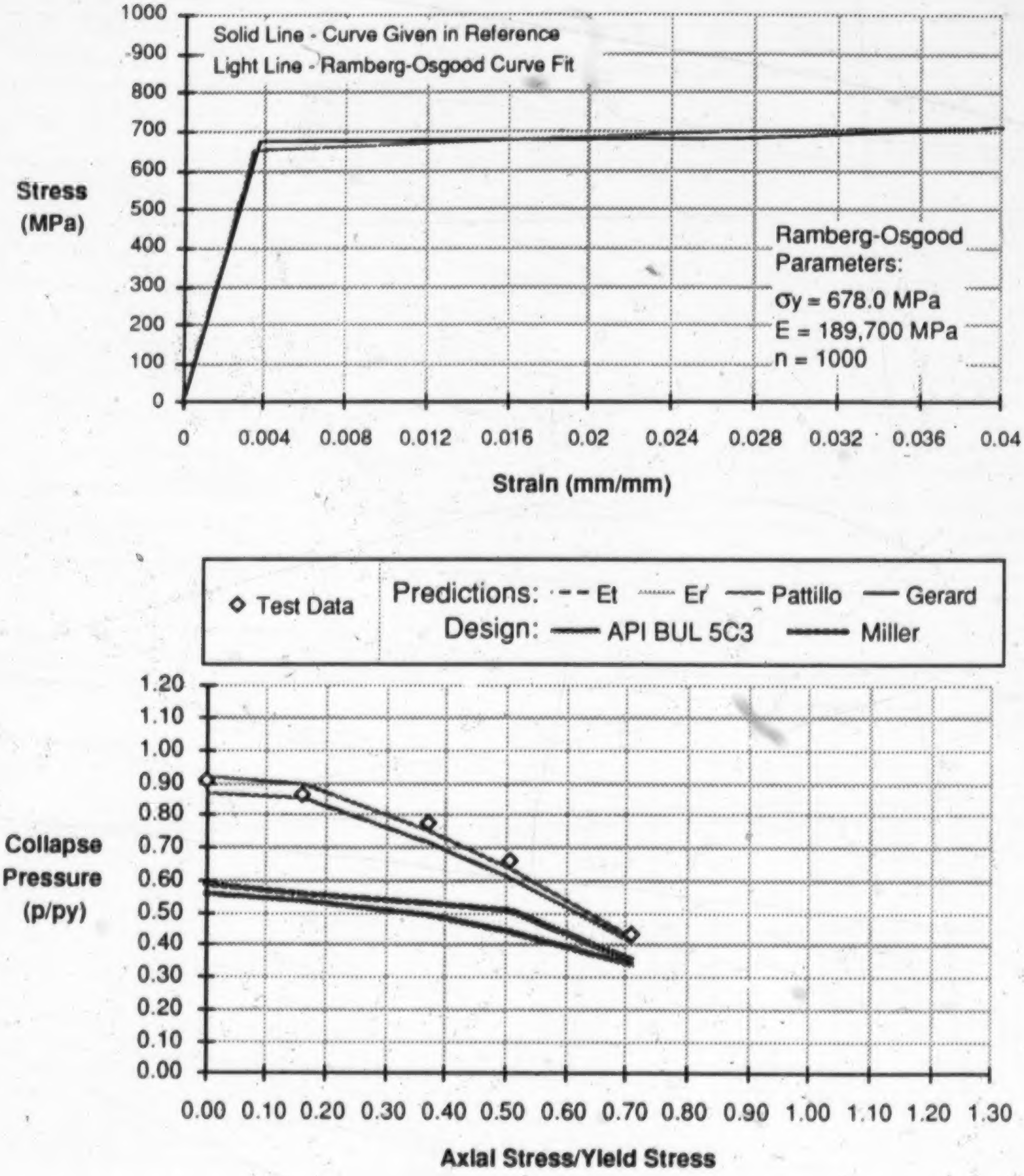

Figure 3.20 - Tamano et al. (1982) Test Group N80-2 (OD/t = 19.3)

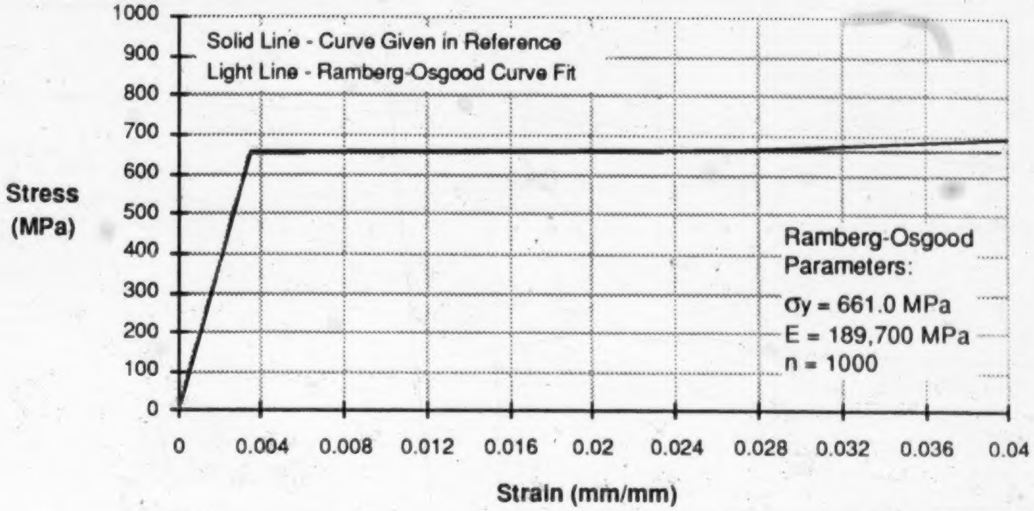

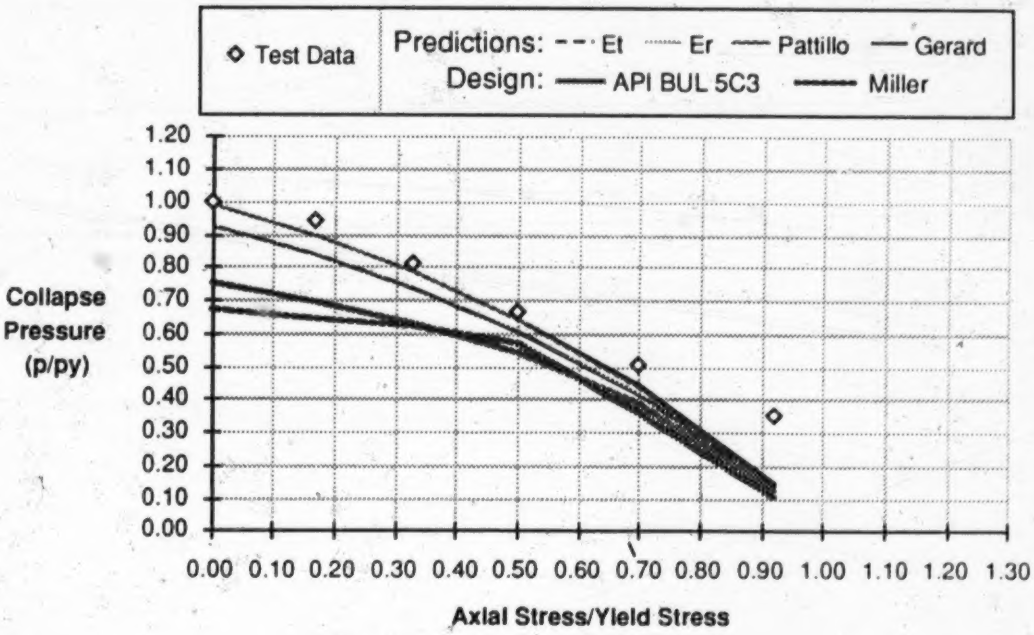

Figure 3.21 - Tamano et al. (1982) Test Group N80-3 (OD/t = 15.2)

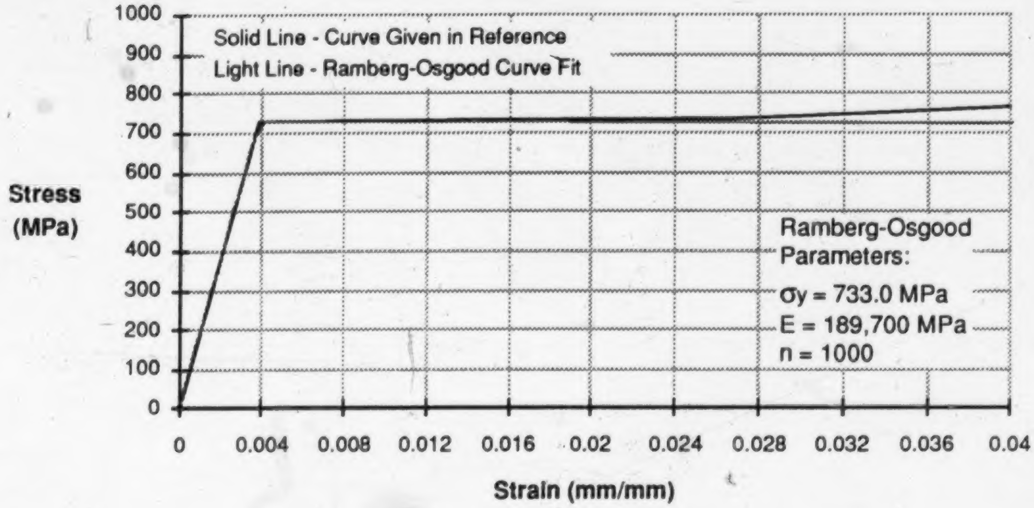

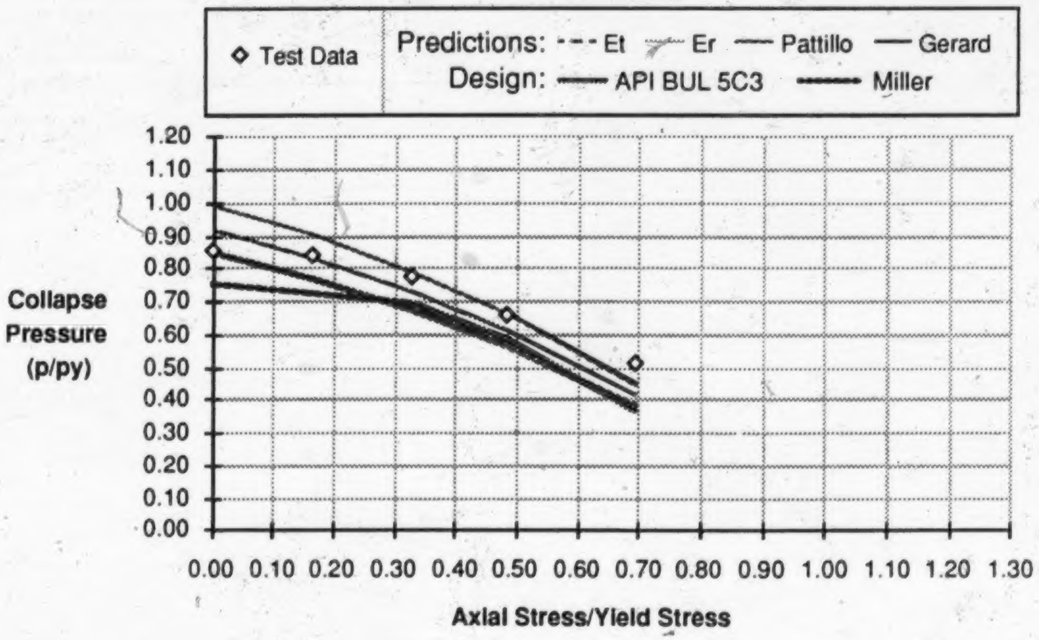

Figure 3.22 - Tamano et al. (1982) Test Group N80-4
(OD/t = 12.6)

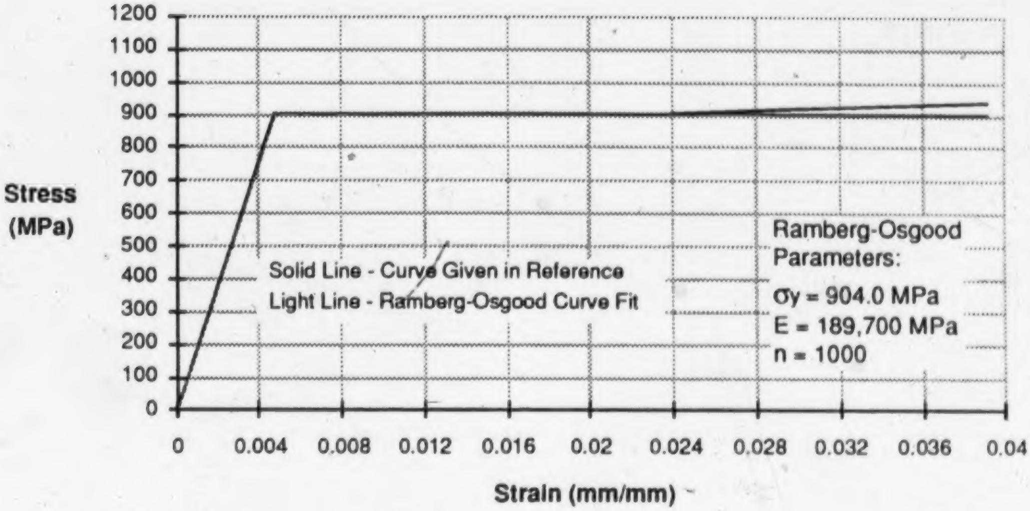

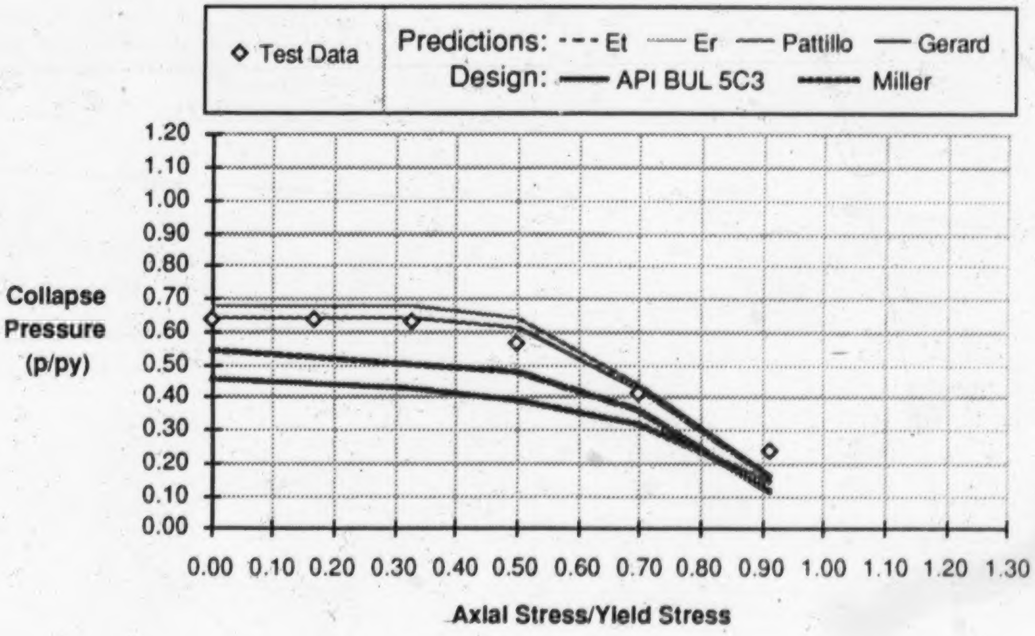

Figure 3.23 - Tamano et al. (1982) Test Group P110-1 (OD/t = 19.4)

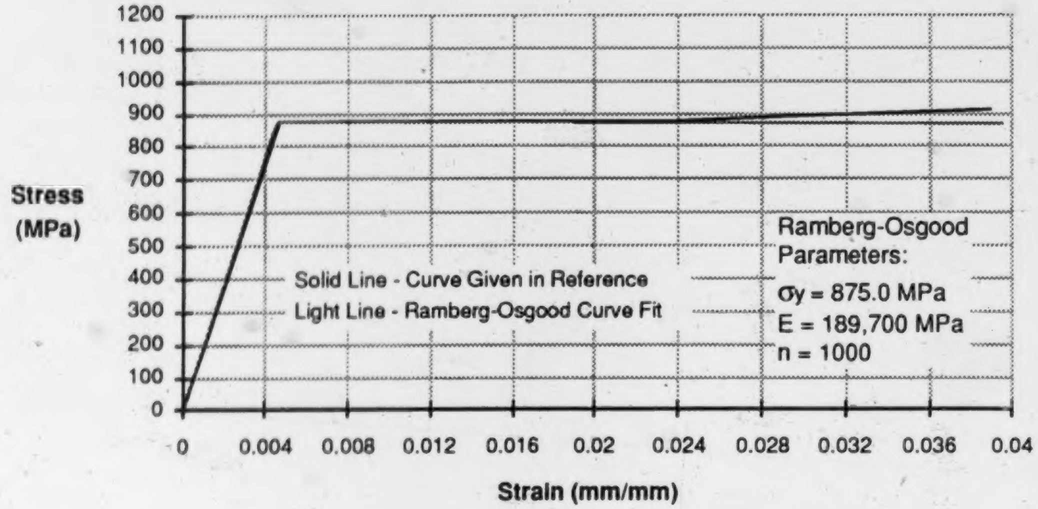

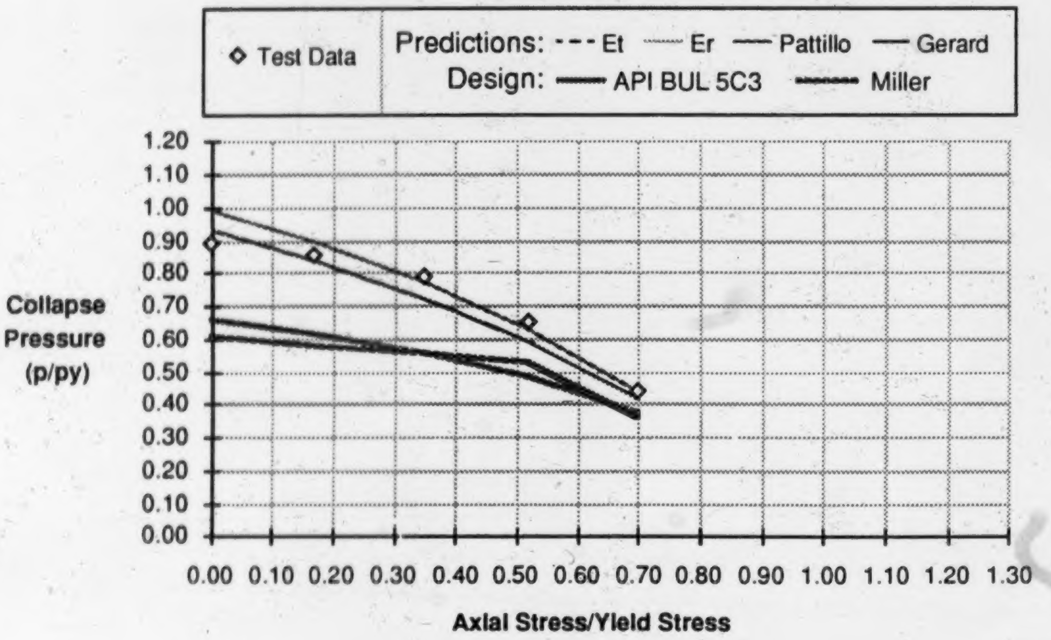

Figure 3.24 - Tamano et al. (1982) Test Group P110-2 (OD/t = 15.8)

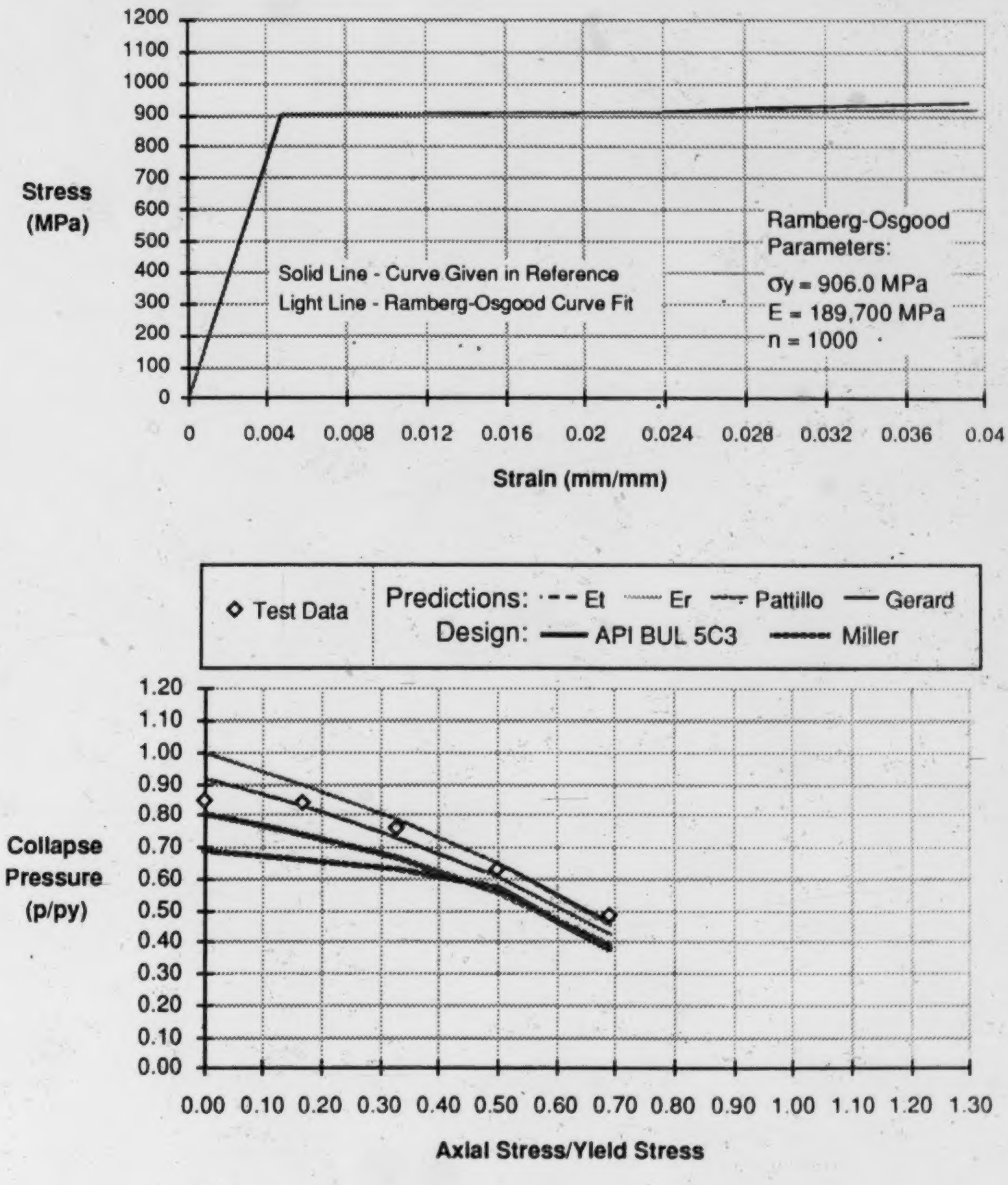

Figure 3.25 - Tamano et al. (1982) Test Group P110-3 (OD/t = 12.8)

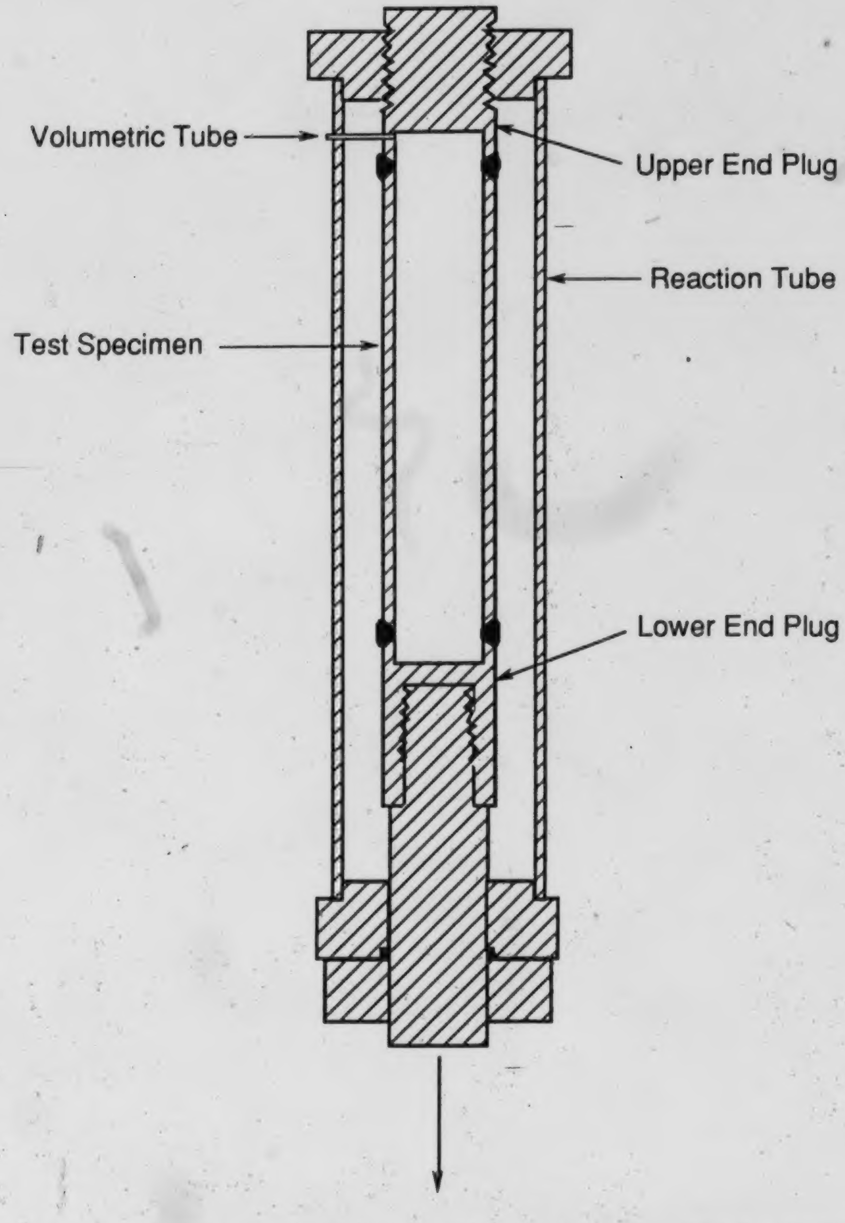
Volumetric Tube
Upper End Plug
Reaction Tube
Test Specimen
Lower End Plug

Figure 3.26 - Collapse Chamber for Gulf Canada (1987) 169mm Casing

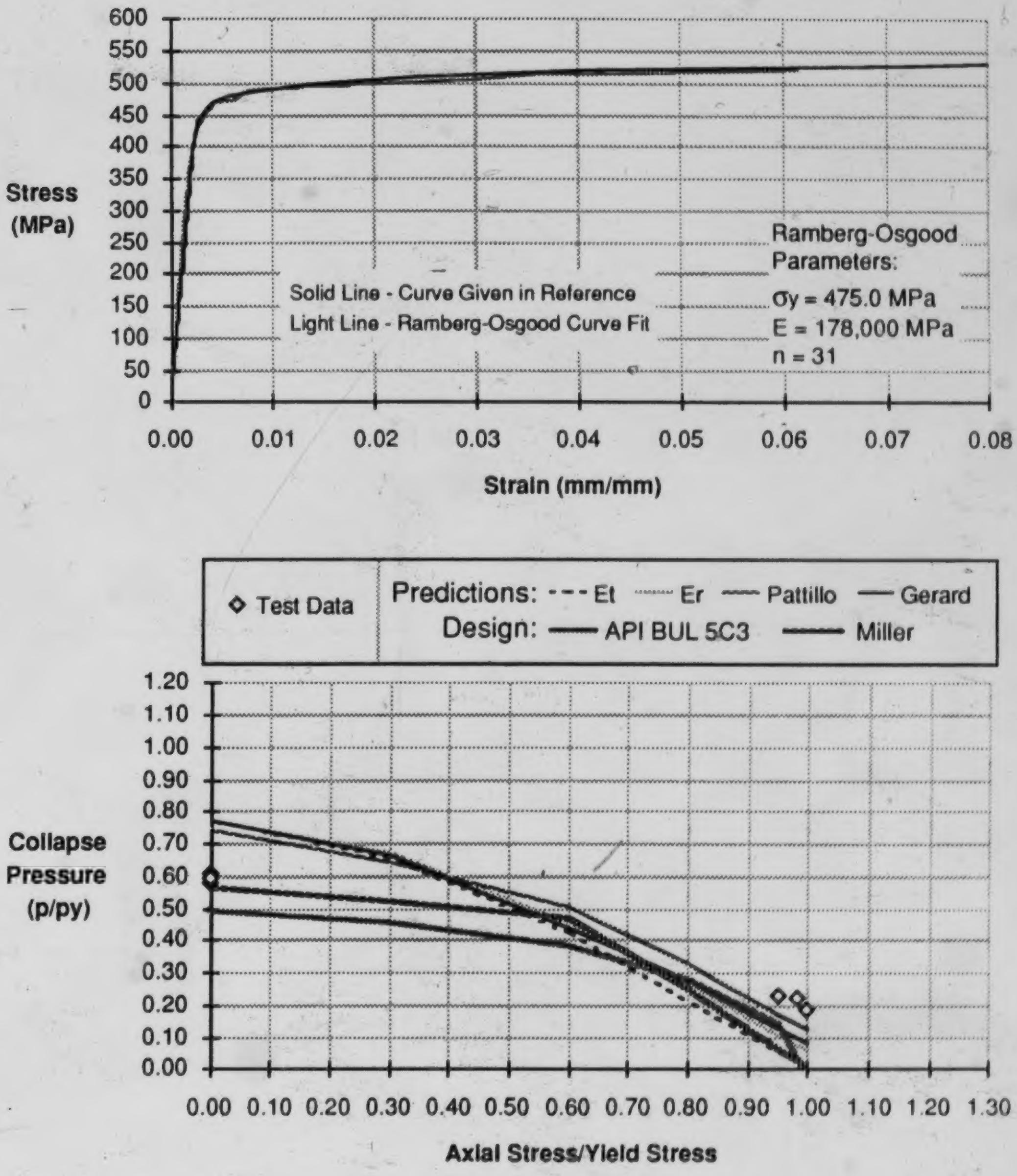

Figure 3.27 - Gulf Canada (1987) Test Group 1 (OD/t = 23.8)

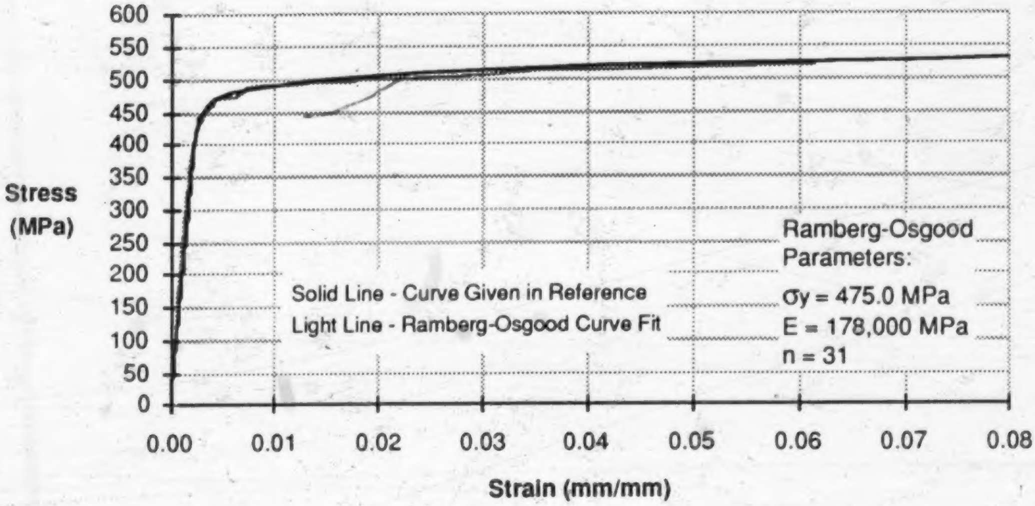

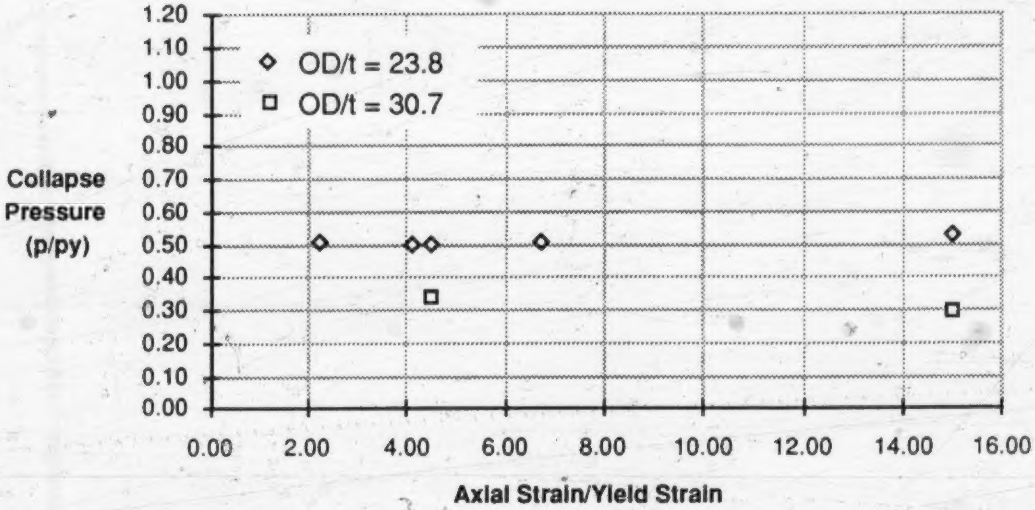

Figure 3.28 - Gulf Canada (1987) Constant Axial Strain Test Data (OD/t = 23.8 and 30.7)

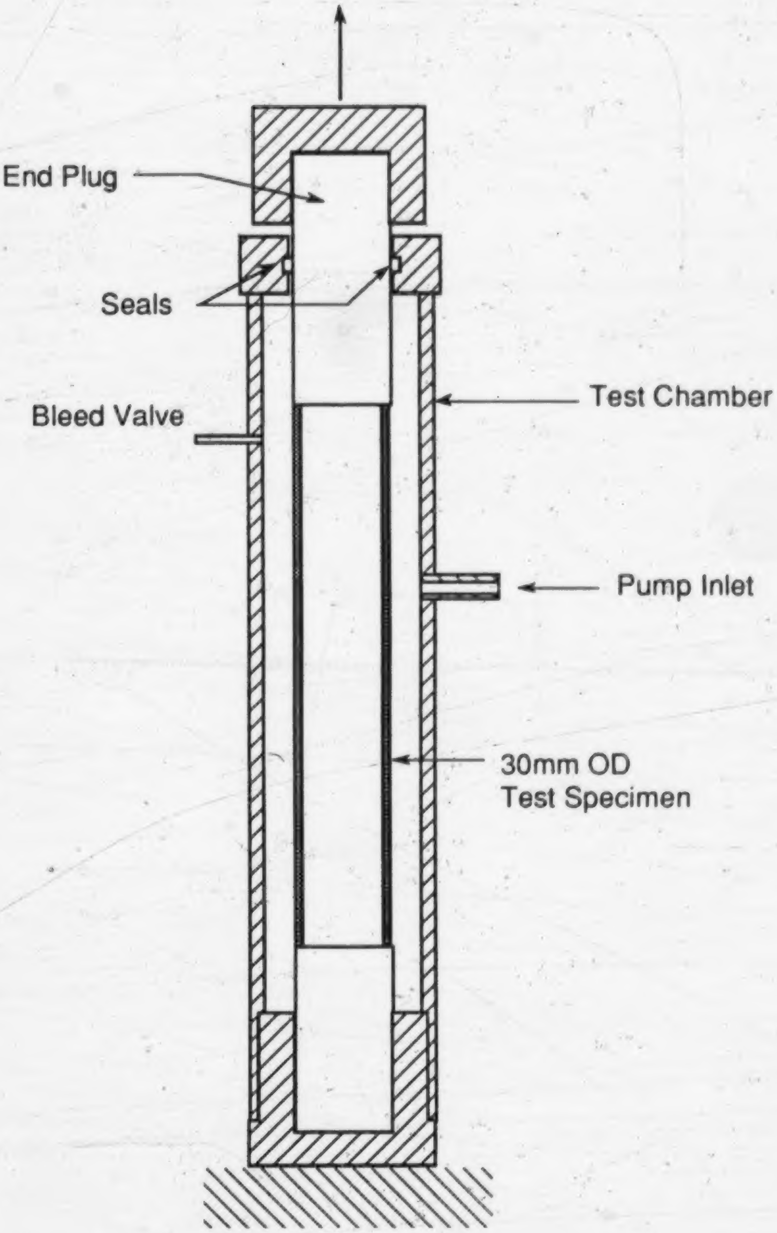
End Plug
Seals
Test Chamber
Bleed Valve
Pump Inlet
30mm OD
Test Specimen

Figure 3.29 - Schematic of Madhavan (1988) Test Apparatus

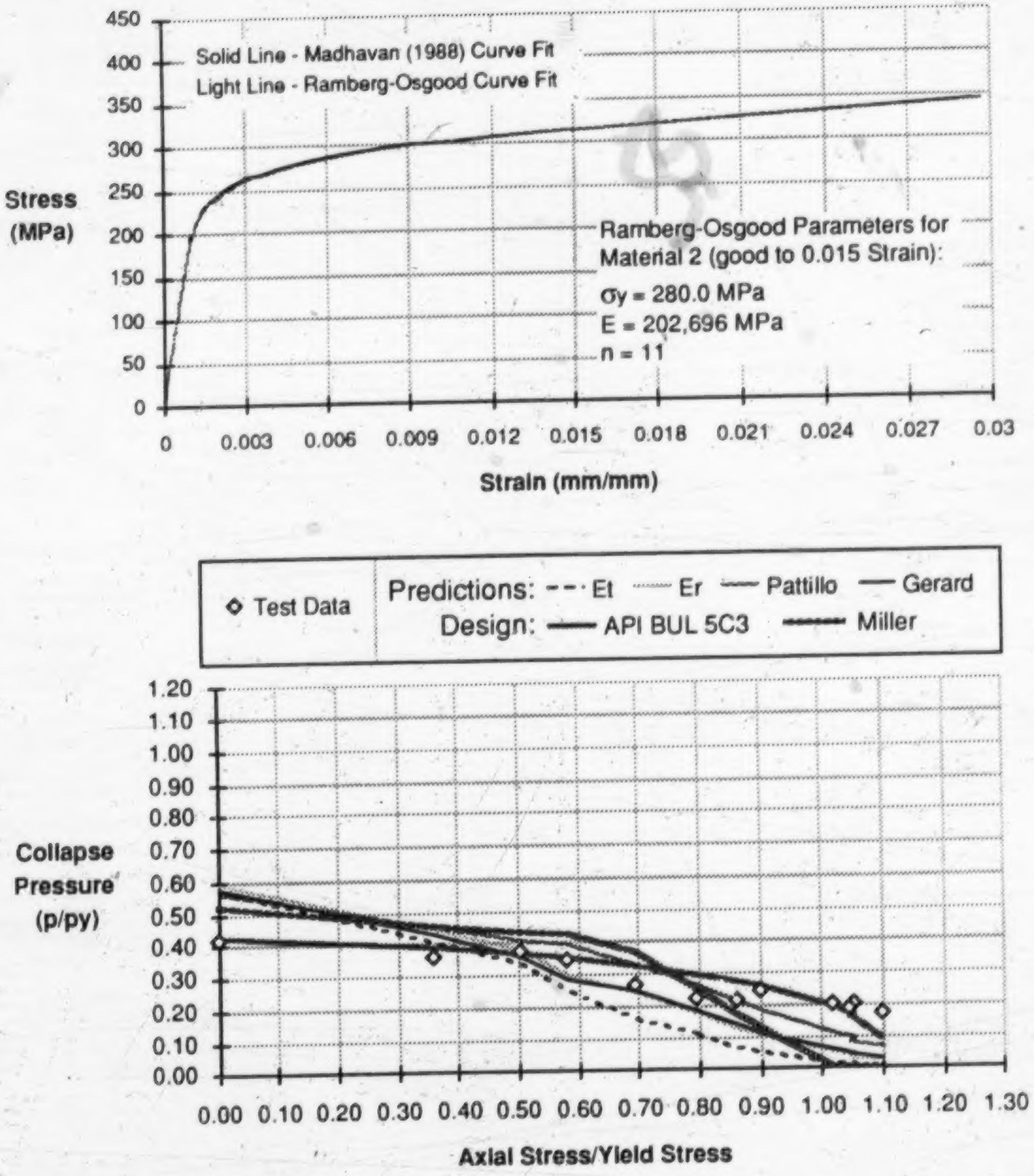

Figure 3.30 - Madhavan (1988) Test Group 1, Stainless Steel (OD/t = 36.7)

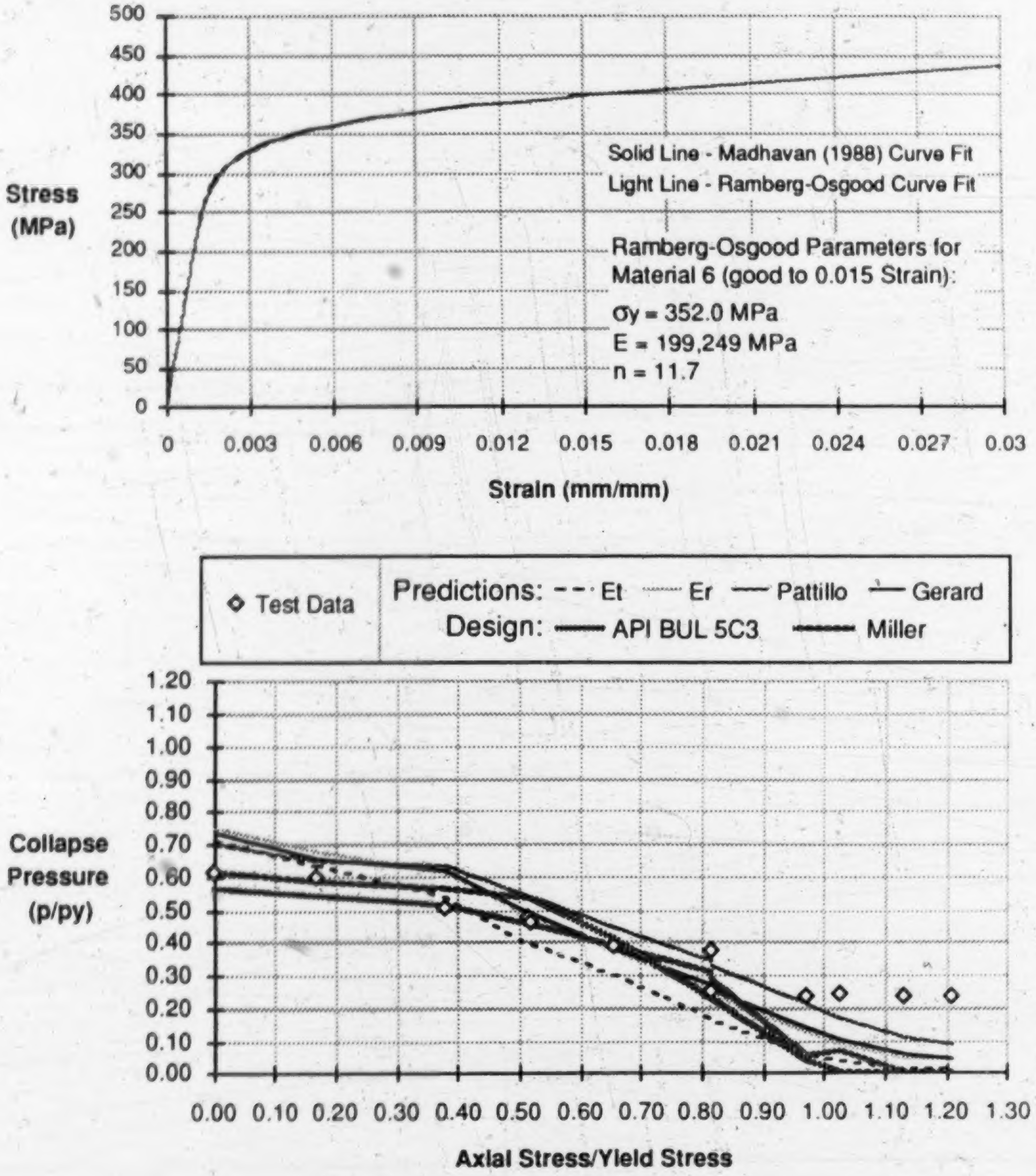

Figure 3.31 - Madhavan (1988) Test Group 2, Stainless Steel (OD/t = 24.5)

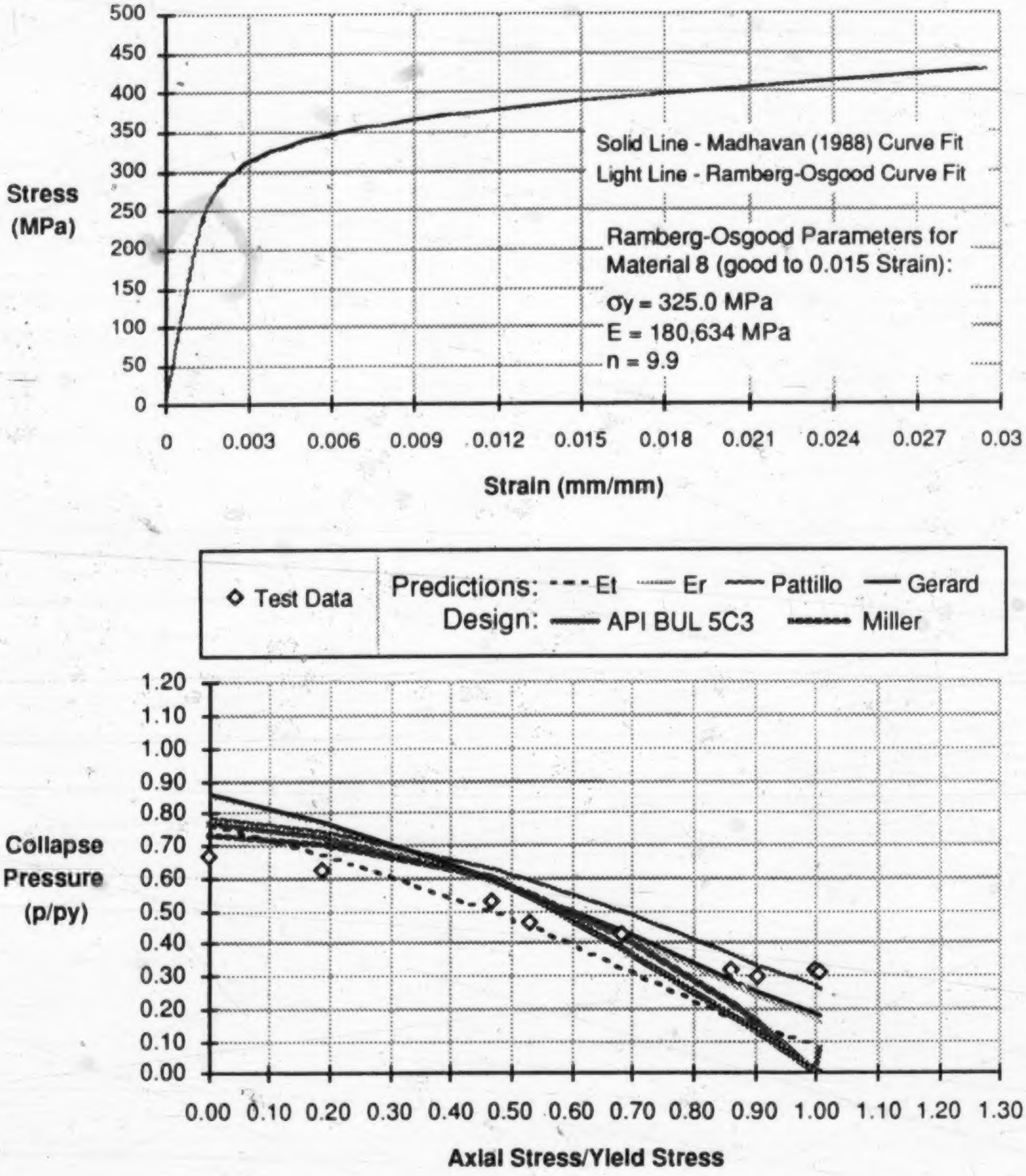

Figure 3.32 - Madhavan (1988) Test Group 3, Stainless Steel (OD/t = 18.7)

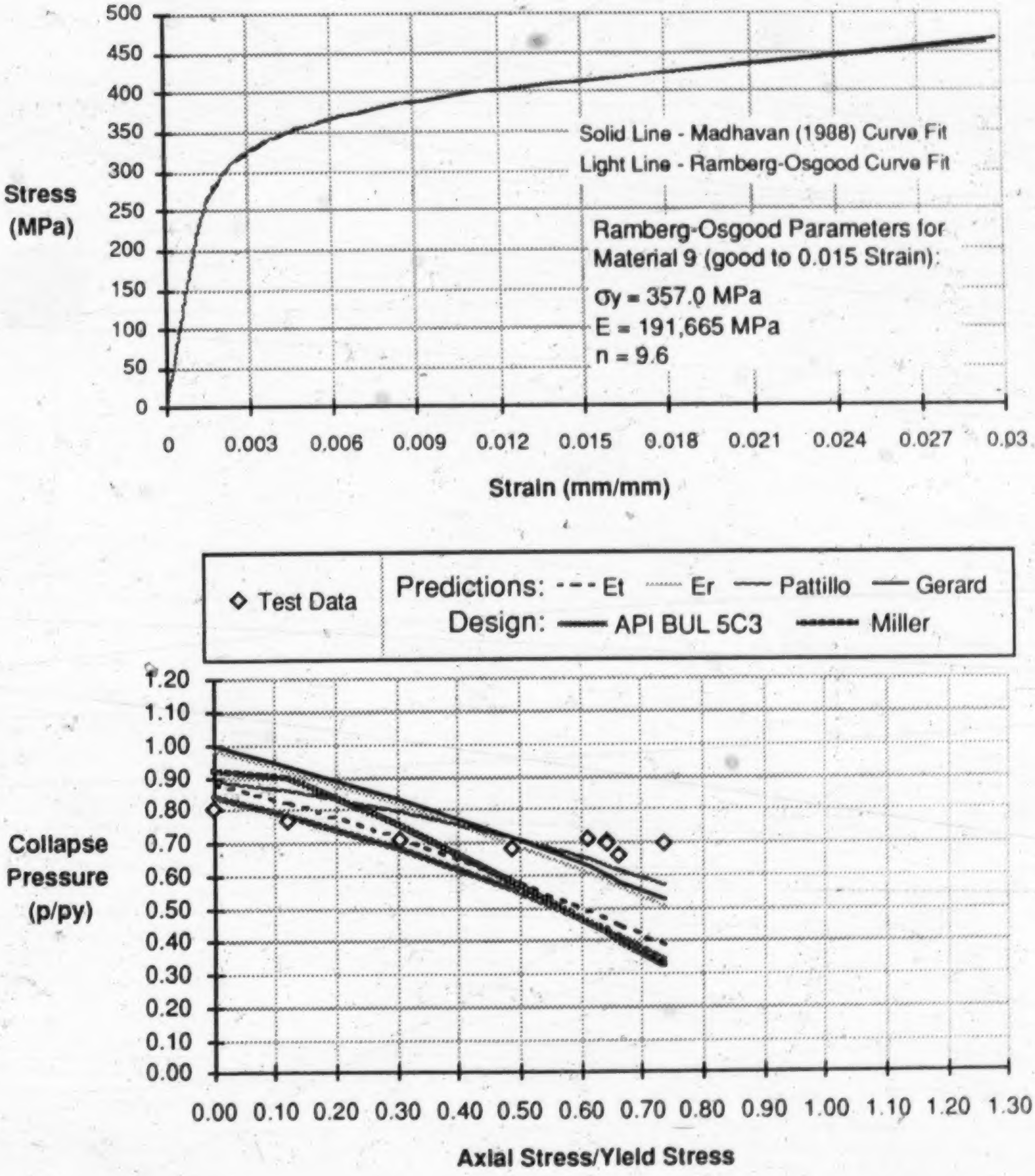

Figure 3.33 - Madhavan (1988) Test Group 4, Stainless Steel (OD/t = 12.1)

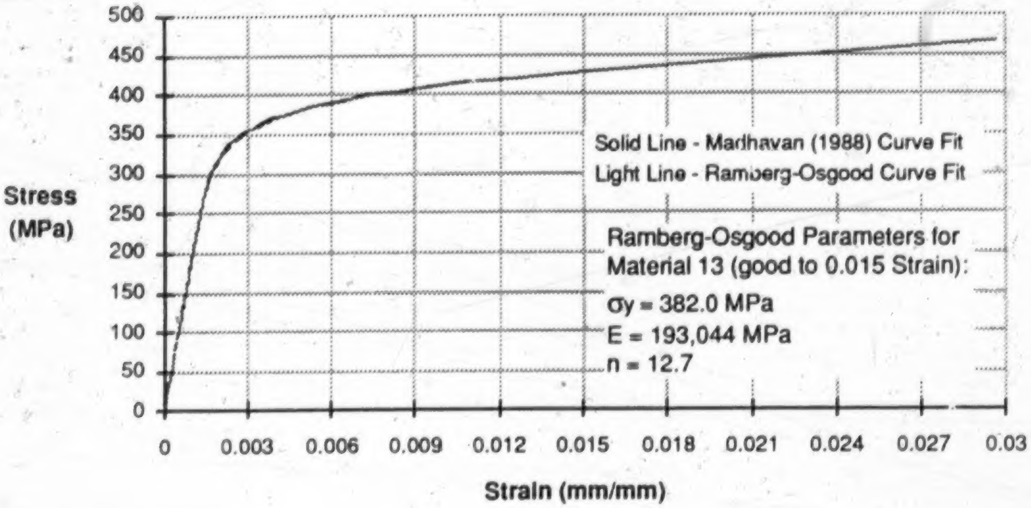

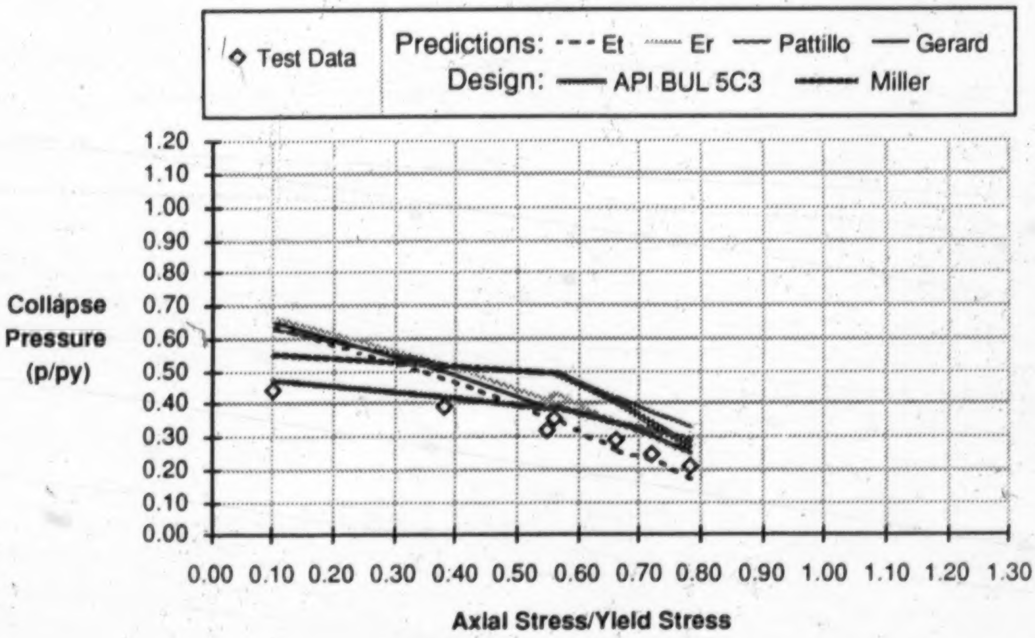

Figure 3.34 - Madhavan (1988) Test Group 5, Stainless Steel (OD/t = 27.3)

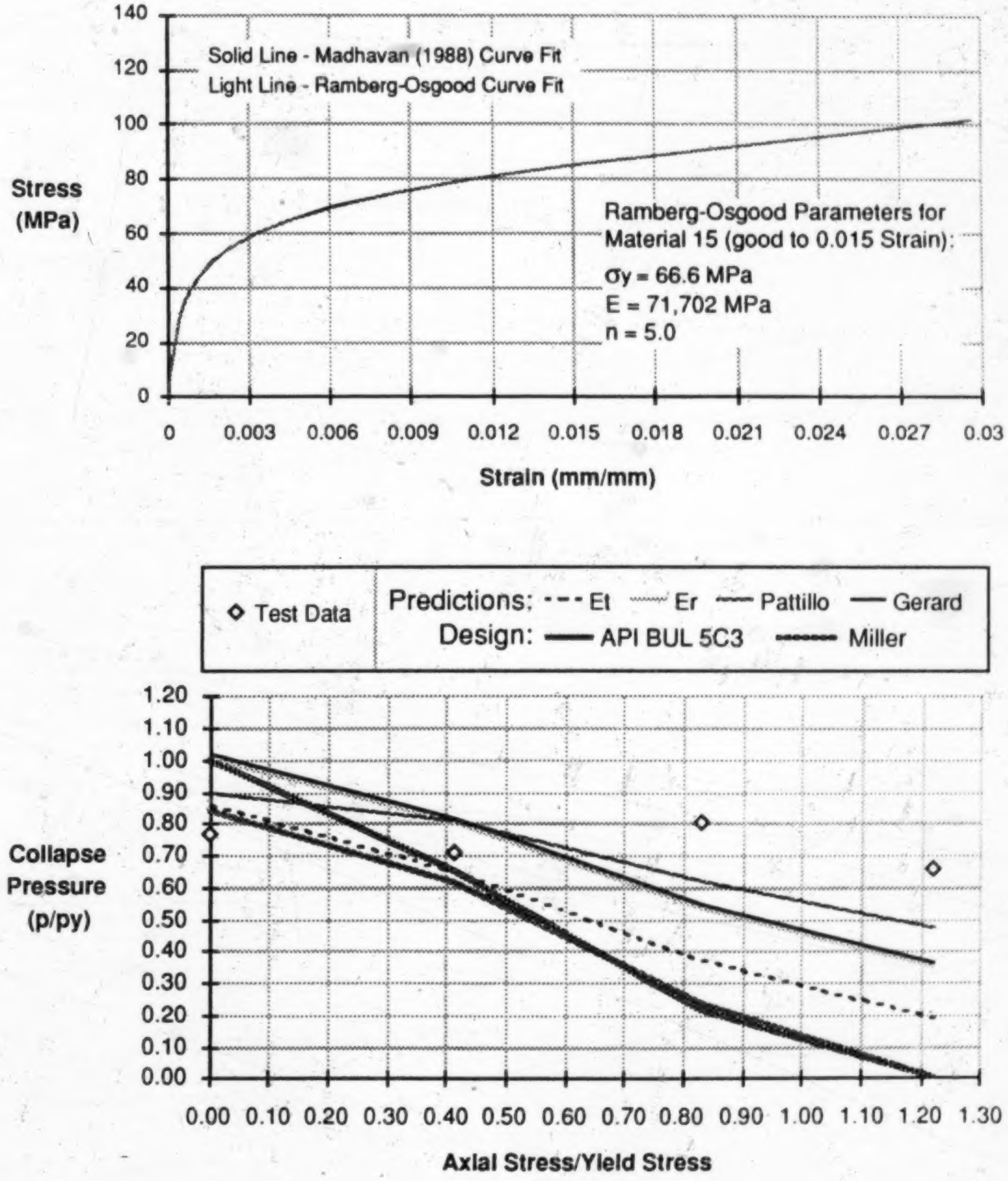

Figure 3.35 - Madhavan (1988) Test Group 6, Aluminum (OD/t = 12.2)

4.0 DERIVATION OF PREDICTION METHOD

Reverting back to the problem of collapse of casing under the environmental loading conditions described in Chapter 2, the predictions of the constant axial load are considered a lower bound condition. The exact loading that occurs in the field is not known for sure because, while the permafrost thaw subsidence is a strain driven problem, other factors like casing slippage may affect the loading condition. Also, it has been noted in Chapter 3 that the loading sequence has very little effect on collapse strength. Therefore, the prediction method described below predicts collapse for cylinders under any combination and loading sequence of axial load and external pressure.

4.1 Prediction Method

The concept used in determining an improved prediction method was one involving the use of the elastic ring buckling equation, reduced by a plasticity reduction factor (PRF), η, and a capacity reduction factor (CRF), α_m. The following prediction method is proposed for use:

$$p_{cr} = \alpha_m (p_c) \qquad [4.1]$$

where:

$$p_c = \eta \frac{2E}{(1 - \nu^2)} \left(\frac{t}{D}\right)^3 \qquad [4.2]$$

$$\eta = \left[\frac{1 - \nu_e^2}{1 - \nu^2}\right]\left(\frac{E_s + 3E_t}{4E}\right) \qquad [4.3]$$

$$\alpha_m = 1-0.2\frac{E_t}{E}\sqrt{\frac{OD_{max}-OD_{min}}{0.01(OD_{nominal})}} \qquad [4.4]$$

The following steps are used to determine the collapse pressure of cylindrical tubes using Equations 4.1 to 4.4:

1. Iteratively determine p_c using a properly modelled effective stress strain curve, and Poisson's ratio equal to 0.3 in the elastic range, and equal to 0.5 in the inelastic range.

2. At the collapse load p_c, determine E_t and calculate α_m in Equation 4.4, knowing the initial ovality of the cylinder, as defined by OD_{min} and OD_{max}.

3. Determine the reduced critical collapse pressure, p_{cr}, using Equation 4.1.

The following sections discuss the use of the plasticity and capacity reduction factors in collapse strength predictions, as well as the reasons for recommending the plasticity reduction factor in Equation 4.3 and the capacity reduction factor in Equation 4.4.

4.1.1 Plasticity Reduction Factor

The plasticity reduction factor was introduced in Chapter 3, and is defined as the critical stress causing buckling divided by the elastic buckling stress for a cylinder, or:

$$\eta = \frac{\sigma_{cr}}{\sigma_e} \qquad [4.5]$$

η is a measure of how much the cylinder has yielded before instability causes buckling. API BUL 2U (1987) and Miller (1981) determine η by calculating Λ, the ratio of the elastic buckling stress to the yield stress. API BUL 2U (1987) indicates that this ratio is a measure of the ratio of the strain in the cylinder at buckling to the yield strain. As Λ increases, η decreases, and because the value of the elastic buckling stress has increased, a net increase will be observed in σ_{cr}.

The different equations for the plasticity reduction factors discussed in Chapter 3 are as given below, rearranged to conform to the format of Equation 4.5:

$$\text{Gerard} \qquad \eta = \left[\frac{1 - \nu_e^2}{1 - \nu^2}\right]^2 \left(\frac{E_s + 3E_t}{4E}\right) \qquad [4.6]$$

$$\text{Red. Mod.} \quad \eta = \frac{\sqrt{E_s E_t}}{E}\left[\frac{1-\nu_e^2}{1-\nu^2}\right]$$

$$\text{or} \quad \eta = \frac{4E_t}{(\sqrt{E}+\sqrt{E_t})^2}\left[\frac{1-\nu_e^2}{1-\nu^2}\right] \qquad [4.7]$$

$$\text{Tan. Mod.} \quad \eta = \frac{E_t}{E}\left[\frac{1-\nu_e^2}{1-\nu^2}\right] \qquad [4.8]$$

It can be seen from these equations that Gerard's (1957) method and the first reduced modulus method both include the secant modulus, and that the critical buckling stress depends on its value. Or, the buckling stress depends on how far along the stress strain curve the cylinder material has proceeded prior to buckling. API BUL 2U (1987) terms this as how efficiently the material has been utilized prior to buckling. This may be one way of interpreting the plasticity reduction factors, but what it does indicate is that the critical inelastic buckling stress depends on an "effective stiffness", whose value lies somewhere between the elastic and tangent stiffnesses. The use of the secant modulus is a convenient way of determining this critical point.

For cylinders that buckle in the elastic range, E_s is equal to the elastic modulus, but when buckling occurs when the material is well into the inelastic range, E_s becomes significantly less in value. The "effective stiffness" is somewhat greater in value than that of the tangent modulus, and as the material progresses well into the inelastic range prior to buckling, the "effective stiffness" becomes less and approaches that of the tangent stiffness.

The following explains, in a qualitative manner, the reasons for the variation in "effective stiffness", and why it is used to determine cylinder buckling strength. Figure 4.1 illustrates the sequence of yielding for two hypothetical cases of a cylinder that buckles inelastically: one that buckles just after the initiation of yielding (cylinder A), and one that experiences significant yielding prior to buckling (cylinder B). The yielding patterns shown in Figure 4.1 are similar to those described by Tomita and Shindo (1982) and Tam and Croll (1988). It is observed in this figure that the section stiffness for cylinder A lies somewhere between that of the elastic and tangent moduli, because portions of the section have yielded while other portions have remained elastic. Because most of cylinder A is still elastic, however, its section stiffness is closer to the elastic value. On the other hand, the section stiffness for cylinder B is closer to that of the tangent stiffness at buckling because most of the cylinder has yielded. Cylinder B has been able to maintain its stability through significant deformations, and the material has progressed well into the inelastic range. These differences in "effective stiffness" for cylinders with different D/t ratios are accounted for in the determination of the plasticity reduction factor.

For a long cylinder subjected to axial tensile load and external pressure, the factors that affect the degree of yielding prior to buckling are not only the OD/t ratio, but also the magnitude of the initially applied axial stress and initial imperfections. The plasticity reduction factors given in Equations 4.6 and 4.7 use the secant modulus as a measure of the amount of yielding that has occurred prior to buckling, but do not consider the effects of imperfections.

For this study, both reduced modulus plasticity reduction factors (Equation 4.7) provide the same degree of accuracy in predicting the buckling strengths for the test data. As was shown in Section 3.5, the plasticity reduction factor defined by Gerard (1957) seems somewhat more accurate in predicting buckling strengths, and is the recommended factor to use for determining the effects of plasticity on cylinder buckling. This is the plasticity reduction factor shown in Equation 4.3 in the proposed prediction method.

4.1.2 Capacity Reduction Factor

Typically, the capacity reduction factor takes into account the effects of initial geometric imperfections (in the form of ovality and eccentricity), material anisotropies, and residual stresses. As was discussed in Section 2.3.2, the effect of residual stresses on buckling strengths is greatest when buckling occurs just as the material is yielding. It will be assumed, however, that residual stresses have been properly accounted for by obtaining a stress strain curve from a coupon specimen that still has residual stresses, or residual stresses have been measured by some other means for inclusion in the stress strain curve.

Material anisotropies were not indicated in most of the test data, and will therefore not be considered in determining the capacity reduction factor. However, if it is known that a particular cylinder is materially anisotropic and the yield strength in both the axial and circumferential directions is known, it was shown in Section 2.3.1 that Madhavan (1988) provides a rather simple method of accounting for the anisotropy.

The capacity reduction factor will thus only consider the effects of ovality. Three capacity reduction factor formulas will be evaluated here: the equation given by

Tokimasa and Tanaka (1986), the equation provided by Nishioka et al. (1976), and a proposed capacity reduction factor, modified from Miller's (1981) formula. The original capacity reduction factor given by Miller (1981) in Equation 3.27 includes the effects of ovality, but does not consider the fact that the effects of initial geometric imperfections are reduced when the material begins to plastify (it is believed that Miller's (1981) plasticity reduction factor accounts for this to some degree). When the material has yielded considerably, the effects of ovality are negligible. The proposed capacity reduction factor accounts for the reduced effect of ovality on buckling.

4.1.2.1 Tokimasa and Tanaka (1986)

Tokimasa and Tanaka's (1986) equation is repeated here:

$$r_\Delta = 1-[0.0856(OD/t)-1.14]\left(1-\frac{2}{A+\sqrt{A^2-4B}}\right) \qquad [4.9]$$

where:

$$A = 1 + 3\Delta_2(D/t) + B \qquad [4.10]$$

$$\Delta_2 = \frac{OD_{max} - OD_{min}}{OD_{max} + OD_{min}} \qquad [4.11]$$

$$B = \frac{\text{calculated collapse pressure}}{\text{elastic collapse pressure}} \qquad [4.12]$$

Equation 4.9 has taken into account the effects of plasticity by using the 'B' term defined in Equation 4.12, as well as the effects of the OD/t ratio and ovality.

It should be noted that the value obtained from Equation 4.9 exceeds unity when OD/t ≤ 13.3. By calculating the elastic buckling limit using OD/t = 13.3, it is known that inelastic buckling will occur for a cylinder of this OD/t only when the yield stress is below about 1240 MPa. For this study, all yield values are well below 1240 MPa, and an upper limit of unity will be imposed on Equation 4.9.

4.1.2.2 Nishioka et al. (1976)

Nishioka et al.'s (1976) equation, modified to neglect the small effect of eccentricity, is:

$$r_{\Delta} = \frac{1}{1 + 3\Delta_2(OD/t)} \qquad [4.13]$$

where OD/t replaces the OD/t_{max} term in the original equation.

Equation 4.13 assumes that post-yield effects can be accounted for by the OD/t ratio only. The other effects of inelastic stiffness and magnitude of axial stress are not considered.

4.1.2.3 Proposed Capacity Reduction Factor

All the factors that determine the capacity reduction factor relate to the degree of material inelasticity prior to buckling. It is therefore proposed to account for this inelasticity by using a modified form of Miller's (1981) equation:

$$\alpha = 1-0.2\frac{E_t}{E}\sqrt{\frac{OD_{max}-OD_{min}}{0.01(OD_{nominal})}} \qquad [4.14]$$

Equation 4.14 uses E_t to account for the OD/t ratio, axial stress magnitude, and inelastic stiffness. It is known that OD/t and σ_z determine how far along the stress strain curve the cylinder material is before buckling occurs. It has also been shown that the effects of ovality diminish as the material becomes inelastic. Therefore, using the ratio of E_t/E in the capacity reduction factor appears justified.

4.1.2.4 Comparison to Test Data

Each of the three capacity reduction factors described above have been substituted into Equation 4.4 of the proposed prediction method to compare their predictive accuracy to the test data. Again, some of the test data reported in Chapter 3 was not used. Madhavan's (1988) reported test results are suspect at the high σ_z/σ_y

ratios. Therefore, only Madhavan's (1988) test results where $\sigma_z/\sigma_y \leq 0.8$ have been used in the comparison. Also, Gulf Canada's (1987) constant axial strain data will not be used in the comparison.

Stuiver and Tomalin (1959) have reported that their test specimens were machined to provide the indicated OD/t ratios, as well as to eliminate any ovalities. The capacity reduction factor has thus been assumed equal to 1 for their data. Ovalities were provided by Tamano et al. (1982) and Gulf Canada (1987) for their data, and are given in Table 4.1. These values were used in the test/predicted comparison for their test data. For the rest of the data, it was assumed that $\alpha = 0.8$. This value uses the maximum ovality permitted by API BUL 2U (1987), and $\alpha = 0.8$ is the API recommended value for the capacity reduction factor. It was also assumed that $OD_{nominal} = (OD_{max}+OD_{min})/2$.

Figures 4.2 through 4.27 illustrate the results of the comparison of the predicted collapse strengths to the test data, using the different capacity reduction factors. Figures 4.22 to 4.27 do not include Madhavan's (1988) data where $\sigma_z \geq 0.8\sigma_y$. Also in the figures are the predictions for a capacity reduction factor equal to one (this assumes no reduction in collapse strength due to initial ovalities). Table 4.2 shows the statistical results, using the mean and coefficient of variation of the test/predicted ratios.

It can be seen from the figures and Table 4.2 that the capacity reduction factors given by Tokimasa and Tanaka (1986) and Nishioka et al. (1976) are conservative and increase the scatter of test/predicted results a small amount, as measured by the coefficient of variation. The OD/t ratio of 36.7 for Madhavan's (1988) test group 1 was apparently too large for use by the Tokimasa and Tanaka (1986) CRF equation. That test group was therefore omitted in the calculation of the mean and COV for all the test data using the Tokimasa and Tanaka (1986) CRF. The coefficient of variation for the test/predicted results using the proposed capacity reduction factor (described in Section 4.1.2.3) was found to be the lowest. It should also be noted that the overall coefficient of variation of the test/predicted ratios using the proposed capacity reduction factor is not much lower than if a CRF = 1 were used. This relates directly to the fact that ovalities were not given for most of the test data. Some of the test specimens were ovalized, while others were not, and using either no capacity reduction factor or the proposed factor will result in both under- and over-predictions, depending on the degree of ovality.

Based on the statistical results of Table 4.2, the recommended capacity reduction factor for use is the proposed capacity reduction factor, as was presented in Section 4.1.

4.2 Summary

The loading condition of constant axial load has been considered in the derivation of the prediction method, providing a lower bound to the problem of casing collapse. The prediction method that has been developed for this loading condition uses Gerard's (1957) buckling equation and plasticity reduction factor, reduced by the proposed capacity reduction factor to account for the effects of initial ovalities. The effects of residual stresses on casing collapse were not included, and are assumed to be accounted for in the determination of the material stress strain curve. Also, the effects of material anisotropies were not included in the prediction method because most of the test data did not indicate any material differences in the axial and circumferential directions. If material differences do exist, and are known for a particular cylinder, Section 2.3.1 outlines a simple method to account for the differences.

The use of the proposed prediction method has provided the most accurate predictions, as measured by the mean and COV of the test/predicted ratios. Figures 4.28 and 4.29 illustrate the test/predicted ratios in relation to the OD/t ratio and the σ_z/σ_y ratio using the recommended method for collapse prediction. The mean and coefficient of variation of the test/predicted ratios are 0.97 and 16.74%, respectively.

Figure 4.29 also indicates an increase in scatter of test/predicted ratios when σ_z/σ_y approaches unity. This figure did not use the suspect Madhavan (1988) data. It is difficult to tell whether or not the data is accurate, or if testing difficulties result when the axial load becomes large. This is one notable area for further study.

Test Group	Ovality Δ $\frac{(OD_{max} - OD_{min})}{OD_{nominal}}$
Tamano K55-1	0.0014
Tamano K55-2	0.0016
Tamano K55-3	0.0018
Tamano N80-1	0.0010
Tamano N80-2	0.0015
Tamano N80-3	0.0011
Tamano N80-4	0.0024
Tamano P110-1	0.0009
Tamano P110-2	0.0009
Tamano P110-3	0.0017
Gulf Const. Load	0.0060

Table 4.1 - Ovalities Given for Tamano et al. (1982) and Gulf Canada (1987) Test Data

Test Data Source	Test Group	Test/Pred Results Using $\alpha_m = 1.0$ for a CRF		Test/Pred Results Using the Proposed α_m for a CRF		Test/Pred Results Using Tokimasa and Tanaka's r_Δ for a CRF		Test/Pred Results Using Nishioka et al.'s r_Δ for a CRF	
		Mean	COV%	Mean	COV%	Mean	COV%	Mean	COV%
Edwards & Miller (1939)	6	0.98	6.42	0.99	6.85	1.04	6.64	1.22	6.44
	7	0.90	20.30	0.95	17.35	1.18	17.31	1.20	19.24
	8	0.95	17.07	1.02	14.94	1.09	15.23	1.26	15.47
	9	0.89	18.50	0.97	12.69	0.96	12.51	1.12	12.57
	10	0.84	10.81	0.86	9.27	1.07	9.19	1.11	10.91
	11	0.88	5.88	0.89	5.84	0.96	6.04	1.11	5.95
	12	0.89	9.62	0.89	9.65	0.89	9.62	1.04	9.62
Stuiver & Tomalin (1959)	1	0.89	18.93	0.89	18.93	0.89	18.93	0.89	18.93
	2	0.92	12.92	0.92	12.92	0.92	12.92	0.92	12.92
Tamano et al (1982)	K55	1.03	17.67	1.08	15.50	1.15	12.85	1.09	17.60
	N80	1.06	29.07	1.10	27.31	1.11	27.25	1.10	28.55
	P110	0.98	13.61	1.01	12.02	1.01	12.98	1.01	13.57
Gulf (1987)*	1	0.75	0.77	0.89	0.74	1.24	1.93	1.02	0.74
Madhavan** (1988)	1	0.97	19.76	1.07	15.45	–	–	1.51	19.76
	2	0.91	8.40	0.97	6.79	1.34	8.85	1.25	8.82
	3	0.85	8.78	0.87	7.97	0.97	7.91	1.09	8.73
	4	1.04	17.75	1.05	17.54	1.04	17.75	1.23	17.75
	5	0.80	8.65	0.86	6.51	1.44	3.79	1.13	8.49
	6	0.81	10.18	0.81	10.06	0.81	10.18	0.95	10.18
All Data* **		0.93	17.85	0.97	16.74	1.06	18.29	1.13	17.88

* - Gulf's (1987) data does not include those tests where $\sigma_z \geq 0.8\sigma_y$

* - Gulf (1987) Test Group 2 (constant axial strain) results were not used

** - Madhavan's (1988) data does not include those tests where $\sigma_z \geq 0.8\sigma_y$

Table 4.2 - Averages and Coefficient of Variations for the Test/Predicted Ratios using Different Capacity Reduction Factors

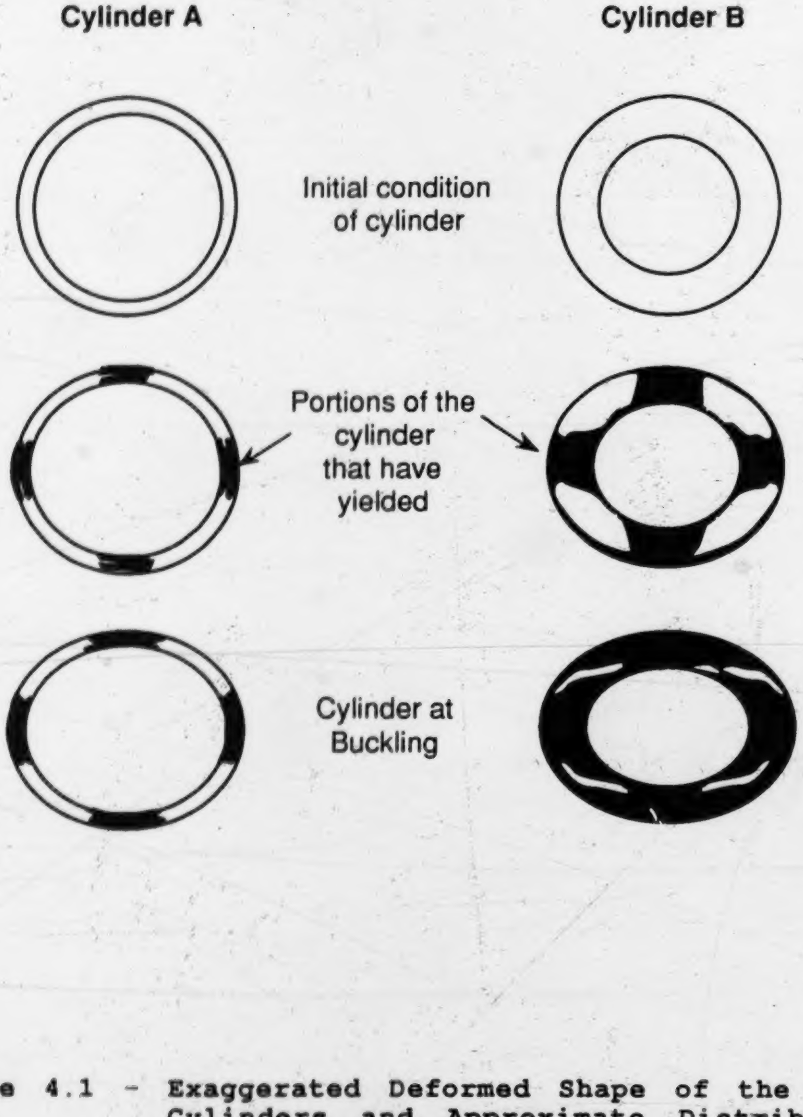
Cylinder A
Cylinder B
Initial condition of cylinder
Portions of the cylinder that have yielded
Cylinder at Buckling

Figure 4.1 - Exaggerated Deformed Shape of the Cylinders and Approximate Distribution of the Inelastic Region

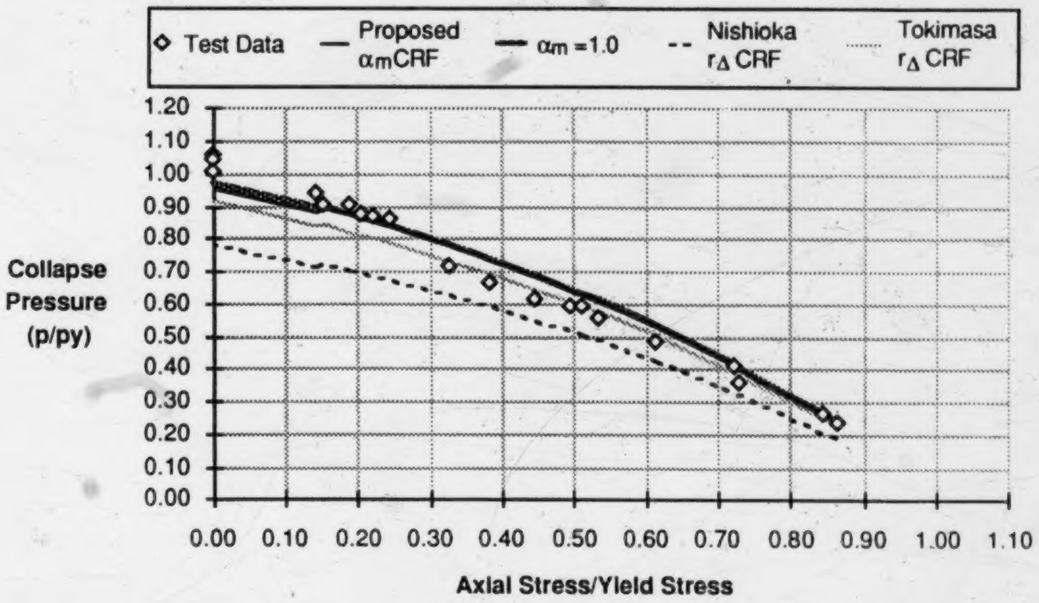

Figure 4.2 - CRF Comparison for Edwards & Miller (1939) Test Group 6 (OD/t = 16.6)

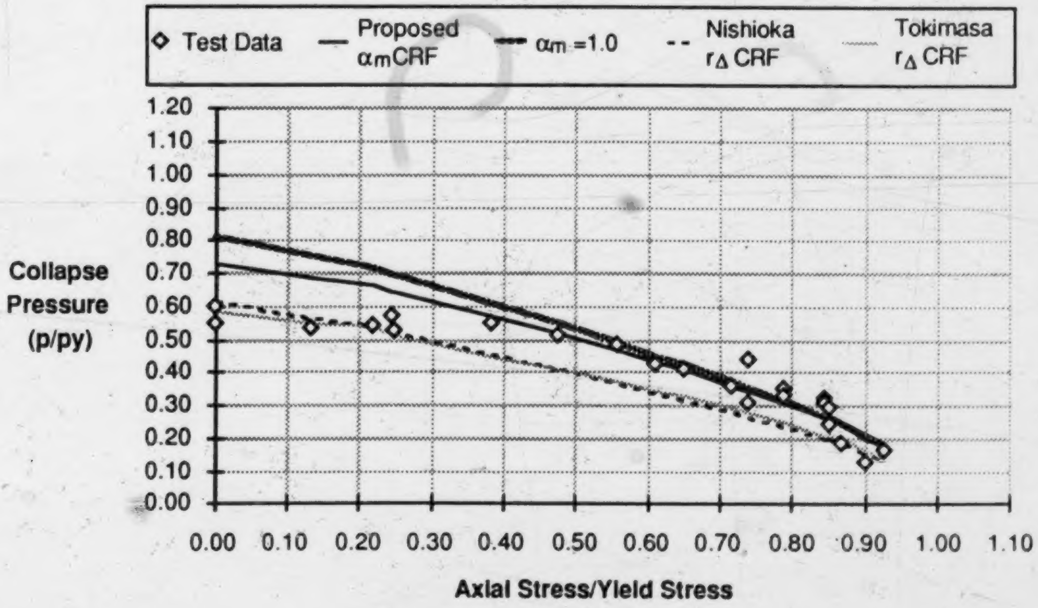

Figure 4.3 - CRF Comparison for Edwards & Miller (1939) Test Group 7 (OD/t = 21.7)

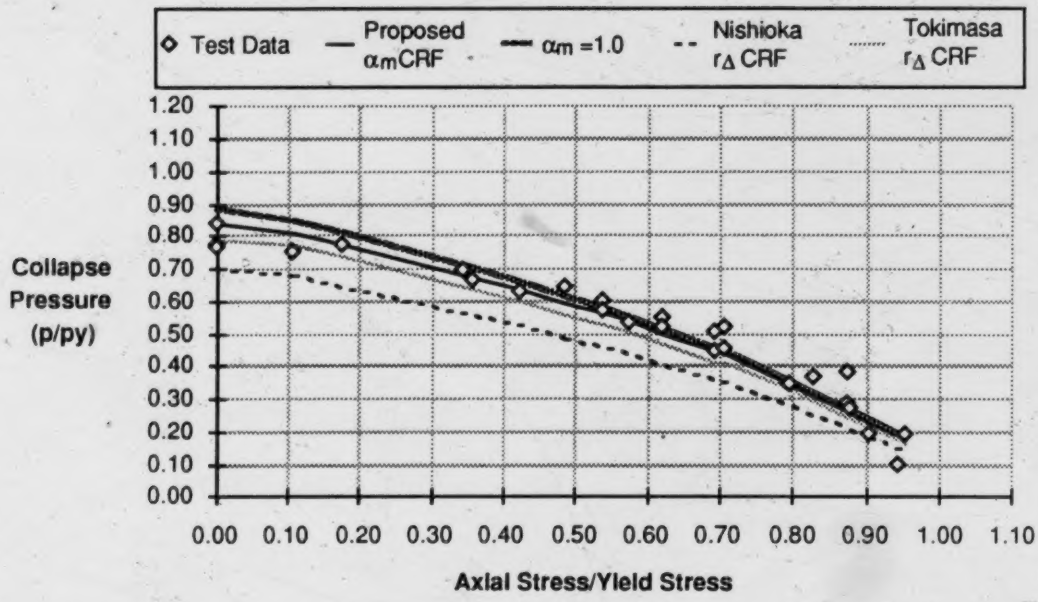

Figure 4.4 - CRF Comparison for Edwards & Miller (1939) Test Group 8 (OD/t = 17.3)

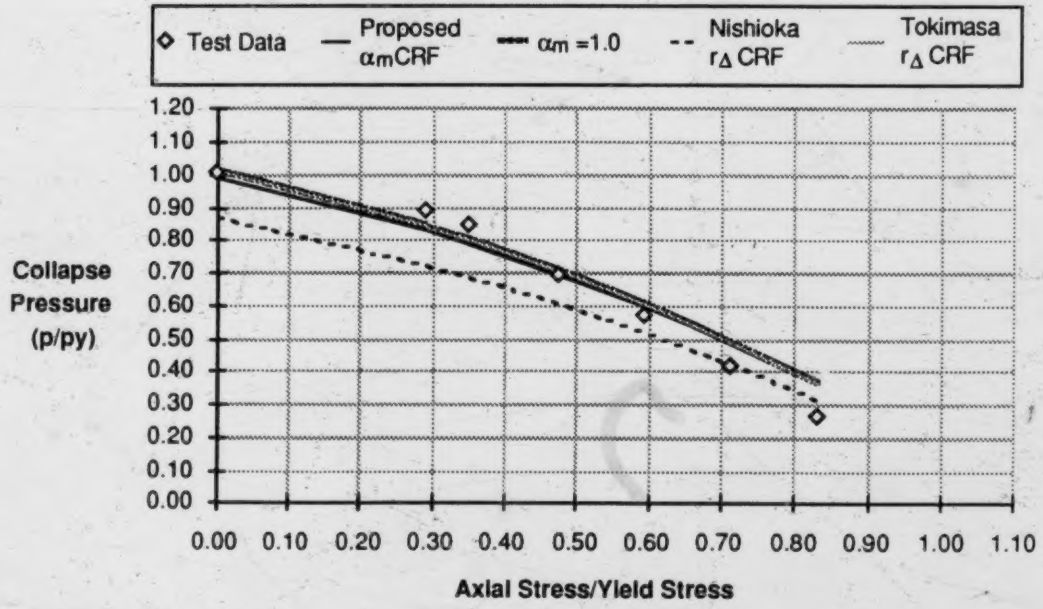

Figure 4.5 - CRF Comparison for Edwards & Miller (1939) Test Group 9 (OD/t = 11.2)

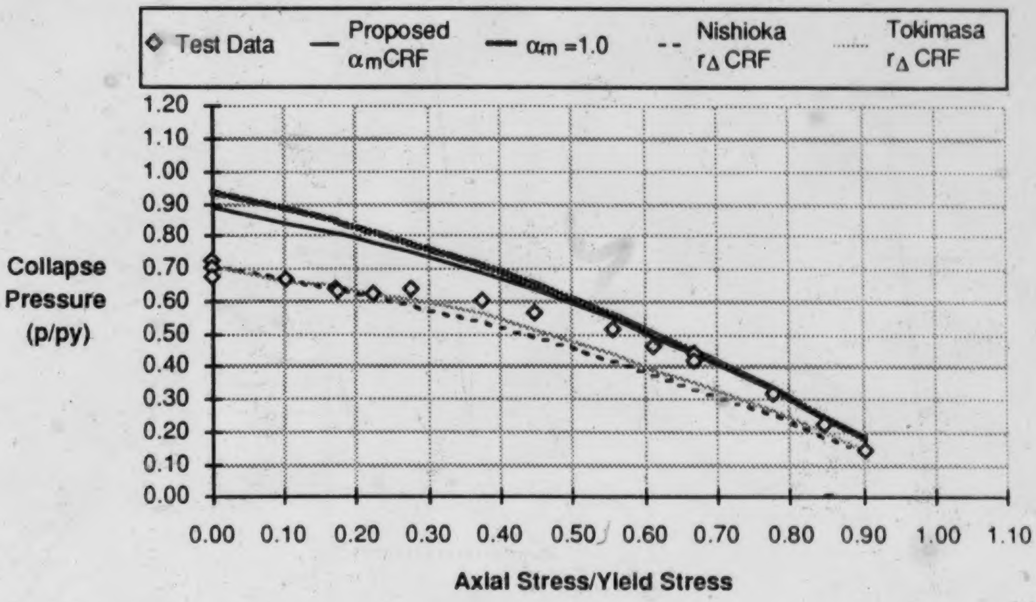

Figure 4.6 - CRF Comparison for Edwards & Miller (1939) Test Group 10 (OD/t = 21.7)

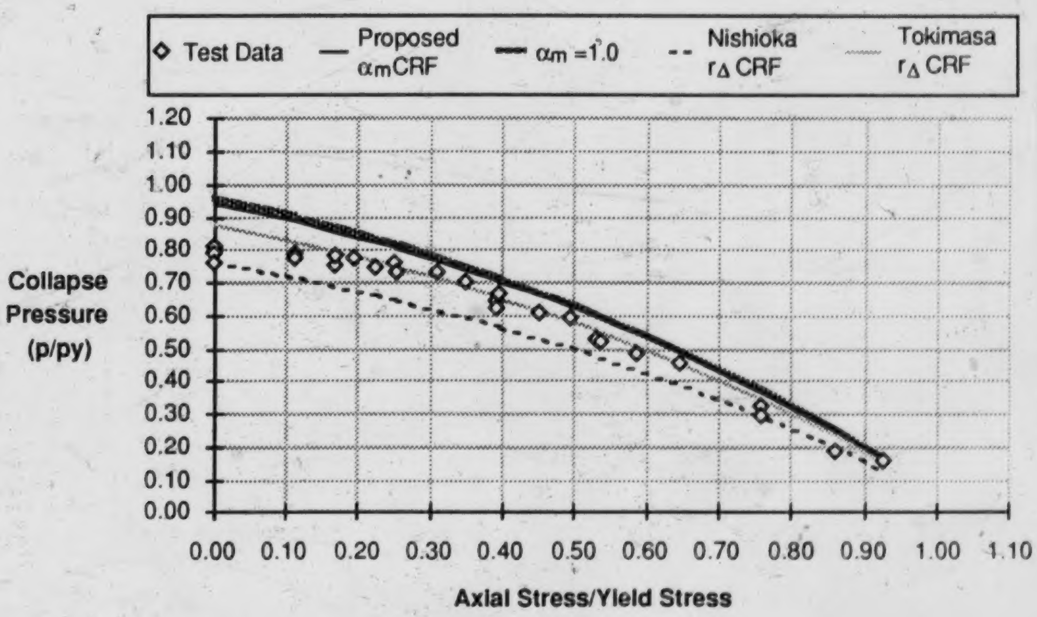

Figure 4.7 - CRF Comparison for Edwards & Miller (1939) Test Group 11 (OD/t = 17.3)

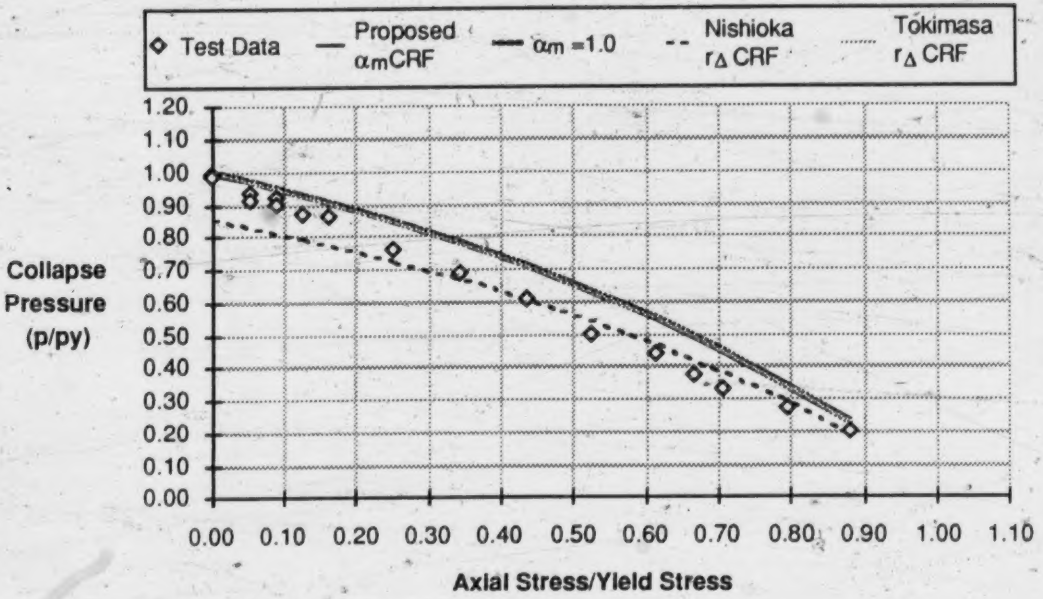

Figure 4.8 - CRF Comparison for Edwards & Miller (1939) Test Group 12 (OD/t = 11.2)

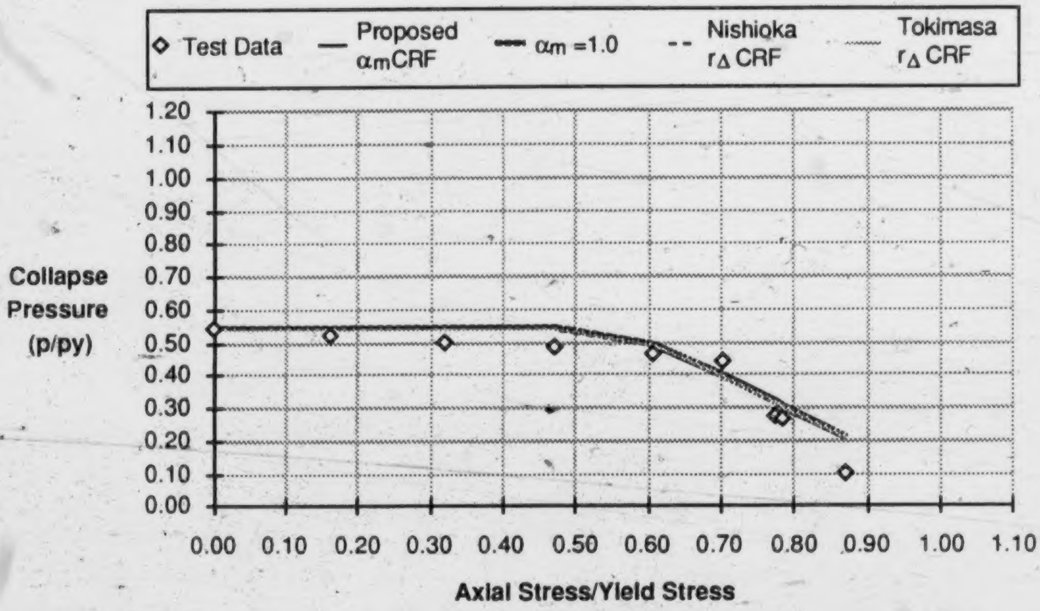

Figure 4.9 - CRF Comparison for Stuiver & Tomalin (1959) Test Group 1 (OD/t = 27.0)

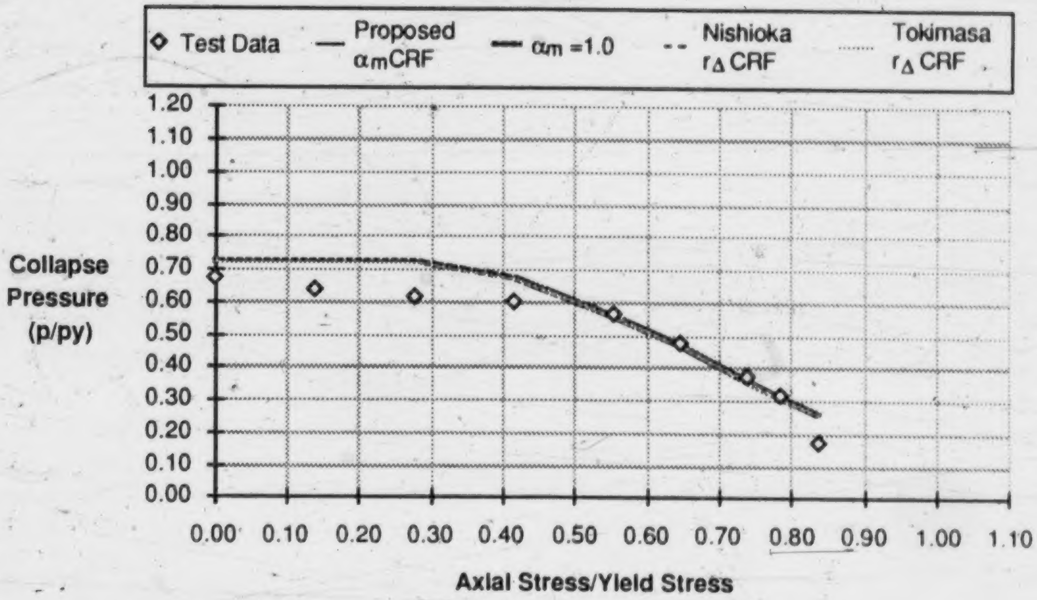

Figure 4.10 - CRF Comparison for Stuiver & Tomalin (1959) Test Group 2 (OD/t = 23.5)

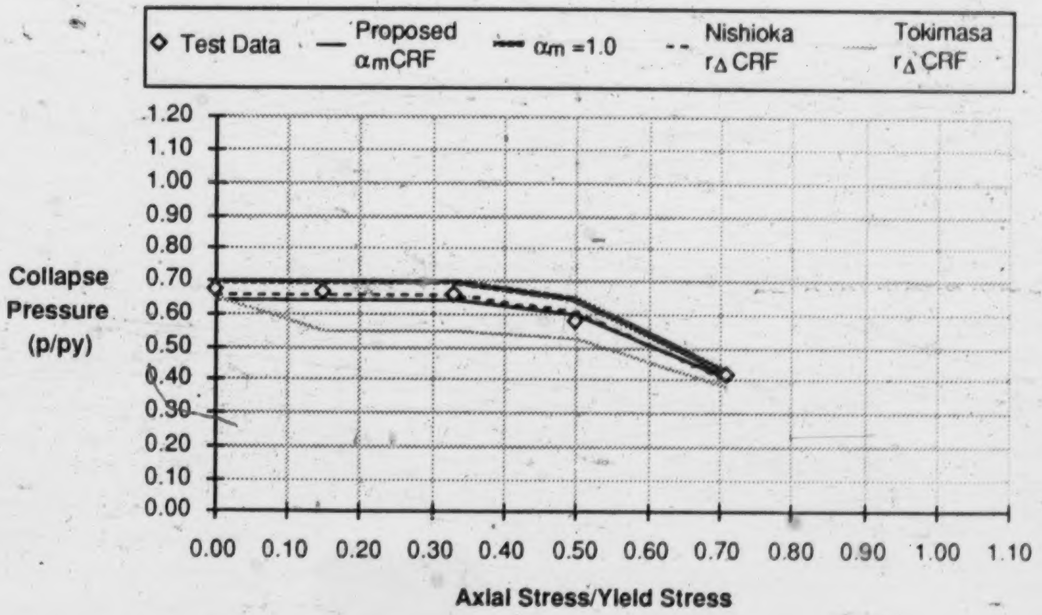

Figure 4.11 - CRF Comparison for Tamano et al. (1982) Test Group K55-1 (OD/t = 25.3)

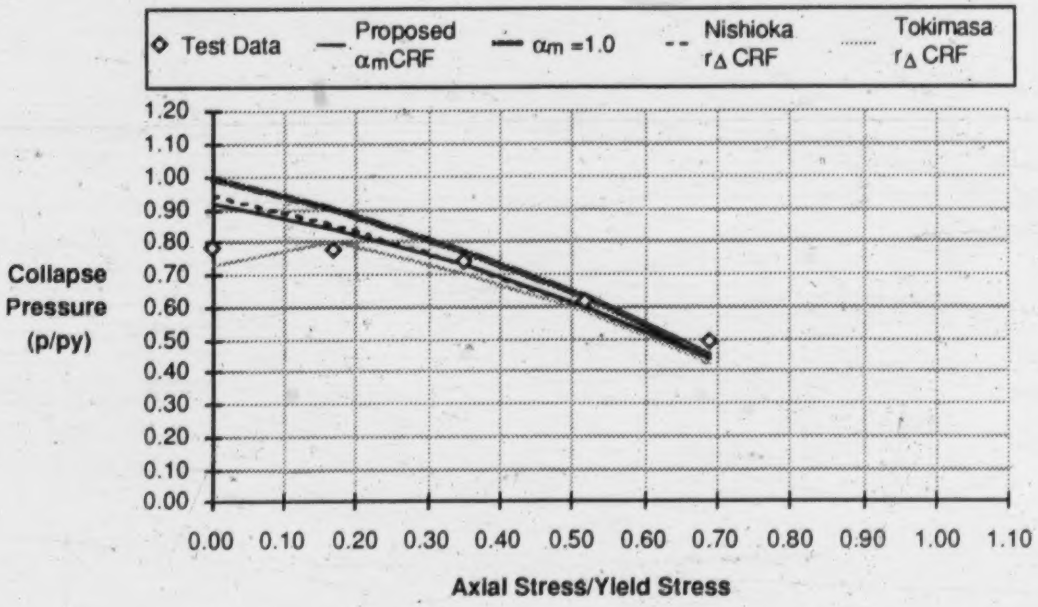

Figure 4.12 - CRF Comparison for Tamano et al. (1982) Test Group K55-2 (OD/t = 21.8)

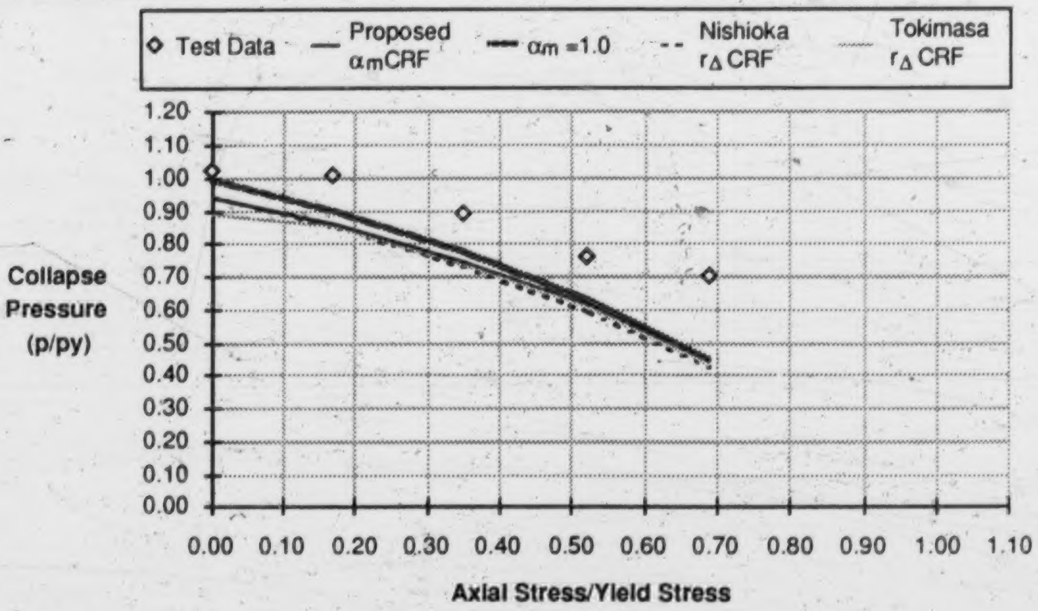

Figure 4.13 - CRF Comparison for Tamano et al. (1982) Test Group K55-3 (OD/t = 18.9)

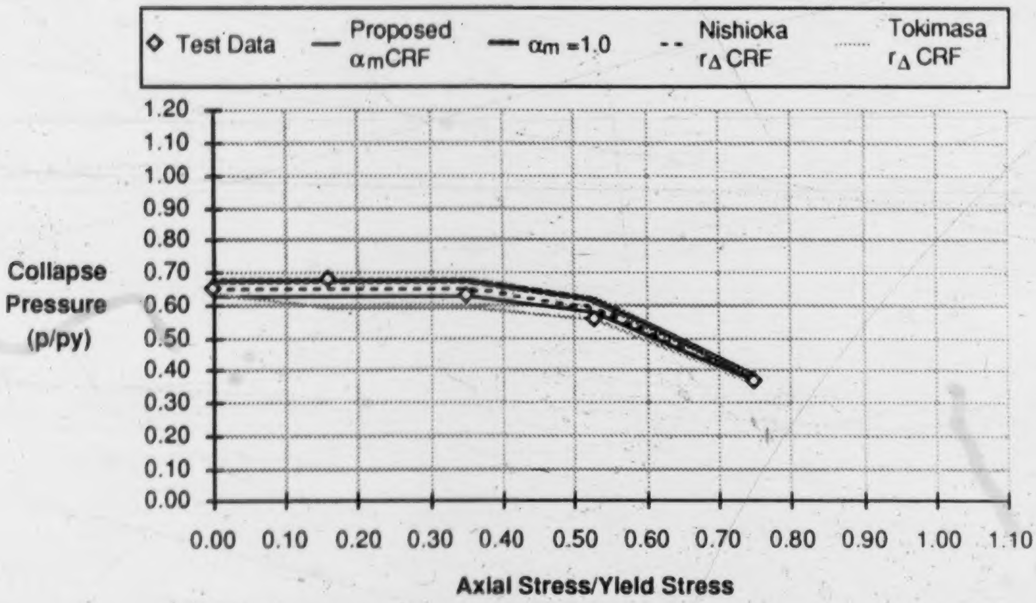

Figure 4.14 - CRF Comparison for Tamano et al. (1982) Test Group N80-1 (OD/t = 22.0)

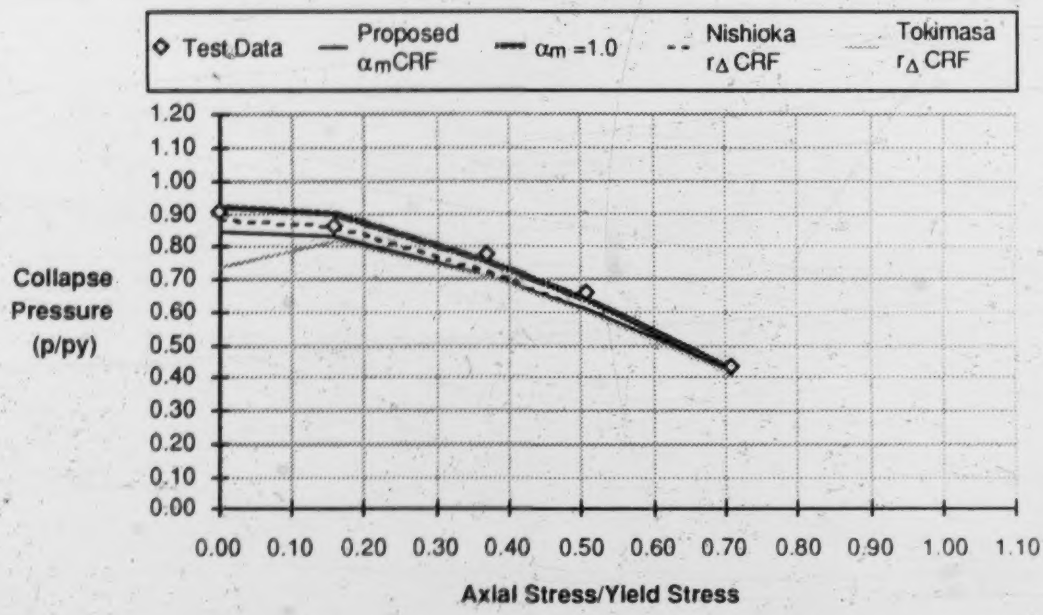

Figure 4.15 - CRF Comparison for Tamano et al. (1982) Test Group N80-2 (OD/t = 19.3)

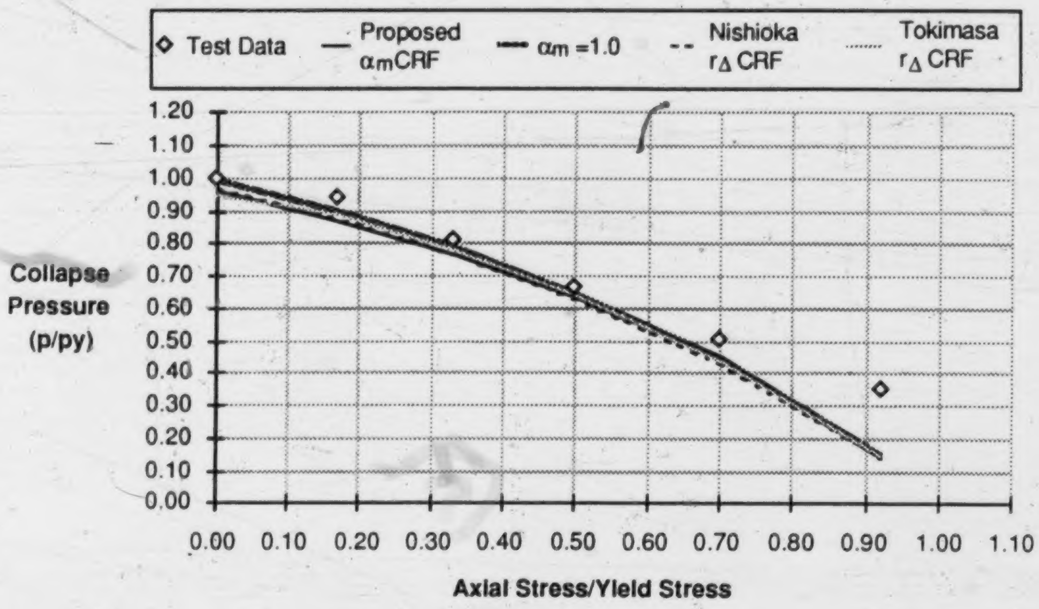

Figure 4.16 - CRF Comparison for Tamano et al. (1982) Test Group N80-3 (OD/t = 15.2)

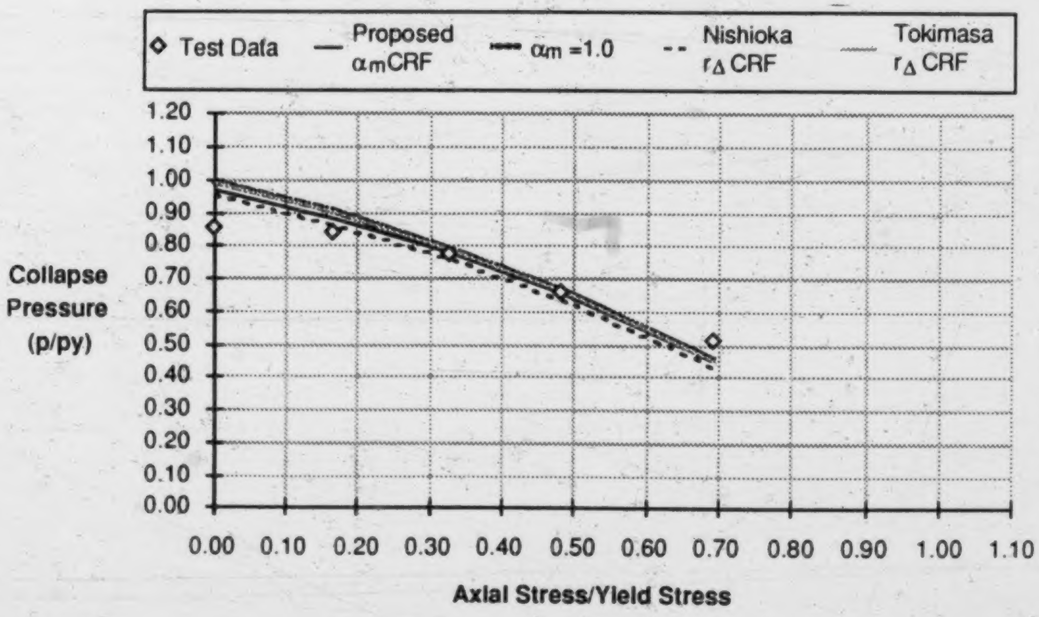

Figure 4.17 - CRF Comparison for Tamano et al. (1982) Test Group N80-4 (OD/t = 12.6)

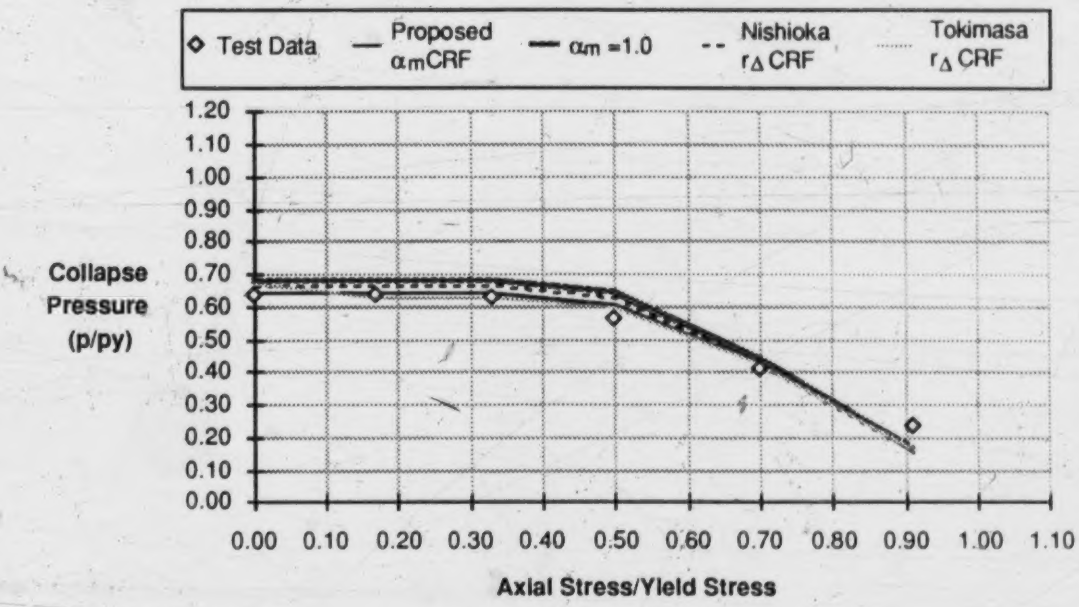

Figure 4.18 - CRF Comparison for Tamano et al. (1982) Test Group P110-1 (OD/t = 19.4)

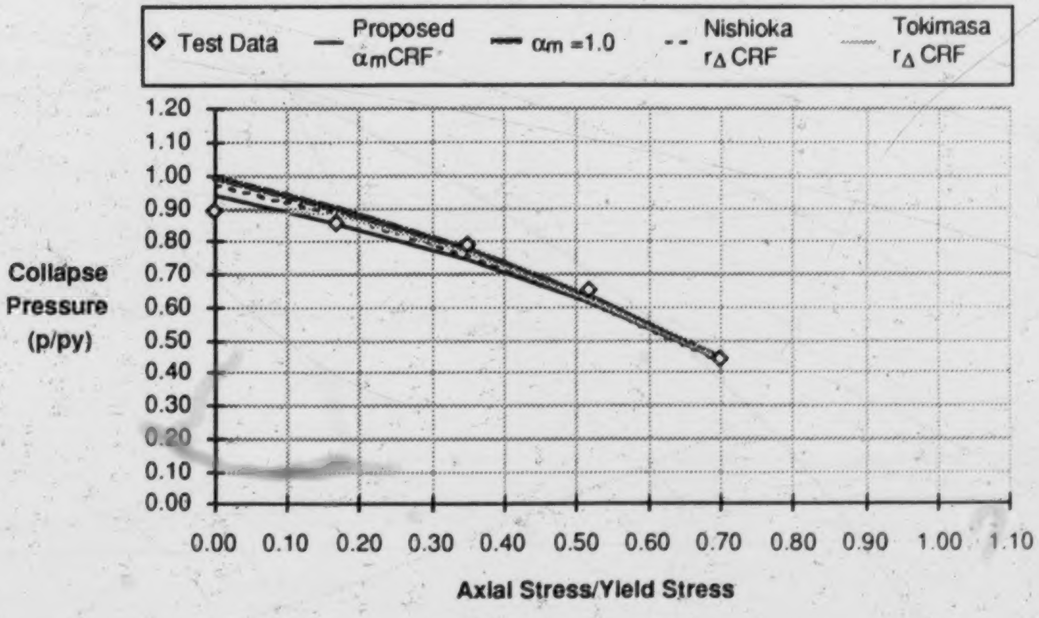

Figure 4.19 - CRF Comparison for Tamano et al. (1982) Test Group P110-2 (OD/t = 15.8)

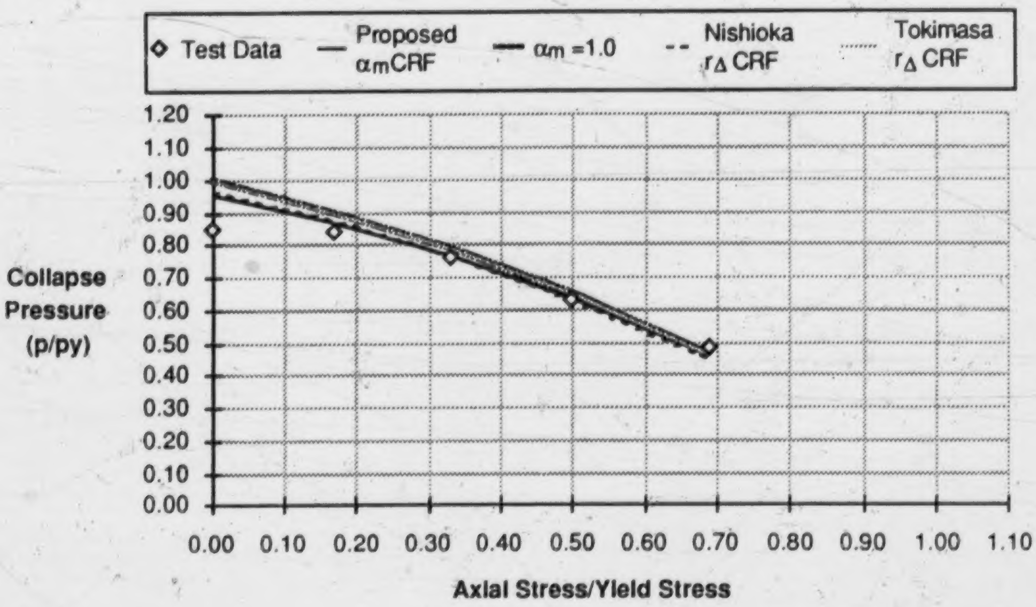

Figure 4.20 - CRF Comparison for Tamano et al. (1982) Test Group P110-3 (OD/t = 12.8)

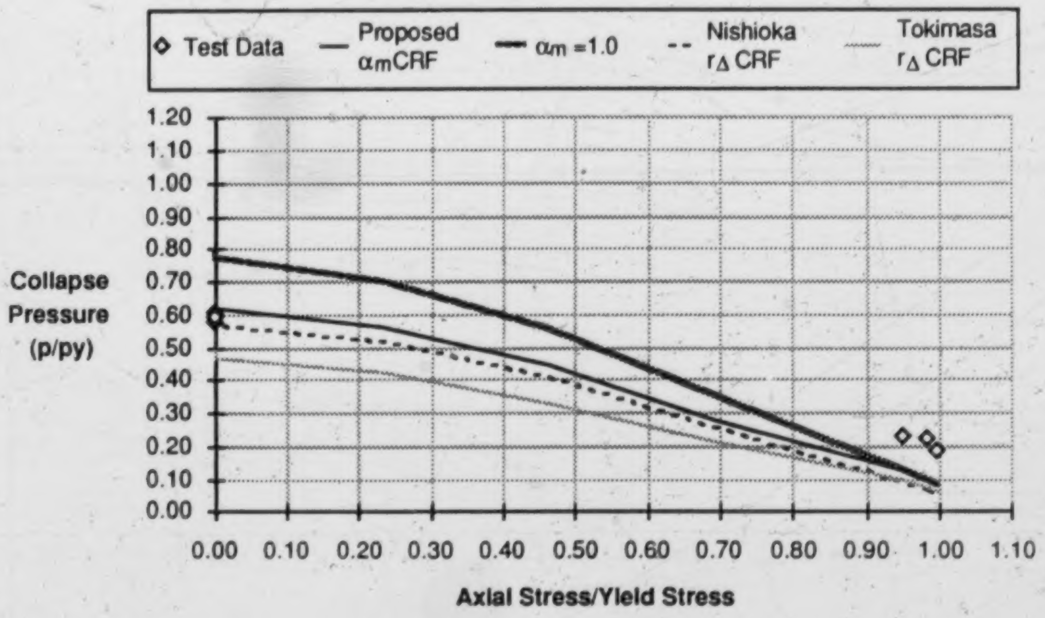

Figure 4.21 - CRF Comparison for Gulf Canada (1987) Test Group 1 (OD/t = 23.8)

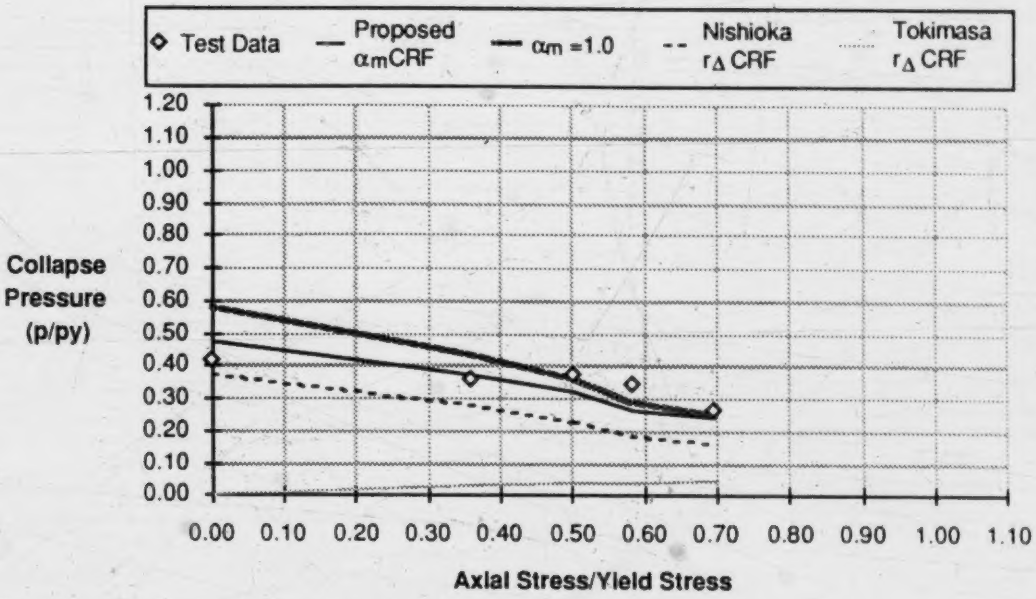

Figure 4.22 - CRF Comparison for Madhavan (1988) Test Group 1 (OD/t = 36.7)

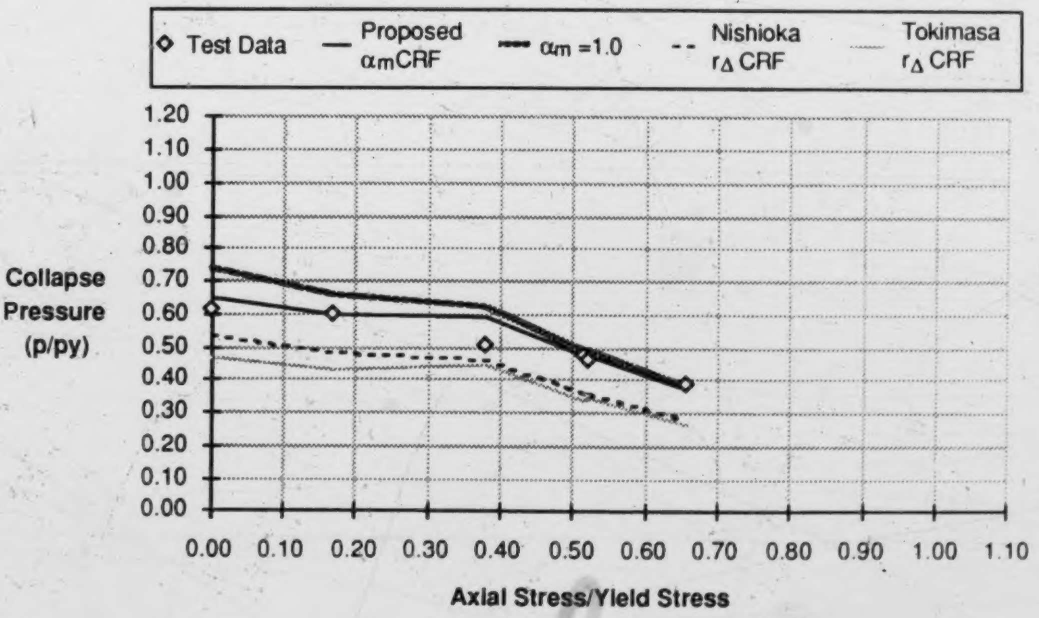

Figure 4.23 - CRF Comparison for Madhavan (1988) Test Group 2 (OD/t = 24.5)

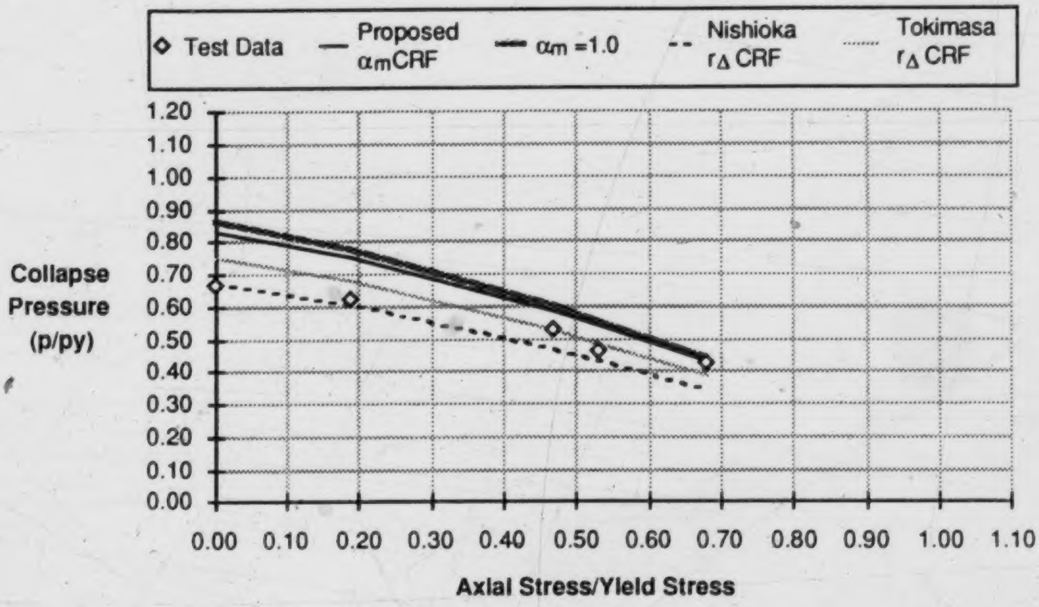

Figure 4.24 - CRF Comparison for Madhavan (1988) Test Group 3 (OD/t = 18.7)

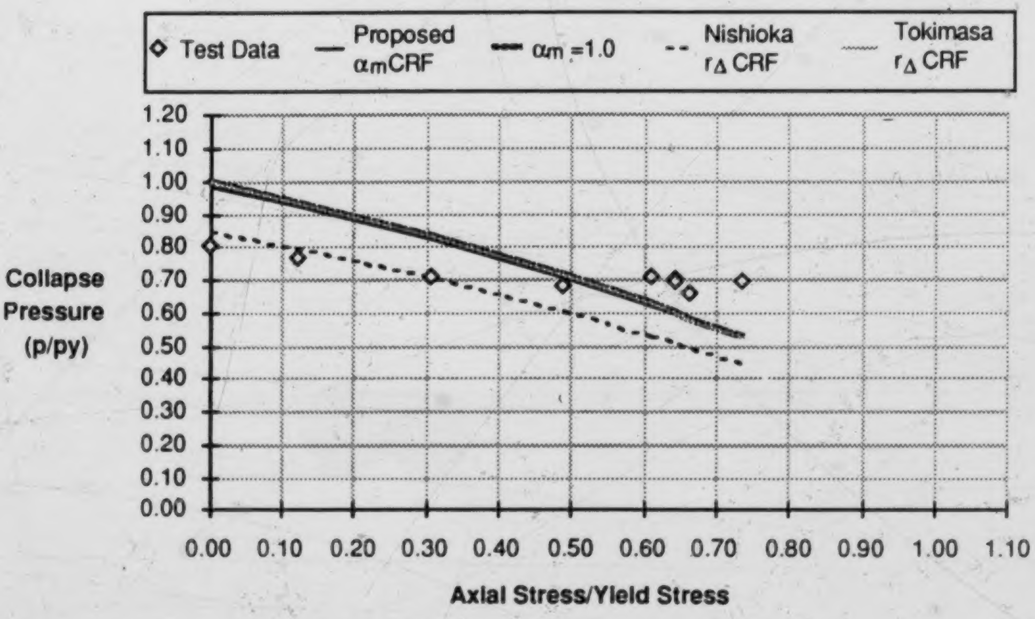

Figure 4.25 - CRF Comparison for Madhavan (1988) Test Group 4 (OD/t = 12.1)

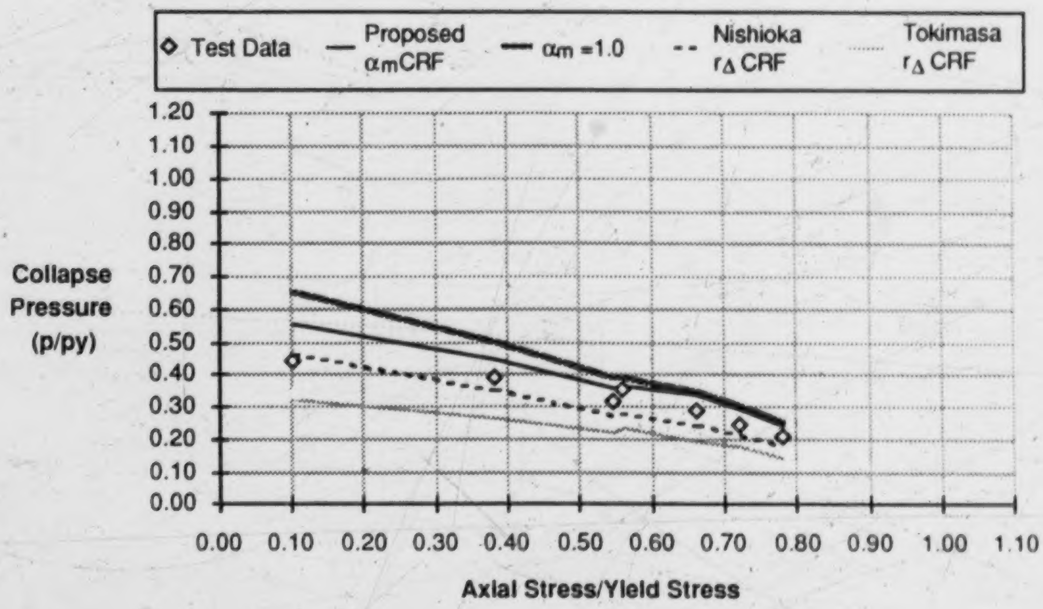

Figure 4.26 - CRF Comparison for Madhavan (1988) Test Group 5 (OD/t = 27.3)

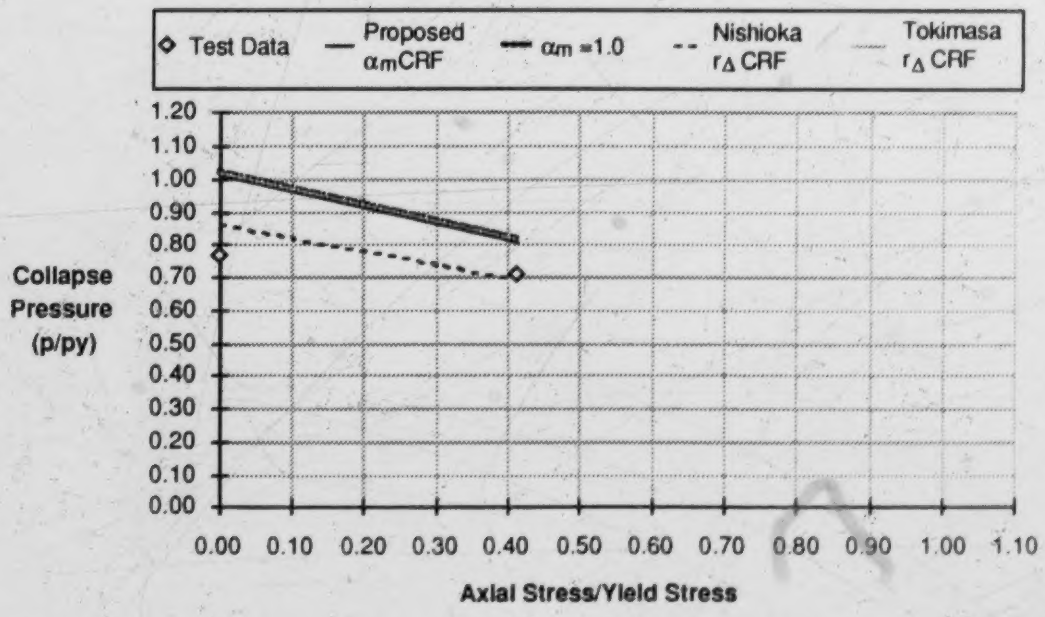

Figure 4.27 - CRF Comparison for Madhavan (1988) Test Group 6 (OD/t = 12.2)

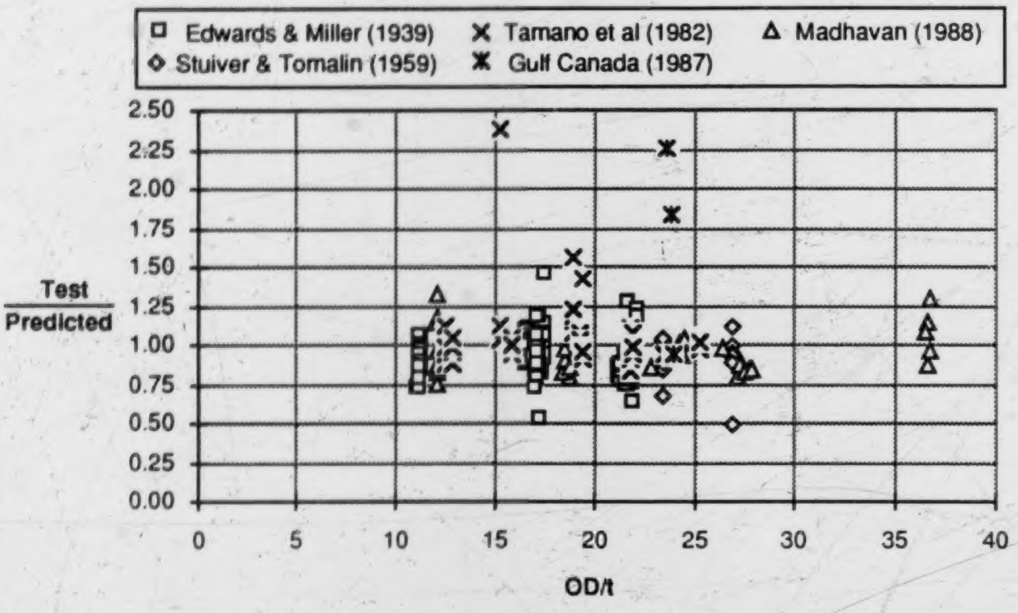

Figure 4.28 - Test/Predicted Ratios in Relation to the OD/t Ratio

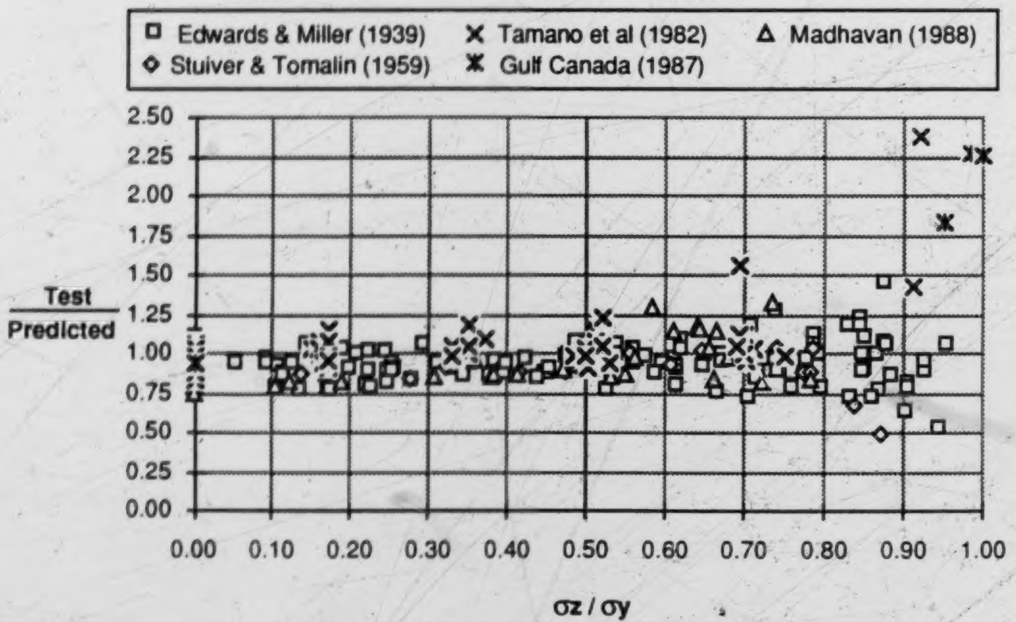

Figure 4.29 - Test/Predicted Ratios in Relation to the σ_z/σ_y Ratio

5.0 PARAMETER STUDY

Using the proposed prediction method described in Section 4.1 and the Ramberg-Osgood (1943) equation to model the stress strain curve, analyses are performed in this chapter to assess the sensitivity of cylinder collapse to variations in the OD/t ratio, the yield stress, the slope of the inelastic portion of the stress strain curve, and the cylinder ovality. The purpose of this chapter is to observe the range of predicted buckling strengths that result from variations in the above mentioned parameters. The axial loading condition considered is one of constant axial load. The variations in the buckling strengths resulting from the parameter study are plotted with axial stress.

In order to effectively perform a parameter study, a general knowledge of the effect of the parameters must be known. This will enable the variation of one parameter, while keeping the others at a value where their influence is greatest. This study has provided the general knowledge necessary to perform an effective parameter study.

5.1 Effect of Inelastic Stiffness

For cylinders that buckle inelastically, the inelastic stiffness of the cylinder material greatly influences the buckling strength. Figure 5.1 illustrates variations in the inelastic stiffness that might realistically occur in a cylinder or casing material (the n variable in the figure represents the exponent in the Ramberg-Osgood equation). The OD/t ratio has been kept at a low value, OD/t = 15, because a casing with a low OD/t ratio will buckle inelastically and be most influenced by inelastic stiffness. The OD/t ratio, however, cannot be too low, or errors will occur, resulting from the assumptions of neglecting radial stresses and assuming a constant value for the circumferential stress through the wall thickness of the cylinder. The yield strength value was selected to represent a lower than normal value for typical casing material. A lower value of the yield strength will ensure inelastic material behaviour. The ovality was selected as:

$$\Delta = \frac{OD_{max} - OD_{min}}{OD_{nominal}} = 0.01 \qquad [5.1]$$

Figure 5.2 illustrates the variation in buckling strength resulting from differences in inelastic stiffness, plotted with the variation in axial stress. The figure clearly illustrates the dramatic increase in collapse strength at the high σ_z/σ_y ratios when n is low, creating a high inelastic stiffness. The differences in collapse strength when the σ_z/σ_y ratio is low is due to the nature of the Ramberg-Osgood relation. Figure 5.1 shows how the proportional limits of stress strain curves differ for the same value of yield strength.

Even though it is not considered in this chapter, the small effects of Poisson's ratio can be seen in Figure 5.2. As was indicated in Chapter 2, the Poisson's ratio model used was one where $\nu = 0.3$ in the elastic range, then, at the elastic strain limit, $\nu = 0.5$. This jump in value from 0.3 to 0.5 is seen as a jump in the curves in Figure 5.2 in the range where $\sigma_z/\sigma_y = 0.6$ to 0.9.

5.2 Effect of Yield Stress

To observe the changes in buckling strength for variations in yield strength, the OD/t value was set equal to 15, again to ensure the material attained its yield value. The inelastic stiffness parameter, n, was set to 20 and the ovality was again set to 0.01.

Figure 5.3 illustrates the variations in yield strength felt to be realistic in a casing material. The corresponding variations in collapse strength are shown in Figure 5.4, plotted with a variation in axial stress. The yield strength of the material does not appear to significantly affect the inelastic buckling strength when the axial stress/yield stress ratio is high. There is, however, some effect of yield strength on collapse resistance when σ_z/σ_y is low. When the yield strength is high, the p/p_y ratio is less for low σ_z/σ_y values. This is because the collapse pressure will increase, but p_y, the pressure causing first material yield, will increase even more. The result is a lower value of the p/p_y ratio.

5.3 Effect of OD/t Ratio

To determine the effect of the OD/t ratio on the collapse strength of cylinders, the value of n was set equal to 20, $\sigma_y = 350$ MPa, and the ovality $\Delta = 0.01$. The range of OD/t ratios typical of casing is between 12 and 36. Figure 5.5 illustrates the assumed stress strain curve, and Figure 5.6 shows the variation in collapse strength with changes in OD/t.

The OD/t ratio is the single most important parameter in the stability of cylinders subject to external pressure. For elastic collapse of geometrically perfect cylinders, OD/t is the only parameter that varies, but the OD/t effects decrease when the cylinder material has exceeded yield and other parameters begin to affect stability. This can be seen in Figure 5.6, where the OD/t ratio has its greatest effect at the low values of σ_z/σ_y, but its effect is diminished when σ_z/σ_y approaches unity.

5.4 Effect of Ovality

To determine the effect of ovality on the buckling strength of casing, the OD/t ratio of 28 was selected to ensure that buckling would occur both elastically and plastically, depending on the σ_z/σ_y ratio. The yield strength was assumed to be 400 MPa, and n was taken equal to 20. The ovality, Δ, was varied from 0 to 0.02 (a value of $\Delta = 0.02$ is twice the accepted API BUL 2U (1987) tolerance).

Figure 5.7 shows the assumed stress strain curve, and Figure 5.8 illustrates the collapse prediction results.

It was discussed in Section 2.3.5 that ovality has its greatest effect when the effective stress of the material has not exceeded the yield value. This was the basis for determining the proposed capacity reduction factor, and this effect can be seen graphically in Figure 5.8.

5.5 Summary

Of the four parameters that were varied in this chapter (inelastic stiffness, yield strength, OD/t ratio, and ovality), the yield strength was found to have the lowest relative affect on collapse strength. Small yield strength effects, however, were observed when the σ_z/σ_y ratio was near zero or near one.

The inelastic stiffness was found to have the greatest effect when the load level exceeded the yield strength. There is no effect of inelastic stiffness on collapse strength when collapse is elastic.

The OD/t ratio was found to influence collapse strength the greatest. Its effect is quite clearly seen in the buckling equation, where the t/OD ratio is to the power of three.

The effects of ovality were found to be significant when the loading combination did not exceed yield, but ovality became insignificant when the cylinder remained stable and the material was allowed to progress past yield.

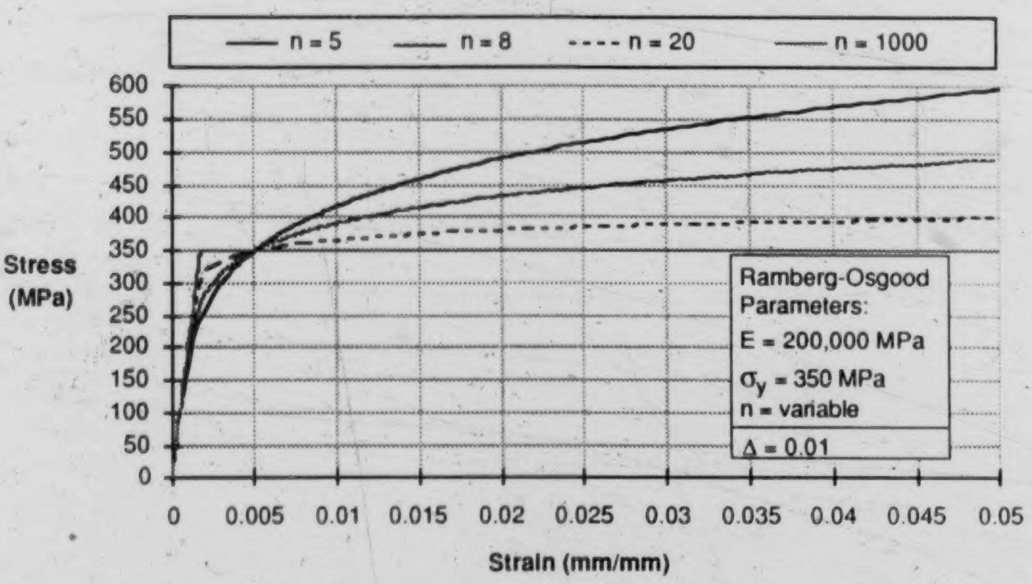

Figure 5.1 - Stress Strain Curves for the Variation in Inelastic Stiffness

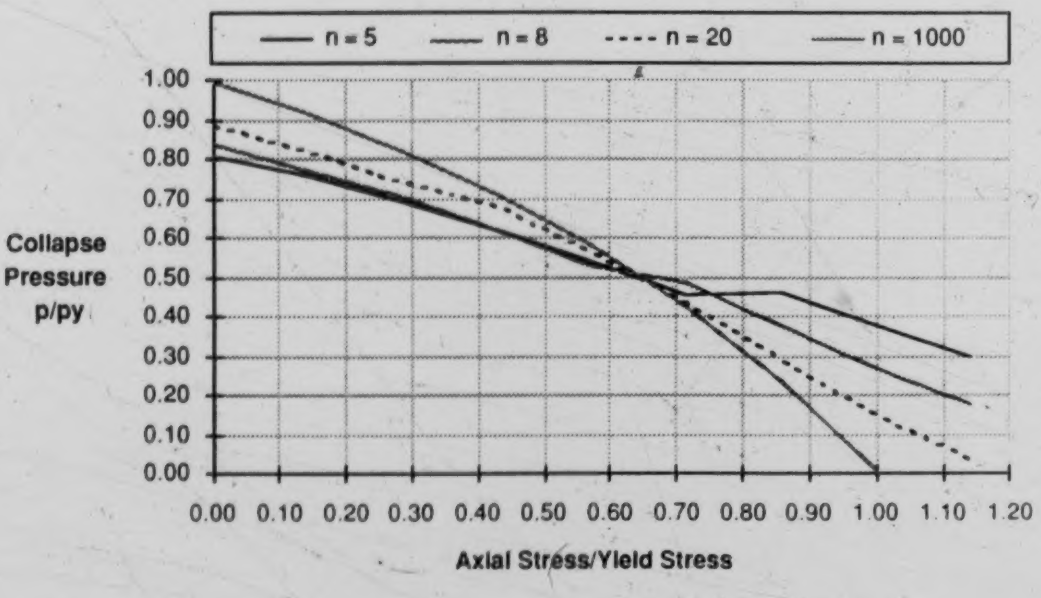

Figure 5.2 - Predicted Collapse Pressures for the Variation in Inelastic Stiffness

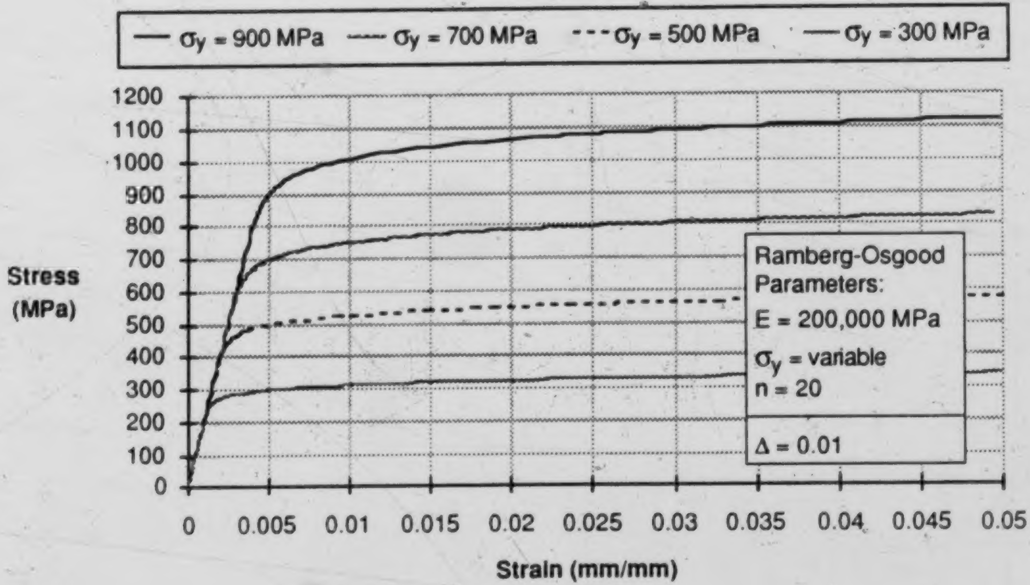

Figure 5.3 - Stress Strain Curves for the Variation in Yield Strength

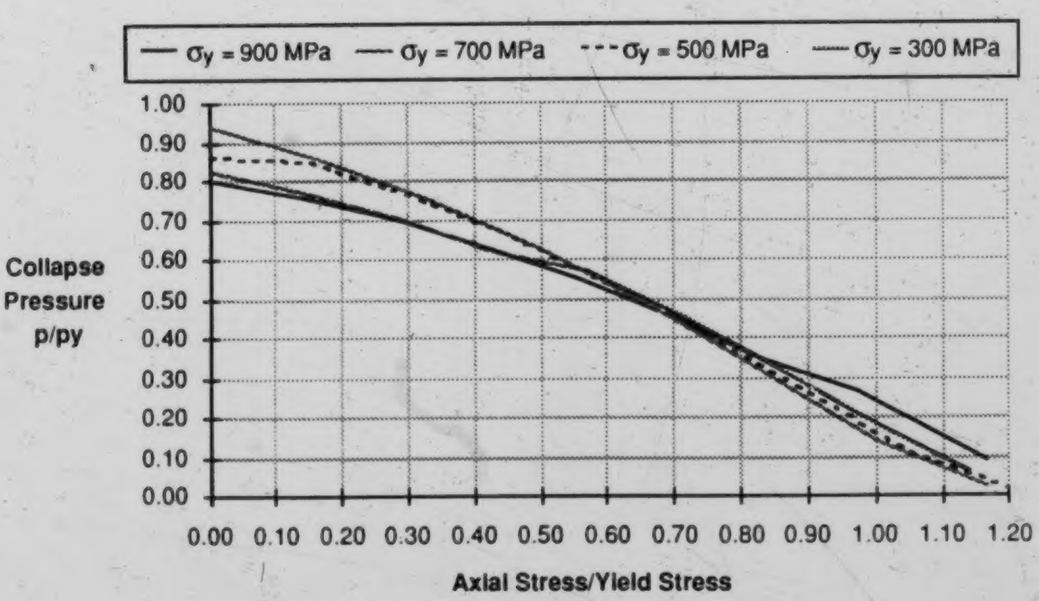

Figure 5.4 - Predicted Collapse Pressures for the Variation in Yield Strength

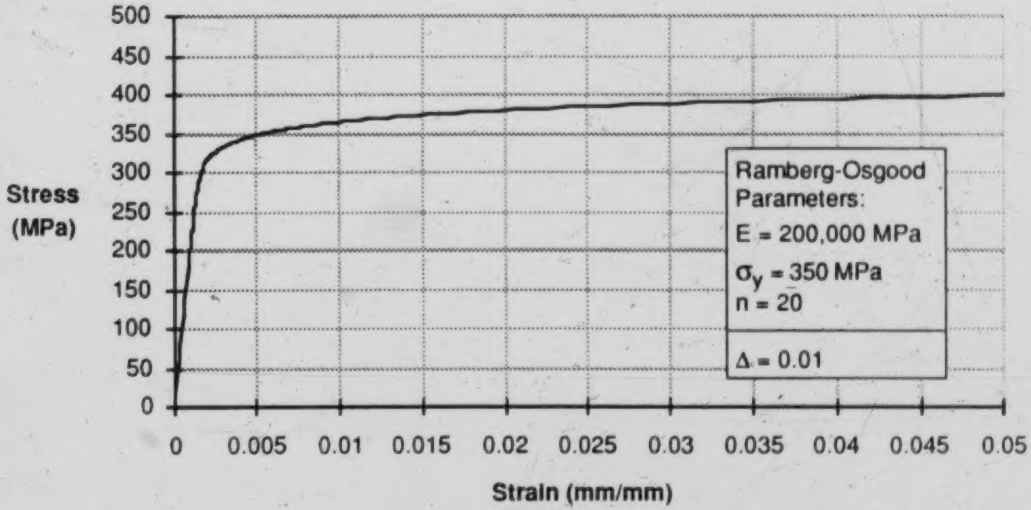

Figure 5.5 - Stress Strain Curve for the Variation in OD/t Ratio

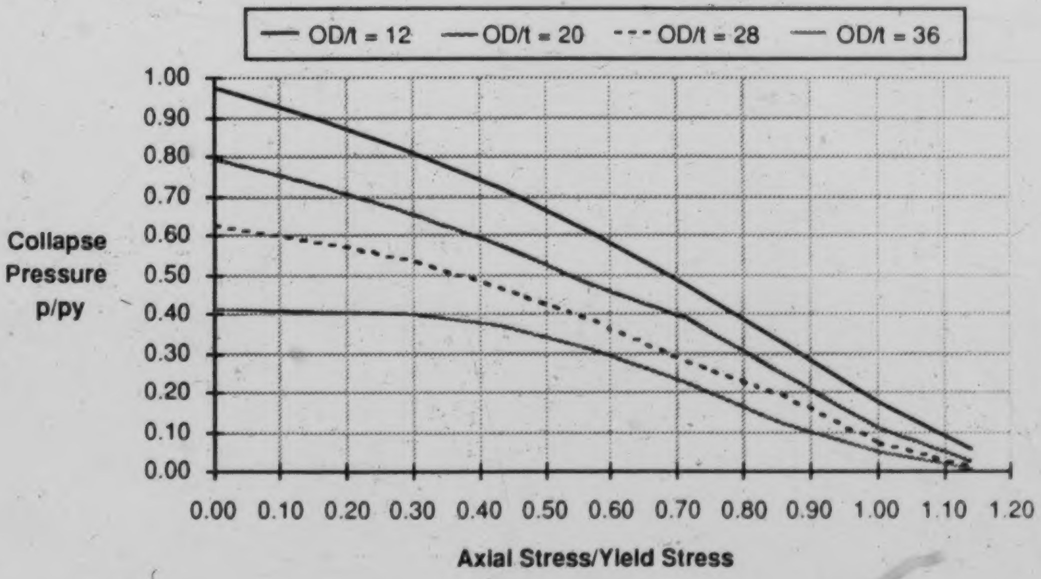

Figure 5.6 - Predicted Collapse Pressures for the Variation in OD/t Ratio

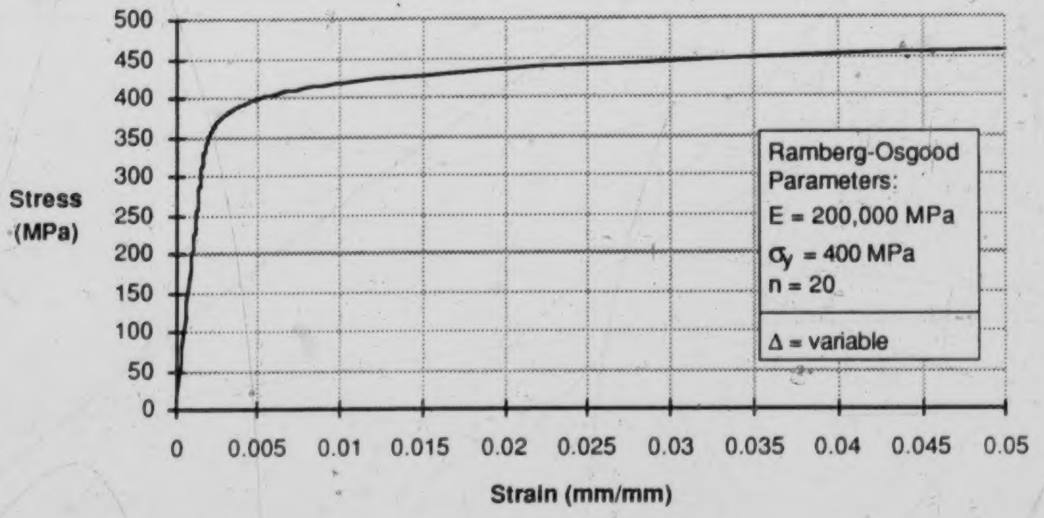

Figure 5.7 - Stress Strain Curve for the Variation in Ovality

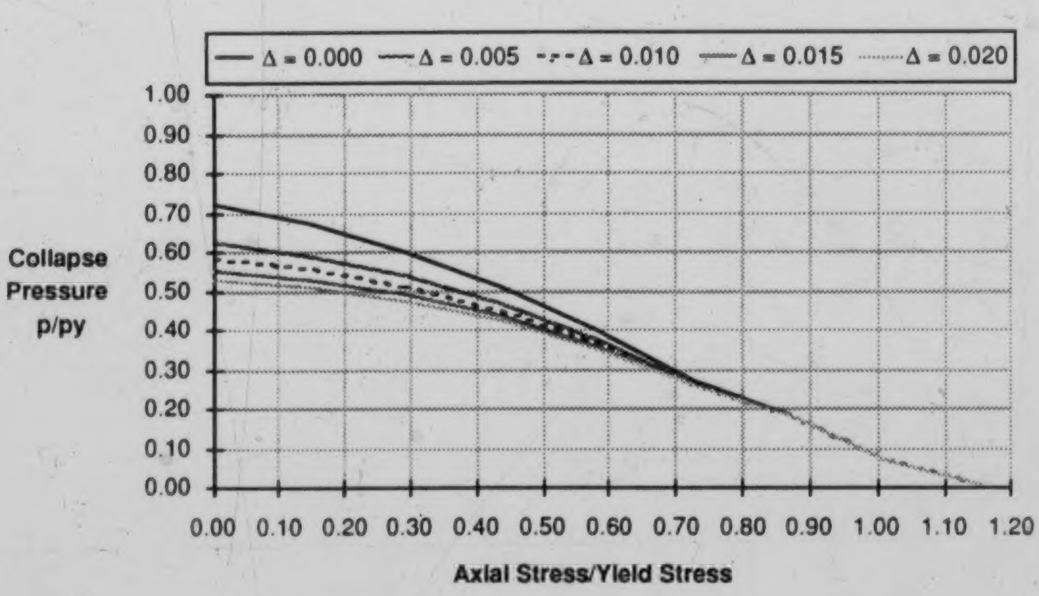

Figure 5.8 - Predicted Collapse Pressures for the Variation in Ovality

6.0 SUMMARY, CONCLUSIONS AND RECOMMENDATIONS

6.1 Summary

The problem of casing collapse in arctic environments has prompted the research outlined in this report. A literature review was performed to determine the factors that affect casing collapse. Test data was gathered for cylinders and tubes under external pressure and constant axial tensile load, as well as external pressure and constant axial tensile strain. Prediction and design methods were also investigated and compared to the test data. A method was proposed to predict the collapse strength of cylinders under the loading condition of constant axial load with external pressure. The proposed method was found to improve prediction accuracy, by measure of the test/predicted ratios. A parameter study was then undertaken to determine the sensitivity of cylinder buckling to variations in four parameters, namely the OD/t ratio, yield strength, inelastic stiffness, and ovality.

6.2 Conclusions

1. An evaluation of several prediction and design methods indicated reasonably good test/prediction and test/design ratios, and that all the prediction and

design methods served their intended purpose with good accuracy.

2. Of the prediction methods found in the literature, Gerard's (1957) method was considered the method of choice, as determined by accuracy and ease of use.

3. An evaluation of the design methods found in the literature resulted in the selection of Miller's (1981) method as the best for use in a design situation.

4. The degree of plasticity was found to affect the sensitivity of collapse to ovality. A modified capacity reduction factor, taking plasticity into account, was proposed for use with Gerard's (1957) prediction method.

5. The recommended method for use in predicting the collapse strength of cylinders subject to axial tensile load and external pressure (described below in Section 6.3) was found to be the most accurate of all the methods evaluated. The resulting mean and coefficient of variation for the test/predicted ratios was 0.97 and 16.74%, respectively.

6. A parameter study revealed that the collapse strength of cylinders is most sensitive to the D/t ratio and

the inelastic stiffness. Collapse strength was affected by ovality only when collapse occurred when the material was below yield.

7. The problem of cylinder collapse under the loading condition of constant axial strain and external pressure involves further study, but the results of a few tests indicate that cylinder collapse is unaffected by the magnitude of the axial strain value.

6.3 Collapse Prediction Recommendation

The recommended prediction method for use in determining the collapse strength of casing under the loading conditions considered in this report is that outlined by Gerard (1957), reduced by the proposed capacity reduction factor described in Chapter 4. This capacity reduction factor includes the effects of initial ovality and how the ovality effect is diminished as the material begins to behave inelastically. The proposed prediction method is restated below:

$$p_{cr} = \alpha_m (p_c)$$

where:

$$p_c = \eta \frac{2E}{(1 - \nu^2)} \left(\frac{t}{D}\right)^3$$

$$\eta = \left[\frac{1 - \nu_e^2}{1 - \nu^2}\right]\left(\frac{E_s + 3E_t}{4E}\right)$$

$$\alpha_m = 1-0.2\frac{E_t}{E}\sqrt{\frac{OD_{max}-OD_{min}}{0.01(OD_{nominal})}}$$

The following steps summarize the procedure:

1. Iteratively determine p_c using a properly modelled effective stress strain curve, and Poisson's ratio equal to 0.3 in the elastic range, and equal to 0.5 in the inelastic range.

2. At the collapse load p_c, determine E_t and calculate α_m, knowing the initial ovality of the cylinder, as defined by OD_{min} and OD_{max}.

3. Determine the reduced critical collapse pressure, p_{cr}.

6.4 Future Research Work

Future work should involve precise testing programs that properly account for the effects of all the parameters influencing buckling resistance. Accurate test results with properly obtained stress strain curves would provide an even better database of test results.

For the loading condition of constant axial load with external pressure, it was found that the scatter of test/predicted ratios increased as the σ_z/σ_y ratio increased. It is not known why the scatter exists, and follow-up work to determine the reasons for this increase in scatter would form the basis for a suitable investigation.

The prediction of the collapse strength of cylinders subject to the loading condition of constant axial strain and external pressure appears to be extremely involved, using plasticity theorems which account for circumferential loading and axial unloading. Collapse predictions for this loading condition is one area for further study.

The effects of ovality, eccentricity, residual stresses, and material anisotropies on collapse strength should also be studied further. Depending on the material state of stress at instability, the influence of these factors can be quite significant.

REFERENCES

API BUL 2U. 1987. Bulletin on the Stability Design of Cylindrical Shells. American Petroleum Institute Production Department, First Edition, May.

API BUL 5C3. 1985. Bulletin on Formulas and Calculations for Casing, Tubing, Drill Pipe, and Line Pipe Properties. American Petroleum Institute, Fourth Edition, February.

API RP 2A. 1982. Recommended Practice for Planning, Designing, and Constructing Fixed Offshore Platforms. American Petroleum Institute, Thirteenth Edition, January.

API RP 2T. 1987. Recommended Practice for Planning, Designing, and Constructing Tension Leg Platforms. American Petroleum Institute, First Edition, April.

Arbocz, J. and Babcock, C.D. 1969. The Effect of General Imperfections on the Buckling of Cylindrical Shells. Journal of Applied Mechanics, American Society of Mechanical Engineers, March, pp. 28-38.

ASME Boiler and Pressure Vessel Code Case N-284. 1986. Metal Containment Shell Buckling Design Methods. Supplement 2 to Nuclear Code Case Book.

Bily, C. and Dick, J.W.L. 1974. Naturally Occurring Gas Hydrates in the Mackenzie Delta, N.W.T. Bulletin of Canadian Petroleum Geology, 22 (3), September, pp. 340-352.

Carman, A.P. 1917. The Collapse of Thin Short Tubes. University of Illinois Engineering Experimental Station Bulletin No. 99, June.

Clinedinst, W.O. 1939. A Rational Expression for the Critical Collapsing Pressure of Pipe Under External Pressure. Drilling and Production Practice, American Petroleum Institute, pp 383-391.

Det Norske Veritas. 1977. DnV Rules for the Design Construction and Inspection of Offshore Structures, Appendix C Steel Structures. Høvik, Norway, pp. C18-C23.

EBA. 1985. Thaw Subsidence Analysis for East Amauligak. Report Submitted by EBA Engineering Consultants Ltd. to Gulf Canada Corporation.

ECCS Technical Committee 8 - Structural Stability. 1984. European Recommendations for Steel Construction: Buckling of Shells. Third Edition, September.

Edwards, S.H. and Miller, C.P. 1939. Discussion on the Effect of Combined Longitudinal Loading and External Pressure on the Strength of Oil-Well Casing. Drilling and Production Practice, American Petroleum Institute, pp 483-502.

Fowler, J.R.; Klementich, E.F.; and Chappell, J.F. 1983. Analysis and Testing of Factors Affecting Collapse Performance of Casing. Journal of Energy Resources Technology, American Society of Mechanical Engineers, 105, December, pp. 574-579.

Galambos, T.V. 1988. Guide to Stability Design Criteria for Metal Structures. Fourth Edition, John Wiley and Sons.

Gerard, G. 1957. Plastic Stability Theory of Thin Shells. Journal of the Aeronautical Sciences, April, pp. 269-274.

Gerard, G. 1962. Introduction to Structural Stability Theory. McGraw-Hill Book Company.

Goodman, M.A. 1977. How Permafrost Thaw/Freeze Creates Wellbore Loading. World Oil, October.

Gulf Canada. 1987. Evaluation of X-56 Casing Subject to Large Tensile Strains and External Pressures. Confidential Report Submitted by the Centre for Frontier Engineering Research to Gulf Canada Corporation, March.

Heise, O. and Esztergar, E.P. 1970. Elastoplastic Collapse of Tubes Under External Pressure. Journal of Engineering for Industry, American Society of Mechanical Engineers, November, pp. 735-742.

Hill, R. 1950. The Mathematical Theory of Plasticity. Oxford University Press.

Hirakawa, K.; Tokimasa, K.; and Tanaka, K. 1982. Effect of L/D on the Collapsing Pressure of Seamless Steel Tubes for Oil Well Casing Under External Pressure. The Sumitomo Search, 27, December, pp. 79-88.

Hirshberg, A.J.; Moyer, M.C.; and Rickenbach, R.M. 1988. Surface-Casing Strain Capacity for North Slope Operations. Society of Petroleum Engineers, SPE Drilling Engineering, September, pp. 289-295.

Hnatiuk, J. and Randall, A.G. 1977. Determination of Permafrost Thickness in Wells in Northern Canada. Canadian Journal of Earth Sciences, 14 (3), March, pp. 375-383.

Holmquist, J.L. and Nadai, A. 1939. A Theoretical and Experimental Approach to the Problem of Collapse of Deep-Well Casing. Drilling and Production Practice, American Petroleum Institute, pp 392-420.

Huang, N.C. and Pattillo, P.D. 1982. Collapse of Oil Well Casing. Journal of Pressure Vessel Technology, American Society of Mechanical Engineers, 104, February, pp. 36-41.

Huang, N.C. and Pattillo, P.D. 1984. The Effect of Length:Diameter Ratio on Collapse of Casing. Journal of Pressure Vessel Technology, American Society of Mechanical Engineers, 106, May, pp. 160-165.

MacKenzie, P.; McKelvie, J.; McDonach, A.; and Walker, C.A. 1986. Measurement of Poisson's Ratio Through the Elastic-Plastic Transition. Strain, February, pp. 13-19.

Madhavan, R. 1988. On the Collapse of Long Thick-Walled Circular Tubes Under Biaxial Loading. Ph. D. Thesis, California Institute of Technology, California, 128 p.

Makogon, Y.F. 1981. Hydrates of Natural Gas. Pennwell Publishing Company.

Mehdizadeh, P. 1975. Casing Collapse Performance. Journal of Engineering for Industry, American Society of Mechanical Engineers, Paper 75-PET-41, pp. 1-8.

Miller, C.D. 1979. Preliminary Commentary on the Metal Containment Shell Buckling Design Methods of the ASME Boiler and Pressure Vessel Code Section III - Division 1, December.

Miller, C.D. 1981. Buckling Design Methods for Steel Structures - A State of the Art. Second International

Symposium on the Integrity of Offshore Structures, University of Glascow, Scotland, July, pp. 397-418.

Mimura, H.; Tamano, T.; and Mimaki, T. 1987. Finite Element Analysis of Collapse Strength of Casing. Nippon Steel Technical Report No. 34, July, pp. 62-69.

Mitchell, R.F. and Goodman, M.A. 1976. Permafrost Thaw-Subsidence Casing Design. Society of Petroleum Engineers, Paper SPE 6060, pp. 1-8.

NASA. 1968. Buckling of Thin-Walled Circular Cylinders, NASA Space Vehicle Design Criteria (Structures), NASA SP-8007.

Nishioka, K.; Yoshihiro, N.; Tetsuro, K.; Hirakawa, K.; Nishikawa, K.; and Tokimasa, K. 1976. An Experimental Study on the Critical Collapsing Pressure of a Seamless Steel Tube for Well Casing Under External Pressure. The Sumitomo Search No. 15, May, pp. 63-74.

Pattillo, P.D. 1985a. How to Apply the New API Axial Load Adjustment, Part 1 - Defining Collapse Resistance. Petroleum Engineer International, March, pp. 40-50.

Pattillo, P.D. 1985b. How to Apply the New API Adjustment for Collapse Resistance of Tubulars, Part 2 - Actual Use of the New Adjustment. Petroleum Engineer International, April, pp. 44-52.

Pattillo, P.D. and Huang, N.C. 1982. The Effect of Axial Load on Casing Collapse. Journal of Petroleum Technology, Society of Petroleum Engineers, January, pp. 159-164.

Pattillo, P.D. and Huang, N.C. 1985. Collapse of Oil Well Casing with Ovality. Journal of Energy Resources

Technology, American Society of Mechanical Engineers, 107, May, pp. 128-134.

Ramberg, W. and Osgood, W. B. 1943. Description of Stress-Strain Curves by Three Parameters. National Advisory Committee for Aeronautics, Technical Note 902, pp. 1-28.

Ratzlaff, K.P. and Kennedy, D.J.L. 1985. Behaviour and Ultimate Strength of Transversely Loaded Continuous Steel Plates. University of Alberta Structural Engineering Report No. 130, November, 114 p.

Simonen, F.A. and Shippell, R.J. 1982. Collapse of Thick-Walled Cylinders Under External Pressure. Experimental Mechanics, February, pp. 41-48.

Southwell, R.V. 1915. On the Collapse of Tubes by External Pressure. Philosophical Magazine, January, pp. 67-77.

Southwest Research Institute. 1987. Tension Collapse of Pipe with High Axial Strain. Report submitted to Gulf Canada Corporation, March.

Stang, A.H.; Greenspan, M.; and Newman, S.B. 1946. Poisson's Ratio of Some Structural Alloys for Large Strains. Research Paper ARP-1742, Journal of Research of the National Bureau of Standards, 37, October, pp. 211-221.

Stephens, M.J.; Kulak, G.L.; and Montgomery, C.J. 1982. Local Buckling of Thin-Walled Tubular Steel Members. University of Alberta Structural Engineering Report No. 103, February.

Stewart, R.T. 1906. Collapsing Pressure of Bessemer Steel, Lap-Welded Tubes, 3 in. to 10 in. in Diameter.

Transactions of the American Society of Mechanical Engineers, 27, pp. 730-822.

Stuiver, W. and Tomalin, P.F. 1959. The Failure of Tubes Under Combined External Pressure and Axial Load. Proceedings of the Society of Experimental Stress Analysis, 16 (2), pp. 39-48.

Tam, C.K. and Croll, J.G.A. 1988. Mechanism Analysis of the Post-Buckling Response of a Circular Ring Under External Pressure. Thin-Walled Structures, 6 (2), pp. 109-128.

Tamano, T.; Mimura, H.; and Yanagimoto, S. 1982. Examination of Commercial Casing Collapse Strength Under Axial Loading. Proceedings of the First Offshore Mechanics/Arctic Engineering/Deepsea Systems Symposium, American Society of Mechanical Engineers, 1, pp. 113-118.

Thompson, J.M.T. and Hunt, G.W. 1983. Collapse, the Buckling of Structures in Theory and Practice, Symposium, University College, London, August - September, 531 p.

Timoshenko, S.P. and Gere, J.M. 1961. Theory of Elastic Stability. Second Edition, McGraw-Hill Book Company.

Tokimasa, K. and Tanaka, K. 1986. FEM Analysis of the Collapse Strength of a Tube. Journal of Pressure Vessel Technology, American Society of Mechanical Engineers, 108, May, pp. 158-164.

Tomita, Y. and Shindo, A. 1982. On the Bifurcation and Post-Bifurcation Behaviour of Thick Circular Elastic-Plastic Tubes Under Lateral Pressure. Computer Methods in Applied Mechanics and Engineering, 35 (2), November, pp. 207-219.

Tschoepe, E. and Maison, J.R. 1983. The External Pressure Collapse Tests of Tubes. Welding Research Council Bulletin 284, April, pp. 1-20.

Workman, G. 1982. User's Guide for PIPEWALL. Applied Mechanics Incorporated, Columbus, Ohio, 19 p.

Yeh, M.K. and Kyriakides, S. 1986a. On the Collapse of Inelastic Thick-Walled Tubes Under External Pressure. Journal of Energy Resources Technology, American Society of Mechanical Engineers, 108, March, pp. 35-47.

Yeh, M.K. and Kyriakides, S. 1986b. Collapse of Deepwater Pipelines. Proceedings of the Offshore Technology Conference, Paper OTC 5215, May, pp. 511-520.